SAHC

The Effect of Bird Excrements on Copper and Bronze

Kristen Balogh

Czech Republic | 2017

ADVANCED MASTERS IN STRUCTURAL ANALYSIS
OF MONUMENTS AND HISTORICAL CONSTRUCTIONS

Master's Thesis

Kristen Balogh

The Effects of Bird Excrements on Copper and Bronze

Czech Technical University in Prague

UPC
UNIVERSITAT POLITÈCNICA DE CATALUNYA

Education and Culture

Erasmus Mundus

ADVANCED MASTERS IN STRUCTURAL ANALYSIS
OF MONUMENTS AND HISTORICAL CONSTRUCTIONS

Master's Thesis

Kristen Balogh

The Effects of Bird Excrements on Copper and Bronze

This Masters Course has been funded with support from the European Commission. This publication reflects the views only of the author, and the Commission cannot be held responsible for any use which may be made of the information contained therein.

Czech Republic | 2017

CZECH TECHNICAL UNIVERSITY IN PRAGUE
Faculty of Civil Engineering
Thákurova 7, 166 29 Prague 6, Czech Republic

MASTER'S THESIS PROPOSAL

study programme: Civil Engineering

study branch: Advanced Masters in Structural Analysis of Monuments and Historical Constructions

academic year: 2016/2017

Student's name and surname: Kristen Balogh

Department: Department of Mechanics

Thesis supervisor: Zuzana Slizkova, Katerina Kreislova

Thesis title: The Effects of Bird Excrements on Copper and Bronze

Thesis title in English see above

Framework content: The visual aspect of bird excrements on bronze and copper cultural heritage is evident. Its chemical and physical contribution to the degradation of metals is still not fully understood. The purpose of the research was to better comprehend bird excrement components and to observe its effect on copper and bronze. Four aspects were tested: 1) change in metal materials, 2) impact of specific dropping components, 3) other environmental conditions, and 4) exposure duration. Pure copper, copper with an established patina, and bronze elements underwent an accelerated aging test with drops of known bird dropping components: 1) Uric acid, 2) Uric acid and sodium nitrate, 3) Uric acid and potassium dehydrate phosphate, 4) Purchased bird droppings, 5) Uric acid and potassium chloride, and 6) Uric acid and potassium sulphate. The accelerated aging took place in a chamber with 100% RH and another chamber with 100% RH and SO2 gas mimicking pollution. Samples were removed at various time intervals to observe changes. The purchased bird droppings and real bird droppings underwent IEC and XRD tests to determine their composition, which proved that the their make-up was different from each other. The used bird droppings consisted primarily of sulphate and potassium, whereas the real bird droppings consisted mainly of phosphorous and ammonium. XRD tests proved that both the used and real bird droppings contained quartz, and weddellite. The used droppings differed from the real as it contained calcite and magnesium hydrogen phosphate hydrate and the real droppings contained aphthitalite and magnesium ammonium phosphate hydrate. The pH tests showed that the added solutions were relatively neutral. Digital microscopy and colourimetry allowed the visual evaluation of the drop surfaces and showed details regarding discolouration and the corrosion process. It is believed that the patina acts as a protective agent for the first stages of exposure. SEM/EDS showed the change in surface texture and also identified the presence of fungi and dust particles. There were no large differences with the SO2 exposure. A longer testing program is recommended with a careful selection of excrement components. Deterring birds is the best protection from metals. Research into the effect of bird deterrent adhesives and gels on metal is recommended.

Assignment date: 7/04/2017 Submission date: 06/07/2017

If the student fails to submit the Master's thesis on time, they are obliged to justify this fact in advance in writing, if this request (submitted through the Student Registrar) is granted by the Dean, the Dean will assign the student a substitute date for holding the final graduation examination (2 attempts for FGE remain). If this fact is not appropriately excused or if the request is not granted by the Dean, the Dean will assign the student a date for retaking the final graduation examination, FGE can be retaken only once. (Study and Examination Code, Art 22, Par 3, 4.)

The student takes notice of the obligation of working out the Master's thesis on their own, without any outside help, except for consultation. The list of references, other sources and names of consultants must be included in the Master's thesis.

.....
Master's thesis supervisor

.....
Head of department

Date of Master's thesis proposal take over: July 2017

.....
Student

This form must be completed in 3 copies – 1x department, 1x student, 1x Student Registrar (sent by department)

No later than by the end of the 2nd week of instruction in the semester, the department shall send one copy of BT Proposal to the Student Registrar and enter data into the faculty information system KOS. (Dean's Instruction for Implementation of Study Programmes and FGE at FCE CTU Art. 5, Par. 7)

DECLARATION

Name: Kristen Balogh

Email: kfbalogh@hotmail.ca

Title of the Msc Dissertation: The Effects of Bird Excrements on Copper and Bronze

Supervisor(s): Zuzana Slížková, Kateřina Kreislová

Year: 2017

I hereby declare that all information in this document has been obtained and presented in accordance with academic rules and ethical conduct. I also declare that, as required by these rules and conduct, I have fully cited and referenced all material and results that are not original to this work.

I hereby declare that the MSc Consortium responsible for the Advanced Masters in Structural Analysis of Monuments and Historical Constructions is allowed to store and make available electronically the present MSc Dissertation.

University: České vysoké učení technické v Praze

Date: July 4, 2017

Signature:

To my new friends and the adventures ahead

ACKNOWLEDGEMENTS

This thesis would not have been possible without the support from all those at SVÚOM and ÚTAM AV ČR laboratories in Prague and CET Telč, Czech Republic. To everyone at SVÚOM, I would like to thank you for consistently helping me find materials, allowing me space to conduct my experiments, and for your friendly attitudes that always made me feel welcome in the office.

For those at ÚTAM AV ČR, I am very grateful for your assistance and guidance throughout this entire process. More specifically, I would like to thank Miloš Drdácký [prof., PhD., DSc.] and Stanislav Pospíšil [doc. Ing., PhD.] for always making me feel welcome at their facilities. Thank you Petra Hauková for helping me conduct my tests and for making me feel more comfortable working in a chemical laboratory again. Jiří Frankl [Ing.], thank you for collecting pigeon excrements for me. It was a job many were not willing to do, but was immensely important for my studies. To Cristiana Lara Nunes [PhD.], I appreciate all of your support and friendship these past couple months. You made the dissertation process fun and exciting!

At CET Telč, I am thankful for you sharing your knowledge about testing procedures and for the immense time you spent guiding and teaching me about the equipment. Jakub Novotný [PhD.], I appreciate you arranging my comfortable stay at the facilities. Petra Mácová and Radek Ševčík [PhD.], thank you for taking the time to help me conduct my testing analyses. A huge thank you goes to Alberto Viani for guiding me through all aspects of my testing: from organizing the equipment use to handling a material I know was not your ideal testing specimen.

I would be remiss to not thank my incredible supervisors Zuzana Slížková [PhD.] and Kateřina Kreislová [Ing., PhD.]. Your knowledge in the field of historical materials is very impressive and I am grateful that you were able to share your expertise with me. Not only were you mentors within the technical aspects of my dissertation, but you also provided guidance with life in Prague and the Czech Republic. Your positive attitudes and friendliness did not go unnoticed and I am lucky to have worked with such inspiring women.

I would like to recognize the SAHC Consortium for providing my scholarship for the duration of the program and their planning of our studies. Thank you to our professors and organizers from the Universitat politècnica de Catalunya and České vysoké učení technické who greatly helped prepare me for the thesis work. More specifically, I would like to thank Petr Kabele [prof. Ing. PhD.] and Alexandra Kurfürstová for their coordination of our theses.

For my friends and family in Canada, I appreciate your utmost support throughout this masters program. Though you were far away, your encouragement and positivity was felt here everyday. Lastly, I would like to extend an enormous thank you to my colleagues from the SAHC program. Not only were you my classmates, but also my friends, engineering gurus, travel agents, therapists, chefs, adventurers, and ultimately my new European family. I cannot imagine conducting my thesis work without your daily inspiration.

ABSTRACT

The Effects of Bird Excrements on Copper and Bronze

This thesis was aimed at understanding the effects of bird excrements on copper and bronze. The current state-of-the-art knowledge regarding copper and bronze material characteristics and degradation processes, along with bird excrement composition was reviewed. Previous studies regarding the effects of bird excrements on various materials were also assessed.

The testing procedure was adapted from an experiment conducted by Bernardi, Bowden, Brimblecombe, Kenneally, and Morselli called *The effect of uric acid on outdoor copper and bronze*. In SVÚOM and ÚTAM AV ČR laboratories in Prague and CET Telč, Czech Republic, four aspects were examined using an accelerated aging test: 1) metal type, 2) specific dropping chemical components, 3) other environmental conditions, and 4) exposure duration. Specimens of pure copper sheets, copper sheets with a developed patina (referred to as the roof sample onwards), and bronze sheets had six different contaminants added to them to mimic bird dropping components: 1) uric acid, 2) uric acid and sodium nitrate, 3) uric acid and potassium dehydrate phosphate, 4) purchased bird droppings, 5) uric acid and potassium chloride, and 6) uric acid and potassium sulphate. The contaminated metals were placed in two chambers, one at room temperature with a relative humidity of 100%, and another chamber at room temperature set at a relative humidity of 100% and included SO_2 gas to imitate that of atmospheric pollution. Samples were removed at various intervals over a span of four weeks.

Ion exchange chromatography (IEC) and X-ray diffraction (XRD) results showed that the purchased bird droppings used in the experiment differed from real droppings collected later. The main anions in the used bird droppings in order from greatest concentration to least were sulphate, chloride, and phosphate, whereas the real bird droppings consisted of phosphorous, chloride, and sulphate. The used droppings primarily consisted of the potassium, calcium, and sodium cations, whereas the real bird droppings contained mainly ammonium, potassium, and sodium. The XRD tests indicated that the used bird droppings contained calcite, quartz, weddellite, and magnesium hydrogen phosphate hydrate. The real bird droppings also contained quartz and weddellite, but the remainder consisted of aphthitalite and magnesium ammonium phosphate hydrate.

The contaminant pH levels were all around pH-5 with slight differences. The digital microscopy showed the changes in surface colour and texture. Visual evaluation showed that changes can be seen from the drops within four weeks and that there are minimal differences between RH and RH + SO_2 exposures. Scanning electron microscopy (SEM) and energy dispersive spectroscopy (EDS) showed the change in surface texture and also identified the presence of fungi and dust particles.

Overall, bird droppings do promote the corrosion process of metals. A patina can act as a protective layer towards corrosion for some time before it begins to deteriorate. A longer study is required to see more developed results. The best protection against bird droppings on metal is to deter the birds from perching on the metal surfaces.

Keywords: copper, bronze, corrosion, bird excrements, patina, SO_2

ABSTRAKTNÍ

Účinky výkalů ptáků na měď a bronz

Diplomová práce řeší problém degradačního působení ptačích (zejména holubích) exkrementů na kovové materiály měď a bronz. Součástí práce je literární rešerše současných znalostí o materiálových vlastnostech mědi a bronzu a o degradačních procesech vyvolaných exkrementy ptáků na povrchu kovových a dalších stavebních materiálů.

Experimentální část práce byla provedena v laboratořích SVÚOM a ÚTAM AV ČR a zaměřila se na studium koroze mědi a bronzu vlivem sloučenin, které mohou být součástí ptačích exkrementů. Byly zvoleny různé podmínky korozního působení a na části zkušebních vzorků byl studován vedle chemického vlivu exkrementů také vliv prostředí - znečištěného ovzduší. Koroze byla studována na 3 typech zkušebních materiálů: destičkách z čistého měděného plechu, destičkách z měděného plechu s rozvinutou patinou a na bronzových destičkách. Zkušební vzorky kovů byly na vymezených plochách kontaminovány různými chemickými látkami, které jsou obsaženy v ptačích exkrementech, a byl sledován vliv těchto látek na povrch kovu ve dvou různých prostředích: při teplotě 20 °C a vysoké relativní vlhkosti (100%) a v prostředí se stejnou teplotou, relativní vlhkostí, ale vyšší koncentrací SO_2 ve vzduchu. Korozní zkoušky byly provedeny v laboratoři s využitím dvou klimatických komor a doba expozice kovových vzorků byla maximálně 4 týdny. Bylo sledováno působení 5 chemických roztoků (připravených z látek, které jsou předpokládanými složkami ptačích exkrementů), a také na trhu dostupný ptačí trus (určený pro krmení ryb), dispergovaný ve vodě. Varianty studovaných látek byly následující: kyselina močová, kyselina močová a dusičnan sodný, fosforečnan vápenatý a fosforečnan draselný, kyselina močová a chlorid draselný, kyselina močová a síran draselný, suspenze koupeného suchého trusu. Chemické složení koupeného trusu bylo stanoveno pomocí iontové chromatografie (IEC) a rentgenové difrakce (XRD). Během práce byl získán vzorek čerstvého holubího trusu, proto byl i tento analyzován stejným postupem a složení trusu z různých zdrojů bylo porovnáno.

Chemické složení obou analyzovaných vzorků holubího trusu se lišilo. Hlavními kationty prodávaného ptačího trusu jsou draselné, vápenaté a sodné ionty, zatímco holubí trus odebraný na fasádě domu v Praze 4 obsahoval hlavně ammonné, vedle draselných a sodných iontů. Anionty byly v obou vzorcích stejné, ale koncentrace jiná: v zakoupeném trusu to byly sírany, chloridy a fosforečnany v klesající řadě, v odebraném holubím trusu naopak fosforečnany, chloridy a nejméně sírany. Mineralogické složení obou trusů bylo obdobné, ale ne totožné: prodávaný trus obsahoval kalcit, křemen, weddellite a hydrát hydrogenfosforečnanu hořečnatého. Odebraný vzorek holubího trusu také obsahoval křemen, weddellite (dihydrát šťavelanu vápenatého) a hydratovaný fosforečnan hořečnato-amonný, ale navíc afthitalit $(K,Na)_3Na(SO_4)_2$, a neobsahoval kalcit.

Pomocí digitální mikroskopie, spektrofotometrie a SEM-EDS byly zjištěny a dokumentovány barevné, chemické a strukturní změny exponovaného povrchu kovových destiček. Znečištění vzduchu SO_2 se během 4- týdenní expozice nijak výrazně neprojevilo. Vedle minerálních složek byly zjištěny stélkaté organismy-houby.

Výsledky prokázaly, že trusy ptáků podporují proces koroze kovů. Patina sehrává roli ochranné vrstvy, ale jen po určitou dobu. Zdá se, že nejspolehlivější ochranou památek před ptáky jsou systémy, které brání ptákům usednout na povrch chráněného objektu.

Klíčová slova: měď, bronz, koroze, exkrementy ptáků, patina, SO_2

LIST OF CONTENTS

1. INTRODUCTION 1

1.1 MOTIVATION AND SCOPE 1

1.2 OBJECTIVES 3

2. LITERATURE REVIEW 5

2.1 COPPER AND BRONZE CHARACTERISTICS 5

2.2 BIRD DROPPING CHARACTERISTICS 11

2.3 CURRENT BIRD DETERRENT SYSTEMS 16

3. METHODOLOGY 20

3.1 TESTING PARAMETERS AND MATERIALS USED 21

3.2 ANALYSES PROCEDURES 25

3.2.1 Bird Excrement Composition 25

3.2.2 Surface Corrosion Products 28

4. RESULTS AND DISCUSSION 32

4.1 TESTING RESULTS 33

4.2 ANALYSES RESULTS 34

4.2.1 Bird Excrement Composition 34

4.2.2 Surface Corrosion Products 38

5. CONCLUSION 73

REFERENCES 75

APPENDIX A – COLOURIMETRY GRAPHS

CHANGE BETWEEN INSIDE AND OUTSIDE OF CONTAMINATED AREAS

CHANGE INSIDE CONTAMINATED AREAS BETWEEN TWO AND FOUR WEEKS

CHANGE OUTSIDE CONTAMINATED AREAS BETWEEN TWO AND FOUR WEEKS (NOT AVERAGED)

LIST OF FIGURES

Figure 1: Abundance of birds flying in Trafalgar Square, London (Finamore, 2016).....1
Figure 2: Left: Bronze statue from the Neptunbrunnen in Berlin, showing possible signs of bird dropping decay. Middle: Pigeons perching on the Turia Fountain in Valencia, Spain. Right: Damage from birds on the bronze Vítězslav Novák statue on the Petřín Hill, Prague. (Photos by: Kristen Balogh).....2
Figure 3: The corrosive layers on an object (Tidblad et al., 2009).....6
Figure 4: Illustration of the effect of relative humidity (left) and temperature (right) for zinc as annual averages in SO_2 polluted atmospheres (Tidblad et al., 2009).....6
Figure 5: Mass gain of zinc samples exposed in air at 95% RH showing the effect of synergy (Tidblad et al., 2009).....8
Figure 6: Illustration of the reactions involved in brochantite formation during patination (FitzGerald et al., 2006).....9
Figure 7: Lowering of the pH induced by four fungal species isolated from pigeon excrements: Aspergillus repens □; Fusarium oxysporum ★; Mucor hiemalis O; Penicillium cyclopium (Bassi & Chiatante, 1976).....12
Figure 8: The structure of uric acid.....13
Figure 9: The oxidation process of uric acid with copper (Vasiliu & Buruiana, 2010).....13
Figure 10: Increase of absorption rate with increasing pH (Vasiliu & Buruiana, 2010).....14
Figure 11: The contaminated areas of the statue (Kreislová et al., 2010).....15
Figure 12: The presence of moolooite can be seen in the diffractogram (Kreislová et al., 2010).....15
Figure 13: Example of a bird trip wire system installed on a building ledge (Absolute Pest Control Ltd., n.d.).....16
Figure 14: Netting around a statue in the Zámek Lednice, Moravia (Photo: Kristen Balogh).....17
Figure 15: Example of bird spikes on monuments in the Luxembourg Gardens, Paris [Photo by Zuzana Slížkova].....17
Figure 16: Example of bird gel application (RS Innovative Solutions, n.d.).....18
Figure 17: Copper with a natural patina was obtained from the roof of Queen Anna's Summer Palace in Prague (Kreislova & Geiplova, 2016; Kreislová & Koukalová, 2012).....21
Figure 18: The copper, roof, and bronze samples with the first four contaminants applied.....24
Figure 19: The distribution of contaminants 1-6 on the metal pieces.....24
Figure 20: The set up of the samples within the RH chamber. The RH + SO_2 chamber was organized in a similar fashion.....25
Figure 21: Crushing the real bird droppings and the magnetic mixing of the contaminants.....26
Figure 22: The IEC Equipment Used.....27
Figure 23: Filtering of the samples to measure pH.....28
Figure 24: The digital microscope and program used.....28
Figure 25: Testing one of the samples with the colourimetry equipment and software.....30
Figure 26: The SEM/EDS system used to analyze the metal surface.....31
Figure 27: The acid solution and the prepared samples for ICP-OES testing.....31
Figure 28: Example of samples removed from 2 weeks of exposure to RH + SO_2. Uric acid + potassium chloride (C5) is dripping onto the uric acid + potassium sulphate (C6) on the copper sample, whereas no dripping can be seen on the roof sample.....33
Figure 29: pH levels of the bird dropping samples used in the IEC testing.....34
Figure 30: The composition of the used bird droppings. Calcite [$CaCO_3$] – red vertical lines; Quartz [SiO_2] – blue vertical lines; Weddellite [$CaC_2O_4(H_2O)_{2.4}$] – green vertical lines; Magnesium Hydrogen Phosphate Hydrate [$Mg(H_2PO_2)_2(H_2O)_6$] – grey vertical lines.....35
Figure 31: The composition of the real dropping sample. Magnesium Ammonium Phosphate Hydrate [$MgNH_4PO_4(H_2O)_6$] – blue vertical lines; Quartz [SiO_2] – fuschia vertical lines; Weddellite

[$CaC_2O_4(H_2O)_{2.4}$] – green vertical lines; Aphthitalite [$K_3Na(SO_4)_2$ – orange vertical lines. The presence of Weddellite and Aphthitalite is ambiguous. 36
Figure 32: pH levels for the sample contaminants removed after four weeks (excluding the used droppings (C4)) 37
Figure 33: Uric Acid (C1) - A) 1 day: Yellow crystals and black corrosion spots; B) 1 week: Larger black corrosion spots; D) 2 weeks: Discolouration; F) 4 weeks: Blue crystal on RH 39
Figure 34: Uric acid + sodium nitrate (C2) - A) 1 day: Dark drop area with yellow crystals visible; B) 1 week: Turquoise crystals visible; C) 2 weeks: The different drop outer ring colours from outside (left) in (right); D) 4 weeks – Discolouration and pitting 40
Figure 35: Uric acid + potassium dihydrogen phosphate (C3) - A) 1 day: Small dark corrosion spots and red crystals; B) 1 week: Blue crystals; C) 2 weeks: The inside versus the outside of the drop area; D) 4 weeks: The darker interior of the RH sample 40
Figure 36: Used droppings (C4) – A) 1 day: Darker outer ring; B) 1 week: Crust formation; C) 2 weeks: Blue crystals forming around RH + SO_2 sample; D) 4 weeks: Mould growth on sample 40
Figure 37: Uric acid + potassium chloride (C5) – A) 1 day: Discolouration; B) 1 week: Not uniform discolouration distribution in the RH + SO_2 sample; C) 2 weeks: Black corrosion areas; D) 4 weeks: Height map of the red layer on the RH + SO_2 sample 41
Figure 38: Uric acid + potassium sulphate (C6) – A) 1 day: Discolouration in RH sample; B) 1 week: Yellow interior of RH + SO_2 sample; C) 2 weeks: Dark interior of RH sample; D) Yellow interior of RH + SO_2 sample 41
Figure 39: Uric Acid (C1) - A) 1 day: Yellow crystals visible; B) 1 week: Black corrosion pits; C) 2 weeks: Eroded surface; D) 4 weeks: Green/brown spots on the salt 43
Figure 40: Uric acid + sodium nitrate (C2) – A) 1 day: No change; B) 1 week: Red area; C) 2 weeks: Spots visible on salt; D) 4 weeks – Eroded surface with red crystals 43
Figure 41: Uric acid + potassium dihydrogen phosphate (C3) – A) 1 day: Darker blue/green contaminant area colour; B) 1 week: Red crystal on the RH sample; C) 2 weeks: Corrosion spots on RH + SO_2 sample; D) 4 weeks: Different outer ring colours 44
Figure 42: Used droppings (C4) – A) 1 day: Black corrosion spots visible; B) 1 week: Mould formation on the contaminant; C) 2 weeks: RH + SO_2 contaminant showing protection from the uric acid + potassium dihydrogen phosphate (C3) dripping; D) 4 weeks: Red crystals around dark outer ring 44
Figure 43: Uric acid + potassium chloride (C5) – A) 1 day: A slightly darker interior; B) 1 week: Salted areas causing pitting in RH + SO_2 sample; C) 2 weeks: Exposed copper around the outer ring in RH sample; D) 4 weeks: Exposed copper interior 45
Figure 44: Uric acid + potassium sulphate (C6) – A) 1 day: Slightly darker outer ring; B) 1 week: Exposed copper in RH sample; C) 2 weeks: More frequent exposed copper areas in RH sample; D) 4 weeks: Exposed copper in RH sample 45
Figure 45: Uric Acid (C1) - A) 1 day: A dark outer ring forming; B) 1 week: Pitting and a pronounced outer ring; C) 2 weeks: Red crystal; D) 4 weeks: Entire spot area is dark 46
Figure 46: Uric acid + sodium nitrate (C2) – A) 1 day: Some blue crystals are seen on the RH sample; B) 1 week: The spot area is slightly darker; C) 2 weeks: Green areas; D) 4 weeks: Dark interior and surrounding turquoise crystals 47
Figure 47: Uric acid + potassium dihydrogen phosphate (C3) – A) 1 day: Black corrosion spots are visible; B) 1 week: More dark corrosion spots; C) 2 weeks: The lighter interior; D) 4 weeks: Red crystals on RH + SO_2 sample 47
Figure 48: Used droppings (C4) – A) 1 day: Black corrosion spots; B) 1 week: Turquoise crystals on RH + SO_2 sample; C) 2 weeks: Yellow interior and pink exterior; D) 4 weeks: Yellow crystals on RH sample 48

Figure 49: Uric acid + potassium chloride (C5) – A) 4 weeks: The black salt contaminant with turquoise crystals; B) 4 weeks: Dark interior with different colour crystals; C) 4 weeks: Various outer ring colours. 48
Figure 50: Uric acid + potassium sulphate (C6) – A and B) 4 weeks: The height differential between the dark interior and exterior; C) 4 weeks: Colour difference between the interior and exterior; D) 4 weeks: Interior 48
Figure 51: The difference in red and green between the inside and outside of drops 50
Figure 52: Total colour change inside the drop areas between two and four week samples 51
Figure 53: Clockwise from top left. The total colour change, the lightness change, the red/green change, and the blue/yellow change in the metals outside the drop areas between two and four weeks. 52
Figure 54: Copper – Outside: The copper sample EDS outside of the spot areas. 54
Figure 55: RH Copper – Uric Acid (C1): The EDS result of RH sample Spot 2 representing the sphere composition. Spots 1 and 3 were primarily Cu. 54
Figure 56: RH + SO_2 Copper – Uric Acid (C1): The EDS result of Spot 3. Spots 1 and 2 were primarily copper. 55
Figure 57: RH Copper – Uric acid + sodium nitrate (C2): The EDS result of Spot 1. Spots 2 and 3 were primarily copper. 55
Figure 58: RH + SO_2 Copper – Uric acid + sodium nitrate (C2): The EDS results of Spot 2 (above) and Spot 4 (below) 56
Figure 59: RH Copper – Uric acid + potassium dihydrogen phosphate (C3): The EDS results of RH Spot 2 56
Figure 60: RH + SO_2 Copper – Uric acid + potassium dihydrogen phosphate (C3): The EDS results of Spot 1, showing higher concentrations of phosphorous and potassium. 57
Figure 61: RH Copper – Used droppings (C4): The EDS results of Spot 4. 57
Figure 62: RH + SO_2 Copper – Used droppings (C4): The EDS results of Spot 2 58
Figure 63: RH Copper – Uric acid + potassium chloride (C5): EDS results for Spot 1 58
Figure 64: RH + SO_2 Copper – Uric acid + potassium chloride (C5): EDS results for Spot 1 58
Figure 65: RH Copper – Uric acid + potassium sulphate (C6): EDS results for Spot 1, showing high concentrations of potassium and sulphur 59
Figure 66: RH + SO_2 Copper – Uric acid + potassium sulphate (C6): EDS results for Spot 2 59
Figure 67: Roof – Outside: The typical diffractogram of the uncontaminated roof patina 61
Figure 68: RH Roof – Uric Acid (C1): The EDS image of Spot 3, showing the presence of iron 61
Figure 69: RH + SO_2 Roof – Uric Acid: EDS results of Spot 2 showing more iron particles. 62
Figure 70: RH Roof – Uric acid + sodium nitrate (C2): The EDS results for Spot 2 62
Figure 71: RH Roof – Uric acid + potassium dihydrogen phosphate (C3): The EDS results for Spot 263
Figure 72: RH Roof – Used droppings (C4): The EDS results for Spot 2 showing the diverse composition 63
Figure 73: RH Roof – Uric acid + potassium chloride (C5): The EDS results for Spot 2. 64
Figure 74: RH + SO_2 Roof – Uric acid + potassium chloride (C5): The EDS results for Spot 3, showing the composition of the remaining crust on the spot surface. 64
Figure 75: RH Roof – Uric acid + potassium sulphate (C6): The EDS results for Spot 1 on the exposed copper section. 64
Figure 76: RH + SO_2 Roof – Uric acid + potassium sulphate (C6): The composition of Drop 1 on the RH + SO_2 sample, showing small amounts of chlorine most likely from the uric acid + potassium chloride (C5). 65
Figure 77: Bronze – Outside: EDS image of the uncontaminated bronze surface 66
Figure 78: RH Bronze – Uric Acid: EDS image of Spot 2 67
Figure 79: RH + SO_2 Bronze – Uric Acid: EDS image of the circular chain element (Spot 3) 67
Figure 80: RH Bronze – Uric acid + sodium nitrate (C2): The EDS image of Spot 2. 68

Figure 81: RH + SO_2 Bronze – Uric acid + sodium nitrate (C2): EDS image of Spot 1 showing the high concentration of lead 68
Figure 82: RH Bronze – Uric acid + potassium dihydrogen phosphate (C3): EDS image of Spot 3 showing a high concentration of carbon, nitrogen, and oxygen 69
Figure 83: RH + SO_2 Bronze – Uric acid + potassium dihydrogen phosphate (C3): EDS image of Spot 1..... 69
Figure 84: RH Bronze – Used droppings (C4): The EDS image of Spot 2, showing the presence of zinc. 70
Figure 85: RH + SO_2 Bronze – Used droppings (C4): EDS image of Spot 3..... 70
Figure 86: RH Bronze – Uric acid + potassium chloride (C5): EDS image of Spot 3 70
Figure 87: RH Bronze – Uric acid + potassium sulphate (C6): EDS image of Spot 3. 71
Figure 88: A) SEM image of the spores found on the bronze sample; B) Research SEM image of penicillium expansum (He, Liu, Mustapha, & Lin, 2011); C) Research SEM image of penicillium cyclopium (Zhang, Sun, Chen, Zeng, & Wang, 2017); D) Microscope image of the mould spores found on the used droppings (C4); D) Research microscope image of penicillium (Conidia, n.d.) 71

LIST OF TABLES

Table 1: ISO 9223 Corrosivity categories for copper based on corrosion rates (Tidblad et al., 2009) ... 7
Table 2: The stability of copper corrosion products in different pH levels ... 8
Table 3: Predicted corrosion loss equations (Kreislova & Geiplova, 2016) ... 10
Table 4: Analytical concentration results of lixiviate (mg/l) (Gómez-Heras et al., 2004) ... 11
Table 5: Cations and anions present in bird droppings (% wt) (Drdácký & Slížková, 2005) ... 11
Table 6: Average non-metal content of bird droppings (wt %) (Lavenburg et al., 2011) ... 13
Table 7: Average metal content of bird droppings (wt %) (Lavenburg et al., 2011) ... 13
Table 8: The composition of the bronze (Kreislova & Geiplova, 2016) ... 22
Table 9: The contaminants applied to the metal products ... 22
Table 10: The chemical properties of the used contaminants (Chemical Book, n.d.; Science Lab, n.d.) ... 23
Table 11: Experimental conditions for the IEC analysis ... 26
Table 12: The experimental conditions for the XRD testing (Viani, 2017) ... 27
Table 13: The IEC results for the bird droppings used in the experiment and the real bird droppings collected (n.d.= not discovered) ... 34
Table 14: Summary of the bird dropping composition phases ... 36
Table 15: Visual transition of the copper under contamination ... 38
Table 16: Visual transition of the roof under contamination. Sometimes a dark green/blue marker was utilized to mark out where the drop was ... 42
Table 17: Visual transition of the bronze under contamination ... 45
Table 18: SEM images for the copper samples ... 53
Table 19: SEM images for the roof samples ... 60
Table 20: SEM images of the bronze samples ... 65

1. INTRODUCTION

1.1 Motivation and scope

When one visits a historical monument, they will often find another community enjoying the structure: birds. Birds, especially pigeons, can be a nuisance to urban areas. According to the theory of ideal free distribution, the suitability of a bird habitat is affected by factors including potential predators, food density, and cover (Fretwell & Lucas, 1968). These factors can often be found around monuments where food is abundant from tourists and shelter can be found within the structures themselves. Pigeon excrements can also be found on the surfaces of which they perch, causing aesthetic unsightliness as well as posing health risks to people. Aside from using nets, bird spikes, or gel to prevent birds from perching on surfaces, some cities such as London have incorporated laws to prevent people from attracting birds by disallowing feeding (BBC News, 2003). The cost of cleaning bird droppings contributes to a large amount of a municipality's expenditures. For example, London's Trafalgar Square costs an estimated £75,000 a year to clean (BBC News, 1999).

Figure 1: Abundance of birds flying in Trafalgar Square, London (Finamore, 2016)

Apart from aesthetic, economic, and health issues posed by bird droppings, excrements also aid in the deterioration of materials. Due to the importance of heritage monuments, there has been an increasing amount of research regarding the understanding of materials and appropriate conservation methods.

It is known that the salts and uric acid in pigeon excrements affect materials differently based on its susceptibility to the chemical compounds. Cities, such as Prague, contain numerous amounts of copper roofs and bronze statues. therefore proper conservation efforts are required. The atmospheric

effects on the deterioration of metal materials have been studied but there is a gap in research regarding the specific effects of bird droppings.

Figure 2: Left: Bronze statue from the Neptunbrunnen in Berlin, showing possible signs of bird dropping decay. Middle: Pigeons perching on the Turia Fountain in Valencia, Spain. Right: Damage from birds on the bronze Vítězslav Novák statue on Petřín Hill, Prague. (Photos by: Kristen Balogh)

The layout of the report is as follows. The first section outlines the objectives of the research and experiments.

The second section describes the main findings from an extensive literature review, including state-of-the-art. It mainly describes the properties of the materials investigated (copper, bronze, pigeon excrements). Also discussed are the current conservation methods related to pigeon droppings on cultural heritage structures.

The third section describes the methodology for the assessment. Samples of copper and bronze elements, as well as samples from a patina-clad copper roof in Prague were exposed to pigeon droppings and salt contaminants to determine individual effects of excrement compositions. As these degradation processes are normally slow acting, accelerated aging in humidity chambers are conducted. Analyses to determine the pigeon excrement components and metal surface corrosion products are determined using ion exchange chromatography (IEC) and X-ray diffraction (XRD, pH testing, digital microscopy, colourimetry, scanning electron microscopy (SEM) and energy dispersive spectroscopy (EDS) SEM/EDS, and inductively coupled plasma optical emission spectrometry (ICP-OES).

The fourth section includes the results and the corresponding analyses. Recommendations for further testing are given following the results from each section.

The fifth and final section presents the final conclusions.

1.2 Objectives

The thesis is aimed at gaining a better understanding of the corrosive products on copper and bronze surfaces exposed to pigeon droppings using accelerated ageing. Its main objectives are the following:

- To understand the material characteristics and deterioration processes of copper and bronze. This includes general corrosion processes and their products.
- To identify the components of bird droppings from previous research studies.
- To indicate the current bird deterrent systems used on cultural heritage monuments.
- To assess previous studies on the effects of bird droppings on metals. This includes reviewing specific experimental procedures and results.
- To determine the composition of collected samples of bird droppings.
- To analyze the effects of bird droppings on the metals surfaces using accelerated ageing. Four main factors are to be studied: 1) metal type, 2) specific dropping chemical components, 3) other environmental conditions, and 4) exposure duration.
- Comparison and assessment of various analytical methods for determination of morphology and chemical composition of affected metal surfaces.
- To provide recommendations for further research

2. LITERATURE REVIEW

The following section describes the composition, chemical and physical characteristics, as well as protective measures for copper, bronze, and pigeon excrements using state-of-the-art knowledge.

2.1 Copper and Bronze Characteristics

Copper is a useful material for construction and architectural elements such as cladding and roofing (Knotkova & Kreislová, 2007). Its properties are heavily dependant on its production. Metallurgical refined copper contains approximately 99.7% Cu and other precious metals are not removed, meaning it can be used directly for rolling (Knotkova & Kreislová, 2007). Areas of corrosion that are exposed to the atmosphere find a change in their mechanical properties such as ductility and strength. After approximately twenty years, the tensile strength decreases by less than 5% and the length changes by 10% (Knotkova & Kreislová, 2007). Corrosion can also result in tarnishing, the formation of patinas or significant deterioration of the surface (Stuart, 2007). The products that result from corrosion depend on the potential reactants of the metal and the environment, and crystals are usually formed on the surface (Stuart, 2007). Common corrosion products of copper are copper oxides, carbonates, and sulphates, but these have the potential of forming a protective layer. These layer products may break down with the presence of chlorides from seawater or ground water (Stuart, 2007).

Copper is often used as an alloy, and when it is mixed with tin, bronze is formed. Zinc and tin increase the breaking strength and hardness of an alloy, whereas lead increases the resistance to corrosion and improves the ease of processing and castability (Knotkova & Kreislová, 2007). Historical types of bronze contain approximately 10-14% tin and they have very good resistance to corrosion. The atmospheric corrosion mass loss of bronze is usually 2/3 that of copper (Kreislova & Geiplova, 2016).

It is important to understand the corrosion process of copper and bronze to better comprehend the effects of bird droppings on the materials. In almost all cases, water is required for corrosion to occur. The water can be ‘absorbed’ onto the metal as a thin liquid film (Tidblad, Kucera, & Sherwood, 2009). This film is the connection to the atmosphere where the attack of corrosive species is increased by the products dissolving in or modifying the properties of the water layer (see Figure 3).

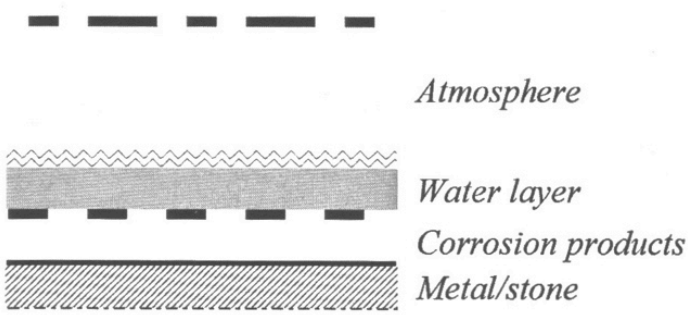

Figure 3: The corrosive layers on an object (Tidblad et al., 2009)

Temperature and relative humidity determine the thickness of the moisture layer and its ability to dissolve gases (Tidblad et al., 2009). Daily fluctuations of humidity and temperature affect the corrosion rate, but it is the long-term effects and annual average values that are of concern. When the water layer is thicker, and thus the relative humidity is higher, the monolayers are more loosely bound, allowing it to act as an ionic medium for dissolving pollutants (Tidblad et al., 2009). The effect of temperature is more complicated, as there needs to be a balance between there being low temperatures to reduce evaporation (increased time of wetness), but not too low that freezing occurs. Research has proven that the optimal measured conditions are around 10°C (see Figure 4). When the annual temperatures are between this and 0°C, optimal conditions occur with a relative humidity of around 80% (Tidblad et al., 2009).

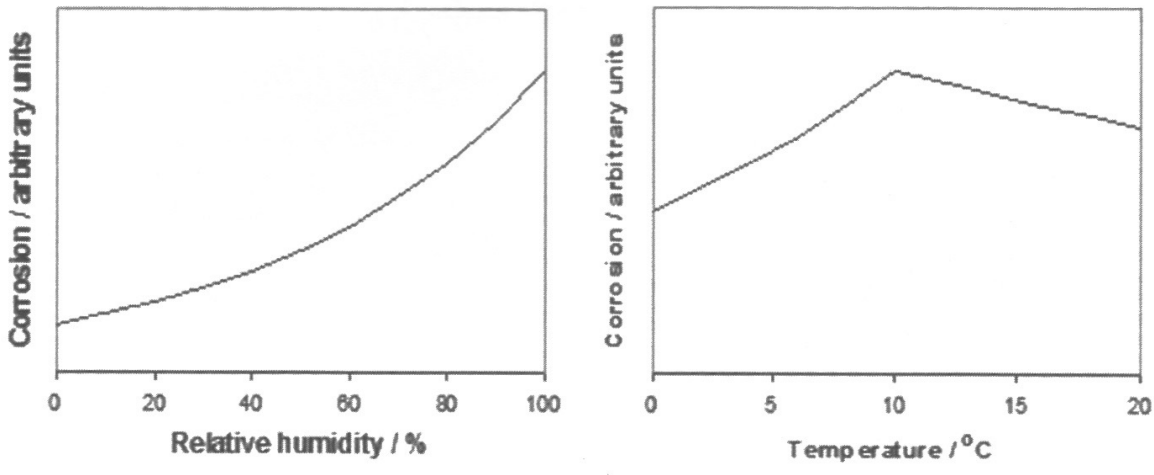

Figure 4: Illustration of the effect of relative humidity (left) and temperature (right) for zinc as annual averages in SO_2 polluted atmospheres (Tidblad et al., 2009)

If the surface area of water becomes very large, such as during rainfall events, the water may dissolve aggressive substances such as chlorides that may cause corrosion. Therefore, rain can decrease the attack (Tidblad et al., 2009). On the contrary, it can also encourage corrosion as it may

dissolve the protective layers depending on its pH. Therefore, environmental factors such as an unsheltered or sheltered location, urban area or rural area, etc. play an important role in corrosion. A sheltered location may decrease the amount of running water over the area, but there is a chance that there will be more stagnant water. Urban areas tend to have more pollutants such as sulphur dioxide (SO_2), which can cause greater corrosion. As the level of SO_2 pollution has generally decreased in the Czech Republic, the rate of corrosion has also been measured to decrease. Therefore the correlation between air pollution and corrosion is strong.

To aid in describing the level of corrosion, ISO 9223 has created five categories for main construction metals. Table 1 illustrates these levels for copper.

Table 1: ISO 9223 Corrosivity categories for copper based on corrosion rates (Tidblad et al., 2009)

Corrosivity	Category	Copper (μm yr^{-1})
Very low	C1	≤ 0.1
Low	C2	0.1 – 0.6
Medium	C3	0.6 – 1.3
High	C4	1.3 – 2,8
Very High	C5	2.8 – 5.6

These values however will be subject to change, as the corrosion rate of metals and alloys exposed to the natural outdoor atmosphere are not necessarily constant with exposure time. Usually, it decreases because the accumulation of corrosion products on the exposed surface acts as a protective layer (Tidblad et al., 2009). Also, the rates are dependent on the type of environment they are exposed to.

As previously mentioned, the presence of SO_2 increases corrosion, especially with copper. When reacted with an oxidizer such as NO_2 or O_3, and when dissolved in water, the sulphite is converted to a sulphate (Clarelli, De Filippo, & Natalini, 2014; Tidblad et al., 2009).

$$SO_2 + H_2O \rightarrow H^+ + HSO_3^- + O_3 \rightarrow 2H^+ + SO_4^{2-} + O_2 \quad (1)$$

The acidic product accelerates corrosion, though in ambient atmospheres the oxidizing agents usually are the dominating corrosive agent as the SO_2 levels are very small. However, synergy – the interaction of various agents or forces – can cause a greater effect than if the individual agents are acting independently (Tidblad et al., 2009). Therefore, consideration of multiple pollutant forces is important to determine the rate of corrosion.

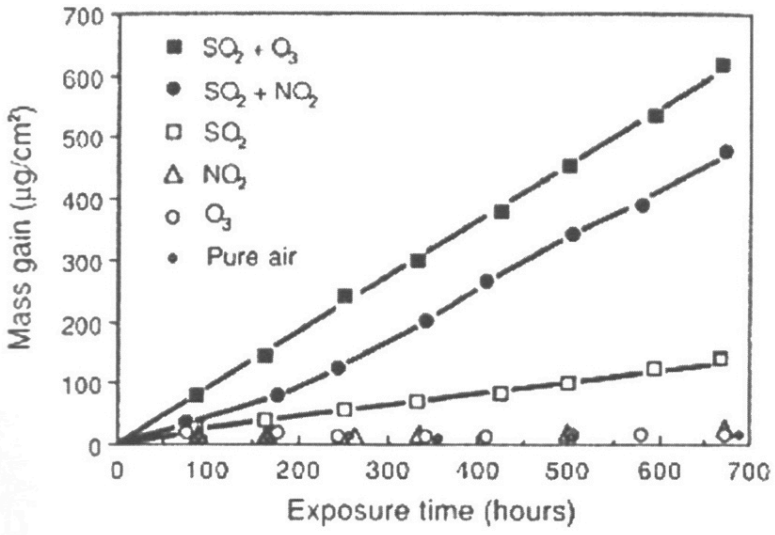

Figure 5: Mass gain of zinc samples exposed in air at 95% RH showing the effect of synergy (Tidblad et al., 2009).

The corrosion of copper can be perceived as aesthetically pleasing as the patina formed becomes a light green colour over time (approximately 10 to 20 years in atmospheric conditions depending on the corrosivity of the atmosphere) (Knotkova & Kreislová, 2007). The development of a patina from the atmosphere includes a number of stages. The first is mostly of the electro-chemical nature, where layers of surface electrolytes are thin and dry out periodically. These reaction products deposit to form solid surface layers which then take part in the corrosion process.

The composition of patina is influenced by the pH of rain because the thermo-dynamical stability of minerals differ (Knotkova & Kreislová, 2007). Table 2 provides the common patina components and their stability in different pH levels.

Table 2: The stability of copper corrosion products in different pH levels (Knotkova & Kreislová, 2007)

Compound	Formula	pH level
Cuprite	Cu_2O	> 4
Brochantite	$Cu_4(SO_4)(OH)_6$	3.5 - 6.5
Antlerite	$Cu_3SO_4(OH)_4$	2.8 - 3.5
Atacamite	$Cu_2Cl(OH)_3$	3.8 - 4.3
Gerhardite	$Cu_2(NO_3)(OH)_3$	4.0 - 4.5
Malachite	$Cu_2(CO_2)(OH)_2$	> 3.3

The main patina components are brochantite, antlerite, and cuprite. Initially, a layer of cuprite (Cu_2O) is formed after wetting (Eqn (2)). Cuprite forms the adhesive layer and is mainly black, brown, red, or orange. The copper sulphates turn into basic sulphates, and they form on the cuprite surface to form solid layers (Knotkova & Kreislová, 2007).

$$2Cu + \frac{1}{2}O_2 \rightarrow Cu_2O \quad (2)$$

Brochantite is formed by the reaction of cuprite, sulphur dioxide, water, and oxygen:

$$2Cu_2O + SO_2 + 3H_2O + \frac{3}{2}O_2 \rightarrow Cu_4(OH)_6SO_4 \quad (3)$$

Brochantite is mainly found in places of direct impact of rain, whereas antlerite is formed by condensed air humidity. These have protective properties and slow down the corrosion of the surfaces and create the blue and green patina. Atacamite and paratacamite ($Cu_2Cl(OH)_3$) are present in atmospheres with natural or technological salinity (Knotkova & Kreislová, 2007). When the patina has not reached a stabilized state, posnjakite ($CuSO_4 \bullet Cu(OH)_6 \bullet H_2O$) can be found. Impurities can also be found on the surfaces such as admixtures of gypsum, and patinas can contain formats, acetates, and oxalates in atmospheres containing anthropogenic and biological effects. These often form darker crusts, and contrast can be seen on elements with green 'stripes' occurring on structures formed by streams of water (Knotkova & Kreislová, 2007). An Australian study determined the characteristics of the different corrosion product colours. The outer layer of brochantite contributes to the green patina. This forms as individual crystals on the surface of the cuprite layer. Thin patinas composed primarily of cuprite are black (FitzGerald, Nairn, Skennerton, & Atrens, 2006). If the patina was thick and the [Fe]/[Cu] ratio was low, then the patina was green. If the [Fe]/[Cu] ratio was around 10%, then the patina is a rust brown in colour (FitzGerald et al., 2006). Figure 6 illustrates the reactions involved with the formation of brochantite.

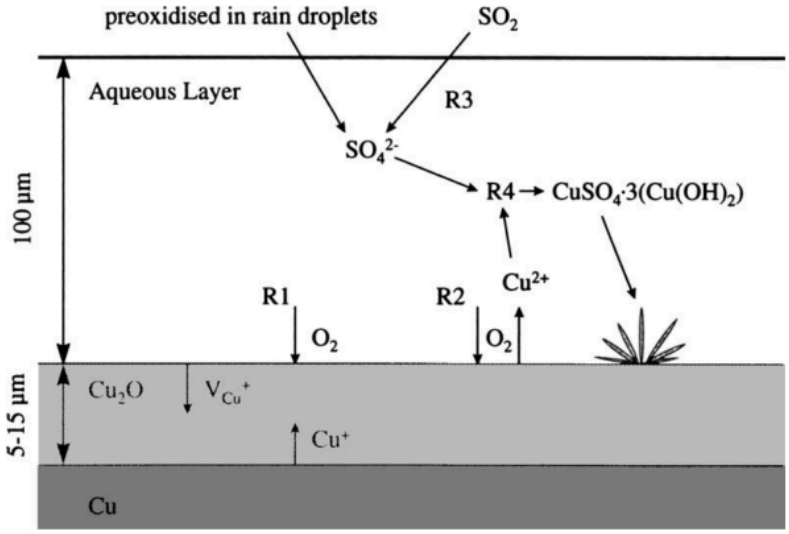

Figure 6: Illustration of the reactions involved in brochantite formation during patination (FitzGerald et al., 2006)

The pH of rainwater can positively and negatively affect the growth of brochantite. Low pH promotes the oxidative dissolution of the cuprite and the precipitation of brochantite. If the environment is humid, has frequent short rain showers, and stagnant water is present, this allows consolidation to occur. Conversely, low pH dissolves both cuprite and the existing brochantite where there are long

rain showers with large amounts of water runoff. Therefore, the amount of copper lost in runoff increases with increasing acidity (FitzGerald et al., 2006).

The corrosion results of bronze are slightly different than that of copper. A study conducted by the National Building and Civil Engineering Institute researched the corrosion stability of different bronzes in simulated urban rain. It was determined that silicon bronze had a higher corrosion resistivity than unleaded bronze and leaded bronze (Fabjan, Kosec, Kuhar, & Legat, 2011). Also, polarization resistances increased for silicon bronze and unleaded bronze, whereas it decreased for leaded bronze. Lastly, the corrosion layer on silicon bronze is more compact and thinner due to its homogeneous microstructure (Fabjan et al., 2011).

Dose-response functions have been derived to estimate the predicted corrosion loss of metals. These research projects include the ISOCORRAG exposure program (53 test sites in 13 countries on four continents), MICAT exposure program (72 test sites in 14 Ibero-American countries), Multi-Assess project (28 test sites in 16 European countries), and the UN ECE ICP exposure program (39 test sites in 12 countries in Europe, USA, and Canada) (Kreislova & Geiplova, 2016). From the collected data, these functions have been created and are summarized below.

Table 3: Predicted corrosion loss equations (Kreislova & Geiplova, 2016)

ISOCORRAG exposure program	Copper	$r_{corr} = 0.0053[SO_2]^{0.26}\exp(0.059RH + f(T)_{Cu}) + 0.0125[Cl^-]^{0.27}\exp(0.036RH + 0.049T)$ $f(T)_{Cu} = 0.126(T-10)\ when\ T \le 10°C, otherwise\ 0.080(T-10)$	**(4)**
	Bronze	$r_{corr} = \frac{2}{3} r_{corr}(Cu)$	**(5)**
Multi-Assess project (copper and bronze: 6-8 %wt Sn, 3-5 %wt Zn, 5-7 %wt Pb)	Copper	$ML_1 = 3.12 + \{1.09 + 0.00201[SO_2]^{0.4}[O_3]RHe^{f(T)} + 0.0878Rain[H^+]\}t$ $f(T)_{Cu} = 0.083(T-10)\ when\ T < 10°C, otherwise\ 0.032(T-10)$	**(6)**
	Bronze	$ML_1 = 1.33 + \{0.00876[SO_2]RHe^{f(T)} + 0.0409Rain[H^+] + 0.0380PM_{10}\}t$ $f(T)_{Br} = 0.060(T-11) when\ T < 11°C, otherwise\ 0.067(T-11)$	**(7)**
UN ECE ICP exposure program (copper and bronze: 6-8 %wt Sn, 3-5 %wt Zn, 5-7 %wt Pb)	Copper	$ML_2 = 0.0027[SO_2]^{0.32}[O_3]^{0.79}RHe^{f(T)}t^{0.78} + 0.050Rain[H^+]t^{0.89}$ $f(T)_{Cu} = 0.083(T-10)\ when\ T \le 10°C, otherwise\ 0.032(T-10)$	**(8)**
	Bronze	$ML_2 = 0.026[SO_2]^{0.44}RHe^{f(T)}t^{0.86} + (0.029Rain[H^+] + 0.00043Rain[Cl^-])t^{0.7}$ $f(T)_{Br} = 0.060(T-11)\ when\ T \le 11°C, otherwise\ 0.067(T-11)$	**(9)**

These equations are useful when determining the corrosion loss of copper and bronze. When the products of copper corrosion are to be removed, there are three cleaning techniques commonly used: 1) cleaning by water under pressure, 2) mechanical or abrasive cleaning (blasting), and 3) chemical cleaning – 'draw-off' and pickling (Knotkova & Kreislová, 2007). Cleaning by water under pressure is often combined with abrasive techniques or chemical cleaning, and removes particles that fall off or are not fixed to the surface. Soluble parts of corrosion crusts are removed or redistributed, and the effectiveness of this method is based on the condition and configuration of a surface and the experience of the staff (Knotkova & Kreislová, 2007). Mechanical (abrasive) cleaning is done by various abrasive and polishing agents, pastes, metal wool, and brushes. This method can be difficult and one runs the risk of exposing layers that will corrode unevenly or cause further damage to the

structure. Lastly, chemical cleaning includes drawing-off and pickling, where pickling removes all layers of corrosion products down to the pure metal (Knotkova & Kreislová, 2007). ISO 8407 states that the pickling period is dependent on the pickling solution, metals, or degrees of corrosion. For historical objects, one should apply the pickling solution repeatedly, wash the objects after each application, and remove the loosened corrosion products and dirt mechanically (Knotkova & Kreislová, 2007).

2.2 Bird Dropping Characteristics

When one sees bird droppings, they will often notice a white and dark section. The white section is uric acid, which is the avian form of urine, and the dark area is the defecation (Jacob, 2015). A bird's digestive tract is different than that of a mammal as they contain a cloaca. This combines excretion and defecation into one dropping (Jacob, 2015). Another component of the bird digestive system that is important to mention is the requirement of grit. The gizzard is part of the digestive tract that acts as the 'teeth' that is comprised of two sets of strong muscles that grind food (Jacob, 2015). Grit, or small stones, aid in the grinding of harder elements that cannot digest by enzymes alone. Therefore, one may notice traces of small elements from stone in their excrements. Few in the field of conservation have investigated the effect of bird droppings on materials. A study conducted in Spain examined the contribution of soluble salts from pigeon droppings to the decay of stones (Gómez-Heras, Benavente, Álvarez De Buergo, & Fort, 2004). It was determined that the droppings contained 4% soluble salts, including halite, sylvite, potassium calcium sulphate, aphthitalite, apatite group minerals, weddellite, and gypsum (Gómez-Heras et al., 2004). To determine this, the concentration of different elements was sought and is summarized in Table 4.

Table 4: Analytical concentration results of lixiviate (mg/l) (Gómez-Heras et al., 2004)

Na^+	K^+	Ca^{2+}	Mg^{2+}	Cl^-	HCO_3^-	SO_4^{-2}	PO_4^{-3}	NO_3^-
935.0	831.8	507.3	139.6	2440.0	1563.3	786.4	263.6	10.0

Ion exchange chromatography was conducted at the Institute of Theoretical and Applied Mechanics (ITAM) in Prague, Czech Republic, to determine the components of bird droppings. The concentration anions and cations are summarized below.

Table 5: Cations and anions present in bird droppings (% wt) (Drdácký & Slížková, 2005)

K^+	NH_4^+	Mg^{2+}	Na^+	Ca^{2+}	PO_4^{3-}	SO_4^{2-}	Cl^-	NO_3^-	NO_2^-	F^-
2.2	0.8	0.2	0.2	0.1	0.14	0.1	0.04	0.01	0.01	0.00

It was also observed that, when interacted with porous limestone, deterioration occurred due to acid attack, which included surface etching of rock forming minerals (Gómez-Heras et al., 2004). Bassi and Chiatante studied the role of pigeon excrements in stone bioteterioration. The four species

of fungi that were grown (mucor hiemalis, fusarium oxysporum, aspergillus repens and penicillium cyclopium) lowered the pH of the system gradually up to 18 days.

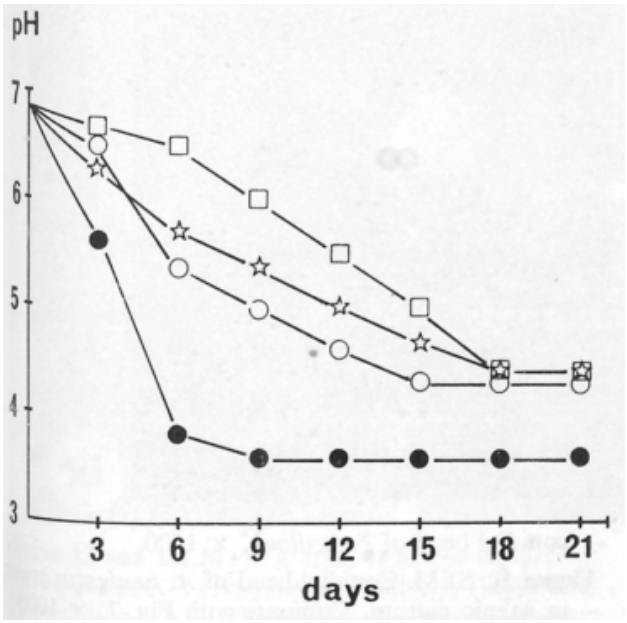

Figure 7: Lowering of the pH induced by four fungal species isolated from pigeon excrements: Aspergillus repens □; Fusarium oxysporum ★; Mucor hiemalis O; Penicillium cyclopium • (Bassi & Chiatante, 1976).

They determined the following conclusions: "1) Pigeon excrement constitutes a highly favourable substrate for microbial growth. A suitable relative humidity of the environment is all that is needed to promote the development of the fungal spores that are either endemic or trapped in the excrement. 2) Some of the fungal species that grow in pigeon excrement secrete acidic products which can contribute to the chemical erosion of the marble surface. 3) Fungal growth actually brings about the erosion of the marble surface in a relatively short time (20 days)" (Bassi & Chiatante, 1976). Though these are the effects on stone, there is still the possibility of microbiological growth on metals.

The composition of bird droppings is also dependent on whether the bird lives in an urban or rural environment. In a study from the University of Delaware, this was investigated to determine the effects of birds and salts on highway structures. The excrement pH values were neutral and the moisture content was >99%. They also were high in volatile organic content, >99% (Lavenburg, Hall, Lewis, Wolfe, & Strange, 2011). Chemically, carbon and oxygen were found to be the major elements in all of the bird dropping samples. Urban environment pigeons had less chemical elements compared to farm grown ones. Also, farm-grown pigeons have Si and F in their feces (Lavenburg et al., 2011). The metal content of the feces is minute compared to the organic and volatile fraction. Potassium and calcium were found to be the major metallic elements (Lavenburg et al., 2011).

Table 6: Average non-metal content of bird droppings (wt %) (Lavenburg et al., 2011)

	C	N	O	P	Cl	S	Si	F
Urban pigeons	48.75	3.73	38.02	1.57	0.47	0.14	0	0
Farm-grown pigeons	36.93	3.97	30.36	1.65	2.58	3.29	2.83	1.28

Table 7: Average metal content of bird droppings (wt %) (Lavenburg et al., 2011)

	Mg	K	Ca	Na	Al	Ti	Fe	Ag
Urban pigeons	0.86	4.80	1.10	0	0	0	0	0
Farm-grown pigeons	0.84	3.00	5.32	1.20	0.42	0.08	0.03	3.70

Urban birds appeared to have both fungi and bacteria, whereas farm-grown birds showed more fungi than bacteria. The fungal species identified was Geotrichum and the bacteria included Staphylococcus-lentus, Corynebacterium-glutamicum, Bacillus-pumilus, Staphylococcus-xylosus, Citrobacteramalonaticu, and Stenotrophomonas-maltophilia (Lavenburg et al., 2011).

The study of bird excrements on metals has also been researched. Preliminary results from tests conducted in Romania concluded that droppings have a negative influence on metals and can cause significant damage (Vasiliu & Buruiana, 2010). One of the major contributing factors to damage in bird droppings is the uric acid. Uric acid ($C_5H_4N_4O_3$) is a heterocyclic compound of carbon, nitrogen, oxygen, and hydrogen (Vasiliu & Buruiana, 2010). Oxidation of the uric acid at alkaline pH occurs with copper and the initial product is dehydro uric acid (Figure 9).

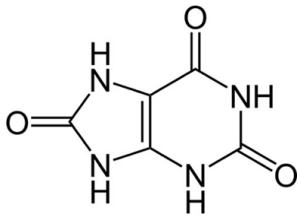

Figure 8: The structure of uric acid

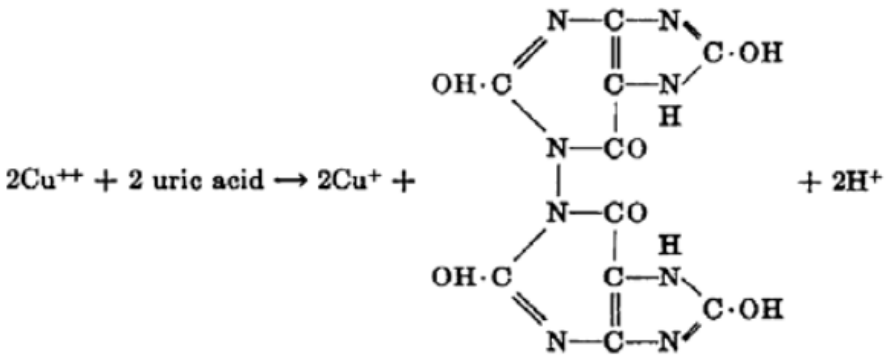

Figure 9: The oxidation process of uric acid with copper (Vasiliu & Buruiana, 2010)

The hydrogen that is extracted from the process above is most likely oxidized as H_2O_2 (Vasiliu & Buruiana, 2010).

$$2Cu^{+} + 2H^{+} + O_2 \rightarrow 2Cu^{2+} + H_2O_2 \quad (10)$$

When the pH increases from 8.2, the oxidation rate also rapidly increases until it reaches a pH of 12.4. The activation rate of copper – uric acid – O_2 system is 70935 J/mol, sustaining the formation of a relatively stable addition compound (Vasiliu & Buruiana, 2010).

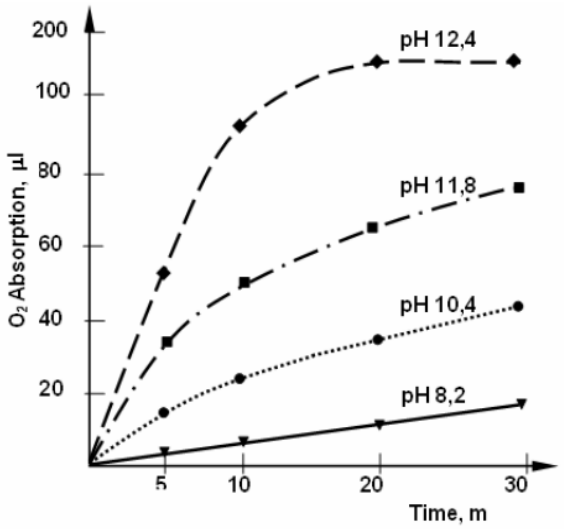

Figure 10: Increase of absorption rate with increasing pH (Vasiliu & Buruiana, 2010)

The reason why a high alkalinity versus a low alkalinity affects the oxidation rate more in this experiment is because this was a full immersion test. Therefore, the lack of atmospheric conditions such as O_2 causes this to occur. This study confirmed that the superficial layers of copper are subject to corrosion due to the uric acid and the metal surfaces are altered. The natural protection layer on the surface of the bronze and copper statues also interacted with the uric acid in time, even if they offered some protection to the bird droppings (Vasiliu & Buruiana, 2010).

An experiment conducted in Balogna, Italy and Norwich, U.K. studied the effect of uric acid on outdoor copper and bronze. Biological degradation happened to uric acid before and after excretion (Bernardi, Bowden, Brimblecombe, Kenneally, & Morselli, 2009). Before excretion, the intestinal microbes transform uric acid into ammonia, short chain fatty acids, and carbon dioxide. Afterwards, external decomposition provides mainly ammonia, which is then nitrified. If this degradation is incomplete, urea and other intermediates are found (Bernardi et al., 2009). Therefore, uric acid and the compounds derived from biodegradation can cause damage to materials (Bernardi et al., 2009). They confirmed that uric acid chemically affects copper and bronzes in that the surface of the metal is modified and copper urates are formed. It also confirms that the patina still reacts with the acid, even though some protection is formed. Droppings leave tarnish marks on copper, water enhances the

corrosion by bird droppings, and it is suggested that cleaning may be appropriate should the conditions remain wet (Bernardi et al., 2009).

The composition of patina layers from various objects in the Czech Republic were studied. Apart from the main products such as cuprite, brochantite, antlerite, atacamite, gerhardite, and malachite, moolooite ($C_2CuO_4 \bullet nH_2O$) can also be found. This is attributed to bird excrements found on metals and was identified at locations sheltered from direct impact of precipitation (Knotkova & Kreislová, 2007). As previously mentioned, the synergistic effects of pollution and particulate matter, such as bird droppings, may cause a more accelerated corrosion rate.

A study of the bronze sculptures of František Palacký in Prague took place to determine the corrosion status. Diffractograms of the patina layer in some areas showed the presence of copper oxalate hydrate ($C_2CuO_4 \bullet H_2O$) – or moolooite on the statue. This was attributed to the dense bird dropping presence on the structure (Kreislová, Knotková, & Koukalová, 2010).

Figure 11: The contaminated areas of the statue (Kreislová et al., 2010)

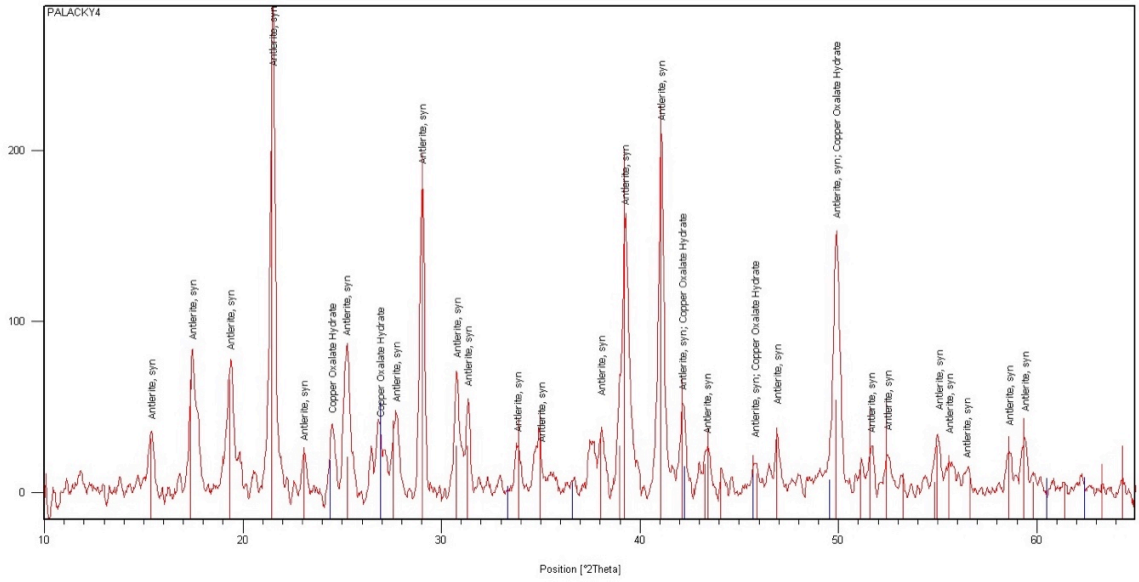

Figure 12: The presence of moolooite can be seen in the diffractogram (Kreislová et al., 2010)

2.3 Current Bird Deterrent Systems

There are different bird deterrent methods available on the market. Many of these are targeted to stone monuments rather than metal, but the principles remain the same. A study conducted by Gra Research Center for Public Buildings analyzed these different methods. The proper choice of product is dependent on the bird species (size, behaviour, and habits), location of building, climatic conditions, time of year, and time of day (Gra Research - Center for Public Buildings, 2016).

The anti-roosting system, “pin and wire”, or “trip wire” is often used to deter pigeons and include a series of parallel wires that are supported by narrow pins held under tension by small springs. Their spacing and differing heights make it difficult for pigeons to gain a foothold on the ledges and makes roosting difficult. These cause minimal damage to buildings, can last up to 10 years, and are environmentally safe. However, they are limited to ledges and are not effective for all species of birds (Gra Research - Center for Public Buildings, 2016).

Figure 13: Example of a bird trip wire system installed on a building ledge (Absolute Pest Control Ltd., n.d.)

Plastic netting systems, or “chicken wire” is used to prevent birds from nesting in recessed portions of a building, in light wells, or under eaves. Polyethylene and Polypropaline are recommended as they can hold a lot of tension, can be different colours, and if hung correctly, can be inconspicuous. These are suitable for large areas, are environmentally safe, can last up to 15 years, and is effective against most bird species. This system is ineffective if there are large gaps and holes where birds can fly through, and is very dependent on accurate installation. Also, it may obscure some architectural elements (Gra Research - Center for Public Buildings, 2016).

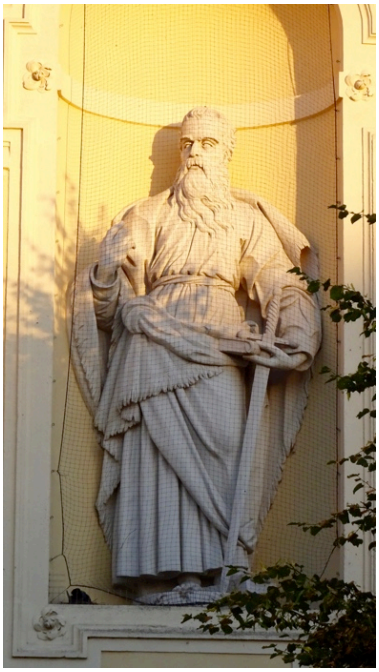

Figure 14: Netting around a statue in the Zámek Lednice, Moravia (Photo: Kristen Balogh)

Rows of metal spires or “porcupine wire” is a physical barrier consisting of rows of needles or spikes pointing vertically upwards that make it difficult for birds to land. They are easy to install, have a long life-span, and are environmentally safe. However, they tend to collect debris between the spikes (bird droppings, feathers, nesting material) and therefore require persistent cleaning. They are ineffective for smaller birds that can nest in-between the spikes (Gra Research - Center for Public Buildings, 2016).

Figure 15: Example of bird spikes on monuments in the Luxembourg Gardens, Paris [Photo by Zuzana Slížkova]

Ultrasonics is for hearing ranges above 20K Hz and produce high frequency sounds to deter birds from roosting. There are no known advantages to this system as the hearing range of birds is roughly the same as humans (Gra Research - Center for Public Buildings, 2016).

Distress signal call systems mimic sounds that birds make when there is a sense of danger. Its effectiveness depends on the type of technology, as birds may be able differentiate between a real distress call and a tape recording. They are best suited for flocking birds and the digitized distress calls are played repeatedly (sometimes as long as two weeks). This system does not obscure the building aesthetics and does not impact or damage the building. It causes noise pollution because it is generally loud, and has the possibility of attracting birds rather than deterring them. Often, birds return once the signal is turned off (Gra Research - Center for Public Buildings, 2016).

Electric wires produce an unpleasant shock when touched or landed on. There are no known advantages, as smaller birds tend to perch on these wires. To add, they are difficult to maintain and install, as complicated connections are required to not damage the structure. They are also difficult to remove and can be unsightly (Gra Research - Center for Public Buildings, 2016).

Gel coating repellents are based on gels of polybutylene. They are intended to irritate bird's feet. There are no known overall advantages as the gels tend to absorb airborne pollutants which can cause them to harden and become ineffective. They only last for short terms (18 months to 2 years) and removal is difficult. The gel also has the potential to damage the surface of the structure (Gra Research - Center for Public Buildings, 2016).

Figure 16: Example of bird gel application (RS Innovative Solutions, n.d.)

Poisoned food includes a variety of chemicals (avitrol or 4-aminopyridine, ornitrol, starlicide, strychnine, and fenthion) that can either cause birds to distress and scare other birds or can simply be highly toxic, These do not show many advantages as they are potentially dangerous to those who

handle the chemicals, are environmentally dangerous, may affect the building materials, and can be inhumane (Gra Research - Center for Public Buildings, 2016).

Trapping is a temporary method that allows a humane means of relocating birds. This requires a substantial amount of human effort and only offers short-term effectiveness. Lastly, there are no advantages to shooting, as there are many limitations and it is inhumane, unethical, and dangerous (Gra Research - Center for Public Buildings, 2016).

One particular study analyzed the statue of Yamato Takeru no Mikoto in Japan as researchers noticed that birds would rarely perch on the monument. A small sample of the bronze showed that the bronze was laced with arsenic. An experiment made from replicating the bronze found that birds would only perch for a short amount of time, only to then avoid the statue all together (Abrahams, 2012). Therefore, another possible approach to bird control could be to modify the composition of some materials to deter birds.

3. METHODOLOGY

3.1 Testing Parameters and Materials Used

The following experiments were conducted in the SVÚOM and ÚTAM AV ČR laboratories in Prague and CET Telč, Czech Republic. There were four main parameters to test the effect of bird droppings: 1) metal type, 2) dropping chemical components, 3) other environmental factors, and 4) exposure duration. The experiment process was inspired by the research conducted by Bernardi, Bowden, Brimblecombe, Kenneally, and Morselli, who studied the effect of uric acid on outdoor copper and bronze (Bernardi et al., 2009). The experiment was modified to test updated knowledge about material compositions mentioned in other studies.

Three metal materials were tested: 1) copper sheet, 2) copper sheet with patina from Prague location, and 3) bronze. The copper samples are normal cold-rolled laboratory grade ~100% Cu. The sheets were prepared by rinsing them with distilled water, scrubbing them with *Dr. House Scouring Powder*, rinsing with distilled water, drying, brushing with a copper wire brush to remove existing patina, and rinsing once more with distilled water and drying. These sheets were already cut into the dimensions 100mm x 70mm x 1mm. The copper with patina was obtained from a previous study on the Queen Anna's Summer Palace roof in Prague, Czech Republic. The thickness of the copper ranged in thickness from 0.35 mm to 0.50mm through its exposure of over 325 years. The thickness of the patina layer was in a range of 7 – 142 μm with an average value of 44 μm. The dominant compound of the patina was brochantite with other compounds such as cuprite and antlerite (Kreislova & Geiplova, 2016). The sheets were cut with industrial metal sheet cutter with the approximate dimensions of 100mm x 70mm to match those of the previously mentioned copper samples.

Figure 17: Copper with a natural patina was obtained from the roof of Queen Anna's Summer Palace in Prague (Kreislova & Geiplova, 2016; Kreislová & Koukalová, 2012)

Lastly, 75mm x 50mm x 5mm samples of bronze were also tested. These were also obtained from a previous experiment by SVÚOM that was attempting to reduce the amount of lead in the

bronze to closely simulate historic copper (Kreislova & Geiplova, 2016). These samples had the following composition.

Table 8: The composition of the bronze (Kreislova & Geiplova, 2016)

Bronze Alloy	Cu	Sn	Pb	Zn	Si	Ni	Fe
Composition (%)	87.0	4.40	3.30	2.90	0.70	1.20	0.16

This type of bronze was chosen for this testing as it had only 2% lead which is similar to historical bronze alloys. Each of the metal samples were numbered with a paint marker, weighed, and photographed. When not in use, the metals were placed in a desiccator to stay dry. The quantity of samples was chosen based on the exposure duration, explained in detail below. These materials were chosen to determine the effects of bird droppings on copper versus bronze, as well as the effect of an established patina.

The dropping components tested included six different contaminants. The first three contaminants were the same as those chosen by the study conducted by Brimblecombe, whereas the fifth and sixth contaminants were chosen based off of major constituents found in previous experiments. Due to the limited time span, real bird droppings were not collected for this testing. The fourth contaminant comprised of pigeon droppings from Belgium that are used as a fish bait product. These solid contaminants were first weighed on an analytical scale (±0.0001g), combined, then mixed with distilled water to form a consistency of a paste. The contaminants of various chemical compositions were then applied as 'drops' to the metals in rows by a glass stirring stick. The approximate dry mass of each of the drops (excluding the bird droppings) was 0.0021g.

Table 9: The contaminants applied to the metal products

Contaminant #	Components	Chemical Formula	Characteristics	Mass
1	Pure uric acid	$C_5H_4N_4O_3$	≥99% crystalline 2,6,8-Trihydroxypurine MW: 168.11 g/mol	1 gram
2	Uric acid and Sodium Nitrate	$C_5H_4N_4O_3$ + $NaNO_3$	Uric acid: See Sol'n 1 Sodium Nitrate: Content (dry matter) min. 99.8%, Mass loss after drying max. 1.0%, Insoluble compounds H_2O 0.004%, Cl: 0.002%, ClO_3, ClO_4: 0.003%, NH_4: 0.003%, SO_4: 0.005%, Heavy metals: 0.0003%, Ca: 0.005%, Fe: 0.0002%, Mg: 0,002%, PO_4: 0.0005%, NO_2: 0.0005%	2:1 ratio (1g $C_5H_4N_4O_3$: 0.5g $NaNO_3$)
3	Uric acid and potassium dihydrogen phosphate	$C_5H_4N_4O_3$ + KH_2PO_4		2:1 ratio (1g $C_5H_4N_4O_3$: 0.5g KH_2PO_4)
4	Bird droppings from package			
5	Uric acid and potassium chloride	$C_5H_4N_4O_3$ + KCl		2:1 ratio (1g $C_5H_4N_4O_3$: 0.5g KCl)

6	Uric acid and potassium sulphate	$C_5H_4N_4O_3$ + K_2SO_4	Uric Acid: See Sol'n 1 Potassium Sulphate: Insoluble compounds: H_2O max. 0.01%, Na: 0.15%, Salts: NH_4: 0.002%, NO_3: 0.002%, Cl: 0.001%, Ca: 0.01%, Heavy metals: (Pb): 0.001%, Fe: 0.0005%, As: 0.0002%, Mg: 0.004%	2:1 ratio (1g uric acid : 0.5g K_2SO_4).

The chemicals had the following general chemical properties.

Table 10: The chemical properties of the used contaminants (Chemical Book, n.d.; Science Lab, n.d.)

	Structure	Form	Melting point	Density	Stability	Solubility	Sensitive
Uric Acid	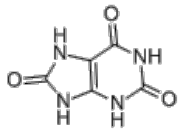	Crystalline	>300°C	1.9 g/cm^3	Stable. Incompatible with acids, bases, oxidising agents	Slightly soluble in water	
Sodium Nitrate	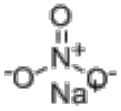	Granular solid	306°C	1.1 g/mL at 25°C	Stable. Strong oxidizer – may ignite flammable material. Incompatible with cyanides, combustible material, strong reducing agents, aluminum	H_2O: 1M at 20°C, clear, colourless	Hygroscopic
Potassium Dihydrogen Phosphate	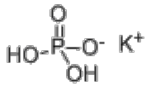	Powder	252.6°C	2.338 g/mL at 25°C	Stable	H_2O: 1.5M at 20°C, clear, colourless	Hygroscopic
Potassium Chloride		Random crystals	770°C	1.98 g/mL at 25°C	Stable. Incompatible with strong oxidizing agents, strong acids. Protect from moisture. Hygroscopic.	H_2O: soluble	Hygroscopic
Potassium Sulphate	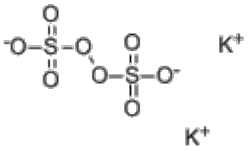	Solid	1067°C	2.47 g/mL	Stable. Strong oxidizer. Incompatible with strong reducing agents, organic materials, combustible materials	H_2O: 0.5M at 20°C, clear, colourless	

Figure 18: The copper, roof, and bronze samples with the first four contaminants applied

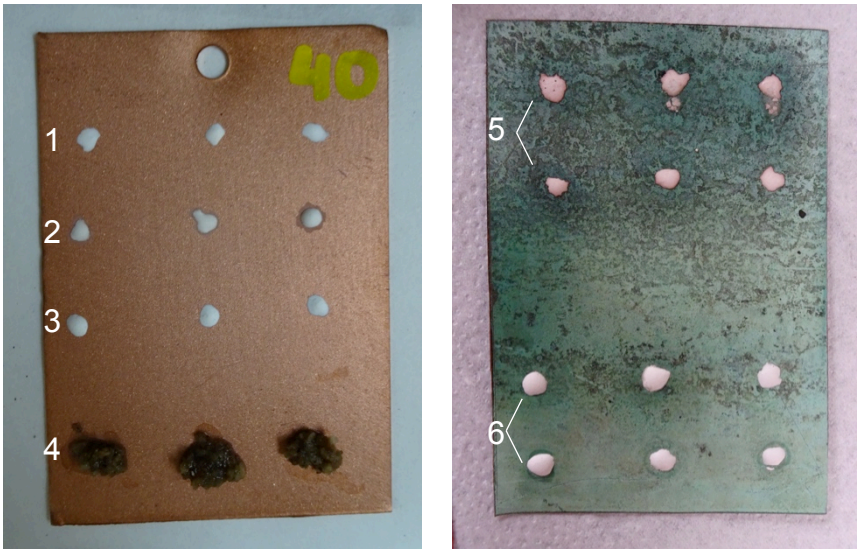

Figure 19: The distribution of contaminants 1-6 on the metal pieces

The samples were exposed to two different environments. Two climatic chambers were utilized, each with 100% RH to accelerate corrosion. These chambers contained a bed of water at the bottom. The general corrosion test in humidity was followed, except that the temperature was not modified and therefore reflected the temperature in the laboratory. Usually, these tests require the temperature to be around 35°C, though to reduce the chance of too much condensation, the temperature was not modified. The humidity and temperature were monitored and tracked throughout the experiment. The difference between the two chambers was that one was infused with SO_2 gas (5.3

$\mu g/m^3$) to mimic air pollution. Therefore, half of the samples were placed in each chamber. This component of the experiment was performed to determine the additional effect of atmospheric pollution on the corrosion of the materials. The placement of the metals also meant that the experiment was performed for an exposed environment rather than a sheltered one.

Figure 20: The set up of the samples within the RH chamber. The RH + SO_2 chamber was organized in a similar fashion.

Lastly, samples were removed at different time steps of exposure to track the rate of deterioration: 1 day, 1 week, 2 weeks, and 4 weeks. Two of each material was removed at these times intervals from each of the chambers. Due to the limited number of materials, only one of the fifth (uric acid and potassium chloride) and sixth (uric acid and potassium sulphate) contaminant samples were removed at each of these time spans. Again, due to the limited number of metal materials, there was only one sample that contained the fifth and sixth contaminants, which was placed in the RH chamber (the one without the SO_2 gas) and was only removed after 4 weeks exposure.

3.2 Analyses Procedures

The following procedures were utilized to analyze the results of the testing program.

3.2.1 Bird Excrement Composition

3.2.1.1 Ion Exchange Chromatography (IEC)

Ion Exchange Chromatography is a method that separates ionisable molecules based on their total charge. The data given from this can be useful in determining the composition of an unknown substance. This test was conducted on bird droppings used in the experiment and on real bird

droppings collected from a colleague's balcony. This information would help determine the difference in properties and to better understand their effects on metals. To prepare, the real bird droppings were first sprayed with a disinfectant for safety reasons, as bird droppings can carry harmful bacteria. It was then crushed and grinded with a mortar and pestle to a fine grain. Three one-gram samples from each of the bird droppings were weighed and placed in a beaker. 100mL of distilled water was then added and the contaminants were mixed for approximately 45 minutes using a magnetic stirrer. After 24 hours, the samples were filtered, the pH values were recorded using an electric pH meter, and they were stored. The contaminants were then diluted 10x to ensure proper testing-equipment parameters were met. An IEC Dionex ISC 5000 was used with a conductivity detector to detect anions and cations. The experimental conditions are summarized below.

Table 11: Experimental conditions for the IEC analysis

Anions	
Mobile Phase	Mixture of 4.5 mM carbonate and 1.4 mM hydrocarbonate
Mobile Phase Flow	1.2 ml min^{-1}
Cations	
Mobile Phase	20 mM MSA (methansulfonic acid)
Mobile Phase Flow	1.0 ml min^{-1}

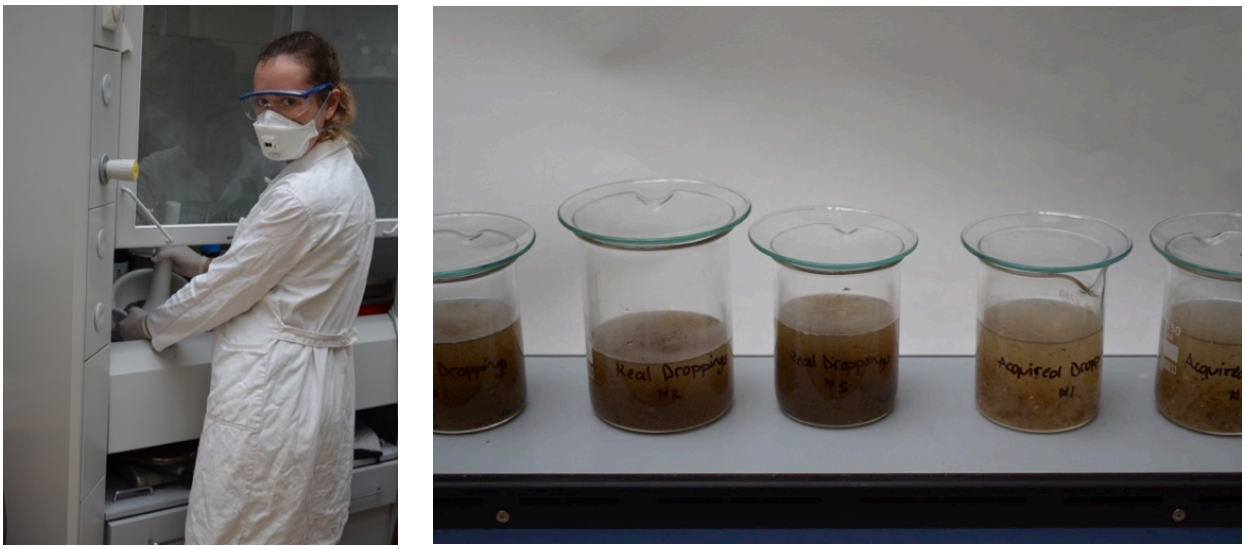

Figure 21: Crushing the real bird droppings and the magnetic mixing of the contaminants

Figure 22: The IEC Equipment Used

3.2.1.2 X-ray Diffraction (XRD)

X-ray diffraction is an analytical technique used to identify the phase of a crystalline material and provides information regarding unit cell dimensions (Dutrow & Clark, 2017). This test was conducted on the used and real bird droppings to determine their compositions. The droppings were further grinded using a mortar and pestle and mixed with ethyl alcohol to improve the crushing process. Each contaminant was spread on the plastic holder using a spatula. The experimental conditions are listed below.

Table 12: The experimental conditions for the XRD testing (Viani, 2017)

Instrument	D8 Bruker
Generator Settings	40mA, 40kV
Tube Position	Line focus
Soller Slits	2.5º
Divergence Slits	0.6mm
Angular Range (2θ)	10-55º
Step size (2θ)	0.01º
Counting time/step	0.04s
Anode material	Cu
Spinning	15 rpm
Sample Holder	Aluminum

3.2.1.3 pH

The pH of water solutions (prepared from the contaminants removed from the metal surface after four weeks of exposure) was determined, as this data would help interpret the surface compositions found in SEM. For example, should the pH match that of which is the ideal pH for the production of brochantite, findings may be correlated. The droppings were removed from the metal

surface via a metal spatula, weighed, and then placed in a volumetric flask. 10mL of distilled water was added to each contaminant. The contaminants were then filtered and the pH was measured using the electric pH meter.

Figure 23: Filtering of the samples to measure pH

3.2.2 Surface Corrosion Products

3.2.2.1 Digital Microscope

At each sample extraction, the cleaned surfaces were observed using a Keyence VHX-5000 digital microscope. A fine-bristled toothbrush and cotton swab were utilized to remove the drops. No other treatment of the samples was required for the microscope readings. This was conducted to see any visible corrosion products and change of the surface morphology.

Figure 24: The digital microscope and program used

3.2.2.2 Colourimetry

The Avantes equipment (AvaSpec-2048, AvaLight-Hal) and AvaSoft 8.0 software was used to measure the colour differences that each of the contaminants posed on the materials. This system measures colour by diffuse-reflected spectrophotometry. The light is reflected by the material, collected in an integration sphere, normalized to the source light of the reflectance, calibrated with the pure white standard (100% reflection) measurement and the black box (zero reflection) over the wavelength spectrum of visible light (Blum, 1997). The analysis is based on the L*a*b* system, or also referred to as the CIELAB system. This cylindrical coordinate system includes the axis of the cylinder as the lightness variable L* (0% - 100%) and the radii is the chromaticity variables a* and b*. The variable a* is the green (negative) to red (positive) axis, and variable b* is the blue (negative) to yellow (positive) axis (Blum, 1997). The tristimulus values X, Y, and Z are utilized to define the variables mentioned above (Blum, 1997).

$$If\ \left(\frac{X}{X_n}\right), \left(\frac{Y}{Y_n}\right), \left(\frac{Z}{Z_n}\right) > 0.008856:$$

$$L^* + 116\left(\frac{Y}{Y_n}\right) 1/3 - 16 \quad \textbf{(11)}$$

$$a^* = 500\left[\frac{\left(\frac{X}{X_n}\right)}{3} - \frac{\left(\frac{Y}{Y_n}\right)}{3}\right] \quad \textbf{(12)}$$

$$b^* = 200\left[\frac{\left(\frac{Y}{Y_n}\right)}{3} - \frac{\left(\frac{Z}{Z_n}\right)}{3}\right] \quad \textbf{(13)}$$

$$If\ \left(\frac{X}{X_n}\right), \left(\frac{Y}{Y_n}\right), \left(\frac{Z}{Z_n}\right) < 0.008856:$$

$$L^* + 903.29\left(\frac{Y}{Y_n}\right) \quad \textbf{(14)}$$

$$a^* = 500\left\{7.787\left[\left(\frac{X}{X_n}\right) + \frac{16}{116}\right] - 7.787\left[\left(\frac{Y}{Y_n}\right) + \frac{16}{116}\right]\right\} \quad \textbf{(15)}$$

$$b^* = 200\left\{7.787\left[\left(\frac{Y}{Y_n}\right) + \frac{16}{116}\right] - 7.787\left[\left(\frac{Z}{Z_n}\right) + \frac{16}{116}\right]\right\} \quad \textbf{(16)}$$

where X, Y, and Z are tristumuls values for the 2° or 10° observer of the specimen, and X_n, Y_n, and Z_n are tristimulus values for the 2° or 10° observer of a perfect reflecting diffuser (Blum, 1997). To determine the differences between two colours, the ΔE* parameter was used:

$$\Delta E^* = [(\Delta L^*)^2 + (\Delta a^*)^2 + (\Delta b^*)^2]^{0.5} \quad \textbf{(17)}$$

The contaminants were removed by a fine brush. An ultrasonic bath was used to clean some specimens. Colour data was collected from the contaminated area and reference areas (not contaminated). Any other tarnish or residual colours on the samples were also collected. As the metals were often inhomogeneous in colour, the uncontaminated colour data collected was averaged

to use one single colour to represent the entire uncontaminated surface. This test was performed on all two-week and four-week samples.

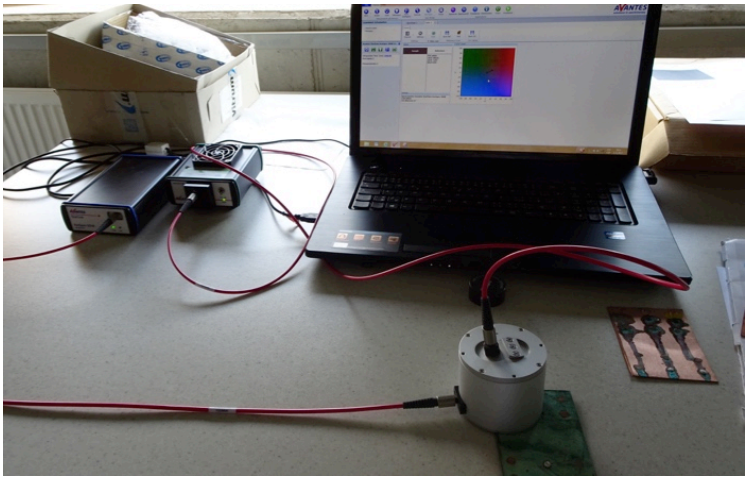

Figure 25: Testing one of the samples with the colourimetry equipment and software.

3.2.2.3 SEM/EDS

A scanning electron microscope (SEM) and Energy Dispersive Spectroscopy (EDS) were used to determine the elemental composition and morphology of the surface of the metals affected by the contaminants. SEM uses a beam of high-energy electrons to generate signals at the surface of the specimens (Swapp, n.d.). These signals provide information about the samples that include external morphology (texture), chemical composition, crystalline structure, and orientation of materials making up the samples (Swapp, n.d.). EDS allows one to identify the particular elements found in SEM and their relative proportions (Hafner, n.d.). The equipment used was the Quanta FEG 450 and the Team software. Little preparation was required for the samples. Since they are conductive metals, they did not require the normal gold or carbon coating. Also, the system was large enough that the samples did not require cutting. For preparation, a small area at the back of the samples was ‘sanded’ to remove dirt and impurities. Conductive tape was applied and the sample was attached to the holder. Markings were used on the samples to aid in navigation to the different drop locations. These tests were conducted only on the surfaces of the four-week samples because the products would be more developed at the longer exposure.

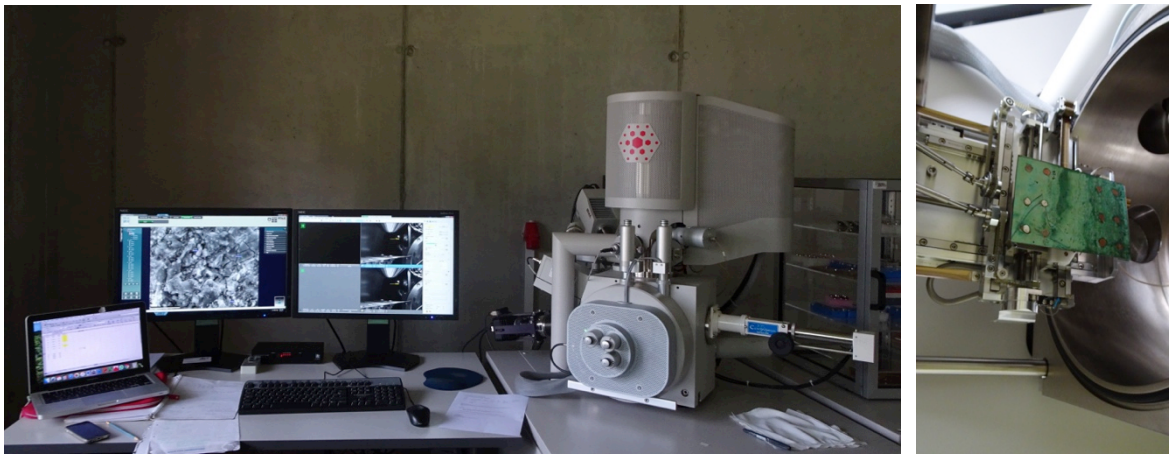

Figure 26: The SEM/EDS system used to analyze the metal surface

3.2.2.4 ICP-OES

Inductively coupled plasma optical emission spectrometry (ICP-OES) detects trace metals. This method was conducted to quantify the amount of metal transferred to the drop contaminant, which can give an indication as to the extent of corrosion that occurred. It was conducted on all two-week and four-week dropping contaminants 1, 2, 3, 5, and 6.

The sample preparation was conducted similarly to Brimblecombe's experiment (Bernardi et al., 2009). To prepare the samples, a drop or two of each sample was removed from the metal surface by the use of a metal spatula. It was then weighed on an analytical scale (±0.0001g) and placed in a 50mL volumetric flask. Afterwards, approximately 10mL of 1:1 HCl and HNO_3 acid mixture was added. The contaminants were then warmed on a burner at approximately 71°C for five minutes or until the entirety of the drops was dissolved. They were then left to cool and distilled water was added up to 50mL. Afterwards, dilution occurred to an appropriate level to conduct the testing.

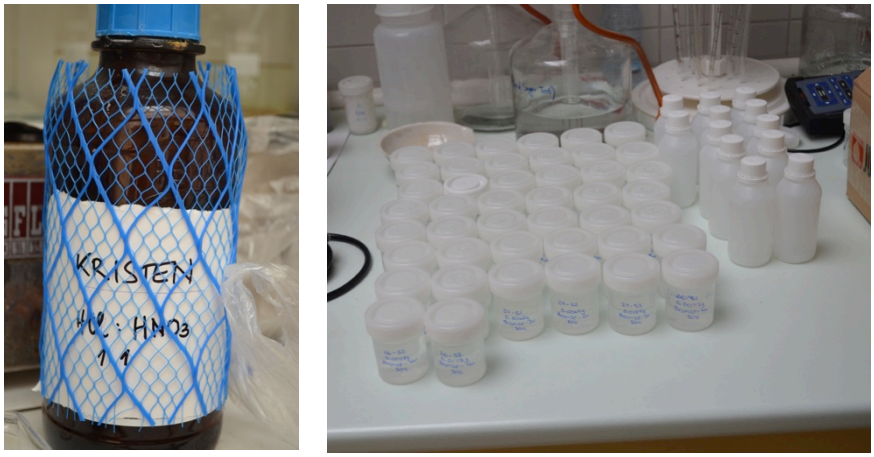

Figure 27: The acid solution and the prepared samples for ICP-OES testing

4. RESULTS AND DISCUSSION

4.1 Testing Results

The relative humidity and SO_2 concentrations were controlled within the chambers as planned. The average temperature was 21°C. Signs of dripping from the contaminants were evident when removing the samples. This was particularly visible from contaminants 2, 3, and 5. This makes sense, as sodium nitrate, potassium dihydrogen phosphate, and potassium chloride are hygroscopic. Due to the orientation of the samples in the chamber, the some contaminant dripped into other contaminants. The sample material also affected the extent of dripping. The smoother the metal, such as copper, the more dripping occurred. Little dripping was observed on roof samples because of their rougher texture. This condition is important to mention, as the results from analyzing drop components may show elements from other drops. To avoid this with future experiments, it is recommended to orient the samples 90º so that if dripping occurs, areas are only affected by the same contaminant. Lastly, the final weight of the removed specimens was not conducted because the change was likely to be very minimal, and it would have been difficult to determine the cause of weight loss or gain. For example, should the metal have been cleaned thoroughly, the loss of weight could be due to the patina removal. Reversely, the weight gain of an element could be due to either contaminant not being removed fully, or the growth of a patina layer. This test would work better in an immersive experiment.

Figure 28: Example of samples removed from 2 weeks of exposure to RH + SO_2. Uric acid + potassium chloride (C5) is dripping onto the uric acid + potassium sulphate (C6) on the copper sample, whereas no dripping can be seen on the roof sample

4.2 Analyses Results

4.2.1 Bird Excrement Composition

4.2.1.1 IEC

The pH levels of the samples were first tested. As can be seen in Figure 29, the used bird droppings are more acidic than the real bird droppings. Overall, the samples are quite neutral.

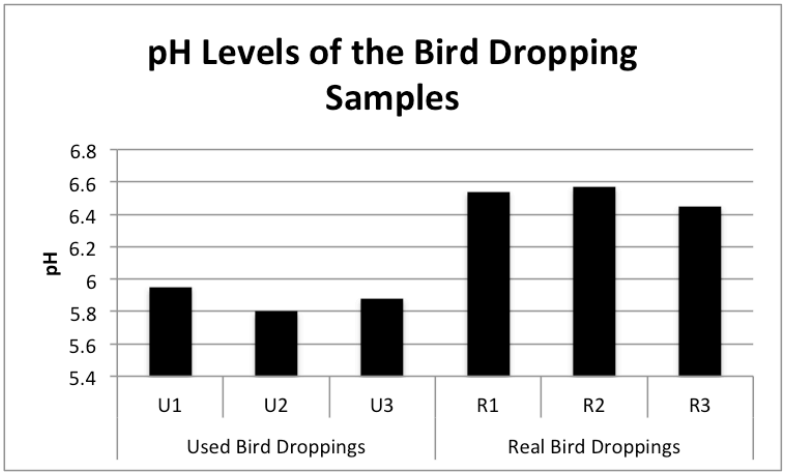

Figure 29: pH levels of the bird dropping samples used in the IEC testing

The results from the IEC tests were averaged as the test was run for each sample twice. The results were as follows:

Table 13: The IEC results for the bird droppings used in the experiment and the real bird droppings collected (n.d.= not discovered)

	F^-	Cl^-	Br^-	NO^{3-}	PO_4^{3-}	SO_4^{2-}	Na^+	NH_4^+	K^+	Mg^{2+}	Ca^{2+}
Used (mg/L)	3.4	15.1	0.2	0.2	7.0	27.5	10.1	0.2	28.5	6.5	24.1
Real (mg/L)	0.0	6.6	n.d.	n.d.	13.8	4.1	5.4	18.0	12.0	1.7	1.3

It can be seen that the two bird dropping compositions were different. The used bird droppings ordered and provided in a package mostly contain the cations potassium followed by calcium. The most concentrated anions were sulphate followed by chloride. The high amounts of calcium were unusual and were probably utilized as a filler material in the mixture. The real bird droppings were primarily comprised of the cations ammonium followed by potassium. Phosphate was the most concentrated anion.

When compared to other studies by Gómez-Heras, Drdácký, and Lavenburg, similar results showed that the main cations were generally potassium, calcium, sodium, magnesium, and ammonium. Other ferrous elements such as silver, aluminum, titanium, and iron were also found in smaller amounts. Similar to other studies, the main anions included sulphate, chloride, phosphate, and

nitrate. Other elements such as fluoride, bromide, bicarbonate, sulphur, and silicon could also be seen in some studies.

Therefore, it is evident that there is no exact composition ratio of bird droppings. The excrements used in the experiment had 'filler' materials such as a fluoride, nitrate, and bromide. It was explained upon receiving this product that it may not be pure pigeon droppings, thus supporting the results seen. If one were to perform this experiment again, it is recommended to use real fresh droppings to obtain more accurate results. Unfortunately, due to the limited time span of the experiment, the tests were conducted with purchased droppings without being able to check their full composition beforehand. If one were to test certain components of the pigeon droppings, it is recommended that they use XRD and/or IEC to first determine its composition, then to determine the salts accordingly, including concentration in those samples. Recommended salt contaminants according to the IEC results are indicated in Section 4.2.1.2.

4.2.1.2 XRD

The X-ray diffraction test produced patterns with vertical bars that indicated the Bragg reflection peaks of phases in the two samples: the bird droppings used in the experiment and the real bird droppings collected later. The results were graphed as follows.

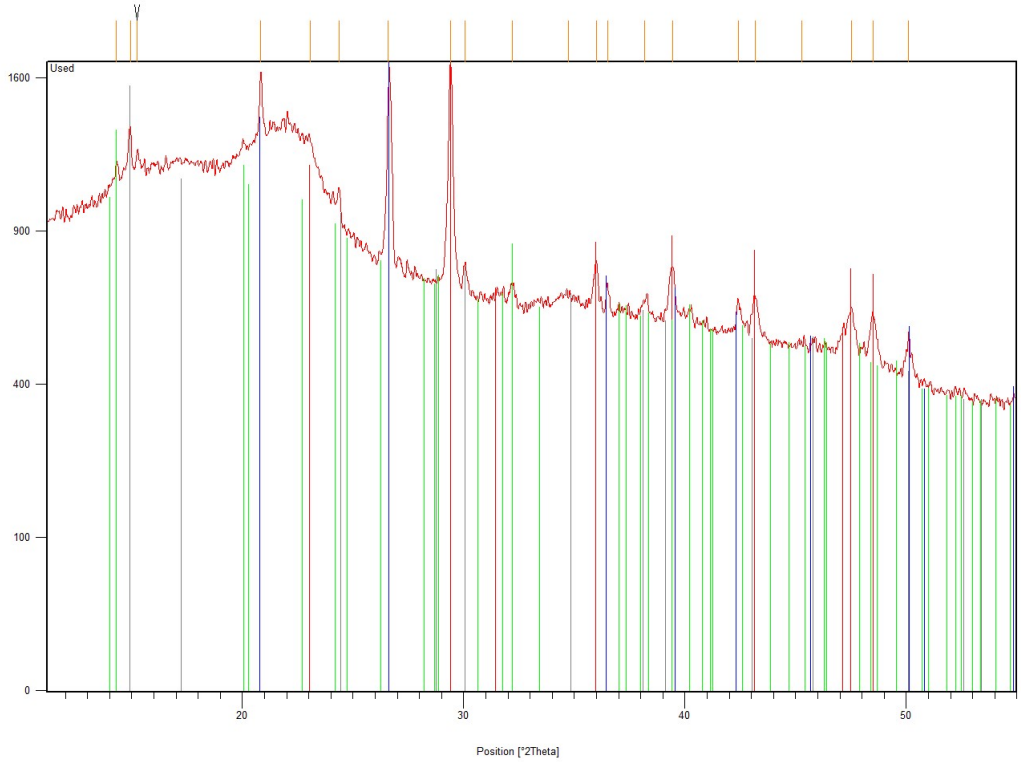

Figure 30: The composition of the used bird droppings. Calcite [$CaCO_3$] – red vertical lines; Quartz [SiO_2] – blue vertical lines; Weddellite [$CaC_2O_4(H_2O)_{2.4}$] – green vertical lines; Magnesium Hydrogen Phosphate Hydrate [$Mg(H_2PO_2)_2(H_2O)_6$] – grey vertical lines.

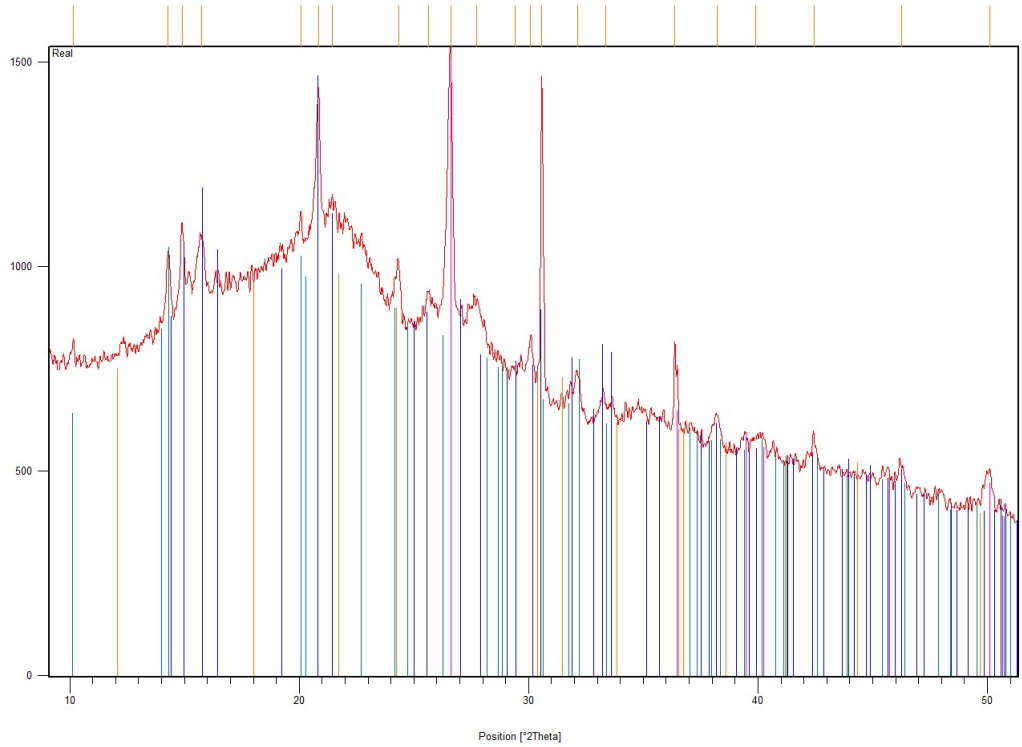

Figure 31: The composition of the real dropping sample. Magnesium Ammonium Phosphate Hydrate [$MgNH_4PO_4(H_2O)_6$] – blue vertical lines; Quartz [SiO_2] – fuschia vertical lines; Weddellite [$CaC_2O_4(H_2O)_{2.4}$] – green vertical lines; Aphthitalite [$K_3Na(SO_4)_2$ – orange vertical lines. The presence of Weddellite and Aphthitalite is ambiguous.

Table 14: Summary of the bird dropping composition phases

Used Bird Droppings	Calcite [$CaCO_3$]
	Quartz [SiO_2]
	Weddellite [CaC_2O_4 $(H_2O)_{2.4}$]
	Magnesium Hydrogen Phosphate Hydrate [$Mg(H_2PO_2)_2$ $(H_2O)_6$]
Real Bird Droppings	Magnesium Ammonium Phosphate Hydrate [$MgNH_4PO_4$ $(H_2O)_6$]
	Quartz [SiO_2]
	Weddellite [CaC_2O_4 $(H_2O)_{2.4}$
	Aphthitalite [K_3Na $(SO_4)_2$]

When these results are compared to those of the IEC test, the real bird droppings show a high correlation as all of the elements identified with IEC are also found with the XRD test. The XRD results of the used bird droppings did not show the presence of F^-, Br^-, NO_3^-, SO_4^{2-}, Na^+, NH_4^+, and K^+. As

also proven by the IEC testing, the samples of the two bird dropping compositions are not exactly the same. Both samples contain calcite, quartz, and weddellite, but there is a slight variation with other components. When comparing the results to the experiment conducted by Gómez-Heras, aphthitalite, and weddellite were also found.

If this experiment was to be conducted again with the results of the real bird samples (IEC and XRD), the following contaminants are suggested: 1) Uric acid; 2) Uric acid and ammonium chloride; 3) Uric acid and sodium sulphate 4) Uric acid and monomagnesium phosphate; 5) Uric acid and potassium chloride; 6) Uric acid and ammonium sulphate; 7) Potassium sulphate; and 8) Real bird droppings. These contaminants allow for the major elements to be tested. Ammonium phosphate was not recommended as it is a highly unstable compound. Also, one must be careful, as ammonium chloride and sodium sulphate are highly soluble in water.

4.2.1.3 pH

The results of the pH testing of the samples proved that most of the samples were around a pH of 5, meaning they are only slightly acidic by the end of four weeks. In general, the pH slightly decreased from Contaminant 1 to 3, then peaked at 5 and reduced again to 6. Therefore, Contaminant 3 was the most acidic and the uric acid + potassium chloride (C5) was the most alkaline. There was a very minimal difference between the RH and RH + SO_2 chambers. These pH levels allow for cuprite and brochantite to be stable and could therefore, along with posnjakite, be the source of the brown/green discolouration on the spot surfaces.

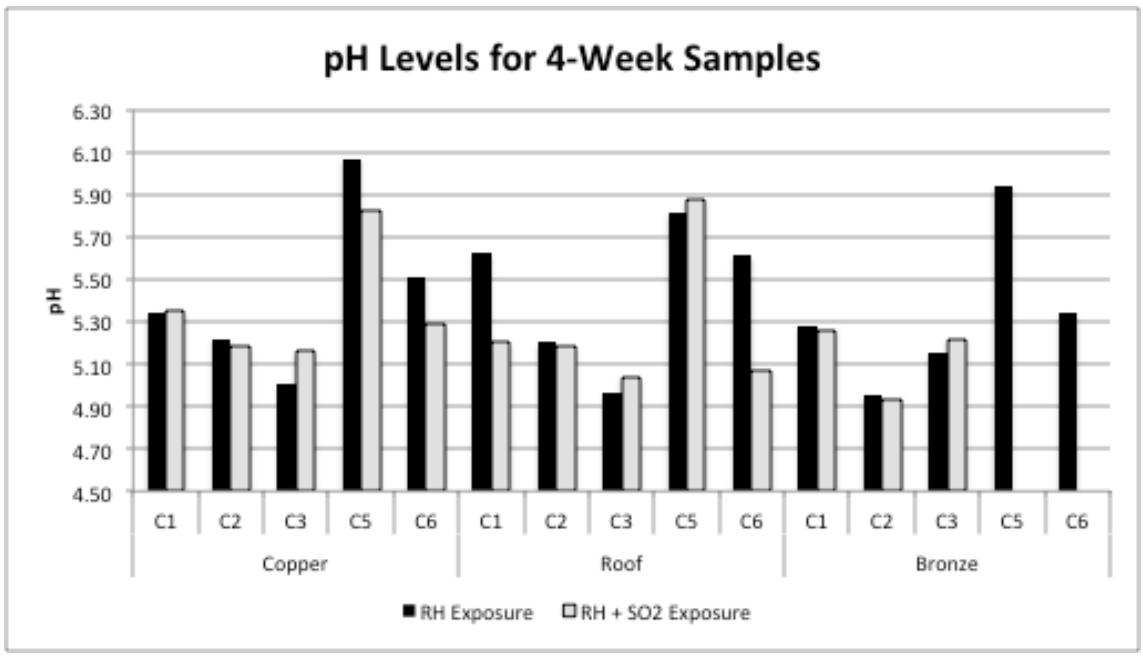

Figure 32: pH levels for the sample contaminants removed after four weeks (excluding the used droppings (C4))

4.2.2 Surface Corrosion Products

4.2.2.1 Digital Microscopy

The digital microscope allowed a good visual assessment of the items. The charts below show a summary of the visual aspects of the drops.

Table 15: Visual transition of the copper under contamination

Contaminant	1 Day Exposure	1 Week Exposure	2 Weeks Exposure	4 Weeks Exposure
RH Exposure				
Uric Acid (C1)				
Uric acid + sodium nitrate (C2)	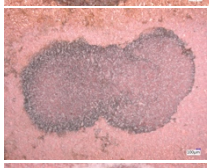		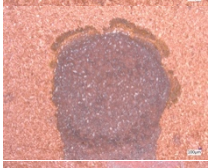	
Uric acid + potassium dihydrogen phosphate (C3)	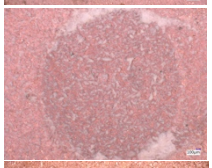			
Used Droppings (C4)			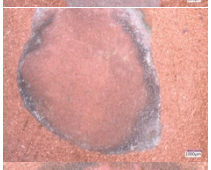	
Uric acid and potassium chloride (C5)			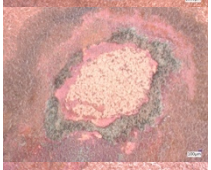	
Uric acid and potassium sulphate (C6)	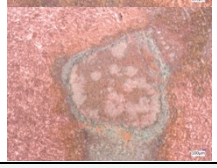		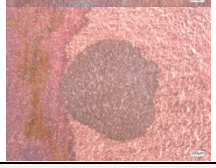	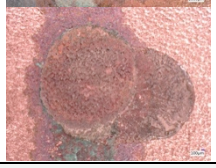
RH + SO_2 Exposure				
Uric Acid (C1)				
Uric acid + sodium nitrate (C2)	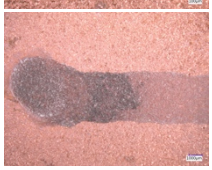		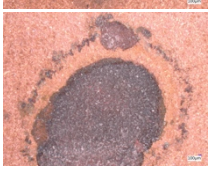	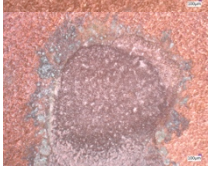

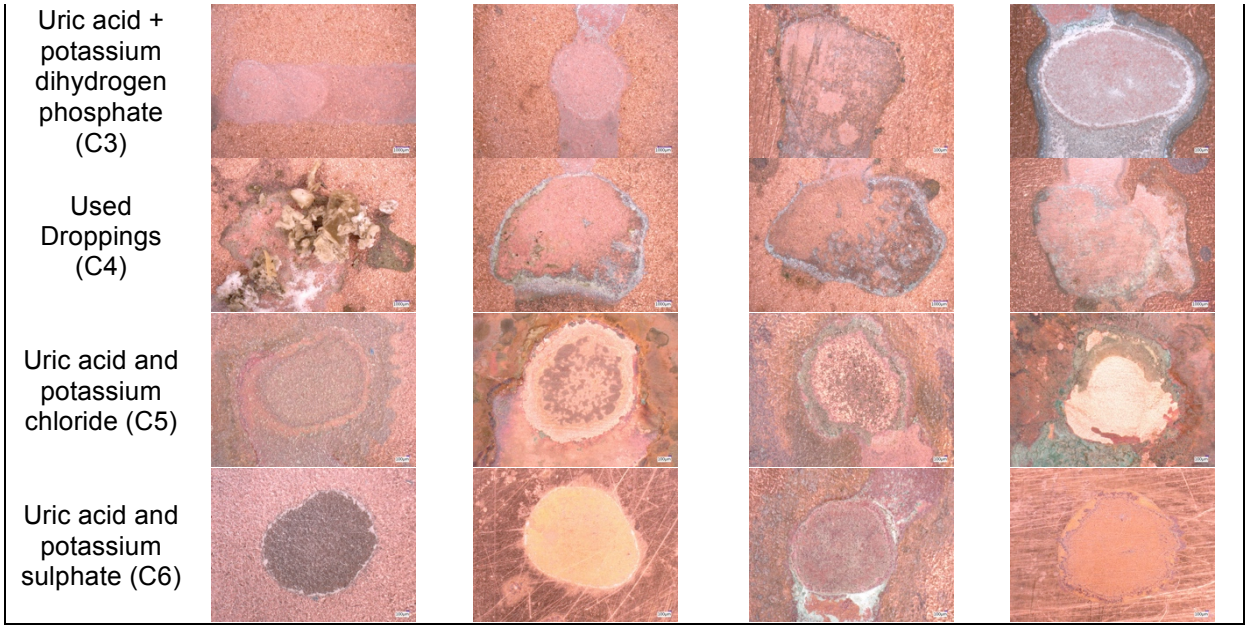

Uric Acid (C1): After one day, yellow crystals could be seen and the black areas proved that corrosion had begun. Larger black areas could be seen after one week, and blue crystals could be seen on the RH + SO_2 samples. Some blue discolouration and random green crystals could be found after two weeks. Lastly after four weeks, the darker areas increased and blue crystals could be seen in the RH samples. Large pits of salt were present in the RH + SO_2 samples. The final darker spot area could be cuprite, which is the initial brown colour that was seen at the beginning of the corrosion process.

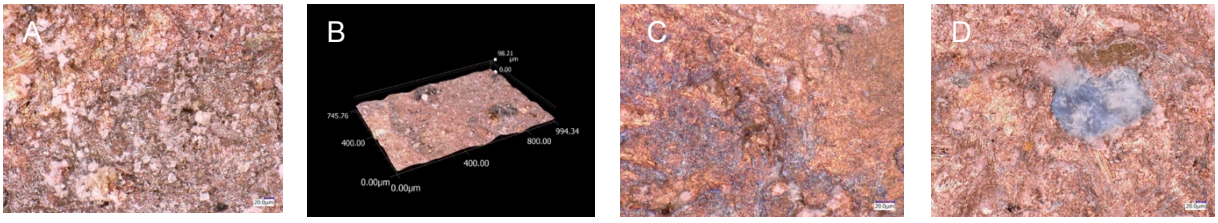

Figure 33: Uric Acid (C1) - A) 1 day: Yellow crystals and black corrosion spots; B) 1 week: Larger black corrosion spots; D) 2 weeks: Discolouration; F) 4 weeks: Blue crystal on RH

Uric acid + sodium nitrate (C2): After one day of exposure, the sample was dark and contained some yellow crystals. Dark corrosion spots could also be seen. The RH + SO_2 sample also had some turquoise crystals. More dark corrosion spots and a turquoise crystal outer ring were present after one week. After two weeks, the damage is more extensive and dark red sections was visible in the RH sample. The RH + SO_2 sample had different compositions for the surrounding outer ring. It also had more dark red sections within its interior. Lastly, after four weeks discolouration had increased and the RH + SO_2 sample had more dark pitting.

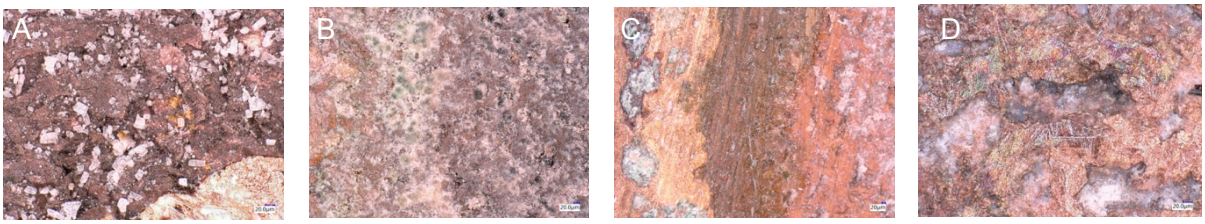

Figure 34: Uric acid + sodium nitrate (C2) - A) 1 day: Dark drop area with yellow crystals visible; B) 1 week: Turquoise crystals visible; C) 2 weeks: The different drop outer ring colours from outside (left) in (right); D) 4 weeks – Discolouration and pitting

Uric acid + potassium dihydrogen phosphate (C3): After one day of exposure, small areas of dark corrosion could be seen. The RH + SO_2 sample had some red crystals visible. Blue crystals and more black corrosion spots were noted after one week. There was not much change after two weeks of exposure, but there was a smoother surface appearance. More blue crystals could be seen surrounding the contaminant. After four weeks, the entire area was darker for the RH sample whereas the area was lighter than its surroundings for the RH + SO_2 sample.

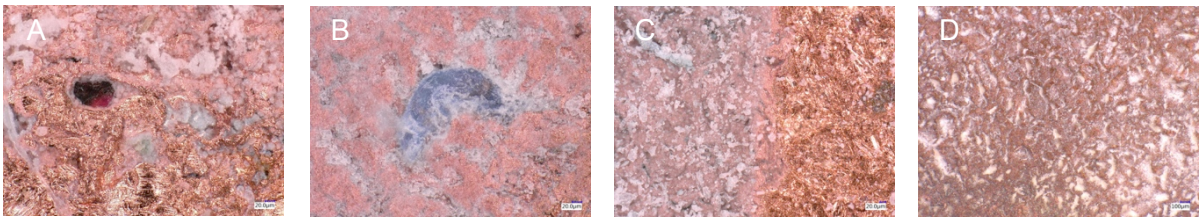

Figure 35: Uric acid + potassium dihydrogen phosphate (C3) - A) 1 day: Small dark corrosion spots and red crystals; B) 1 week: Blue crystals; C) 2 weeks: The inside versus the outside of the drop area; D) 4 weeks: The darker interior of the RH sample

Used droppings (C4): After one day of exposure, dark corrosive areas could be seen and a dark outer ring had formed. The RH + SO_2 sample also had blue and pink crystals. After one week, mould was growing on the sample and a crust had formed. The RH + SO_2 had a lighter pink interior. A dark outer ring and black corrosive spots had increased after two weeks. The RH + SO_2 sample was still lighter on the inside and had blue crystals forming. Lastly, the sample was entirely covered in mould and more blue crust could be seen.

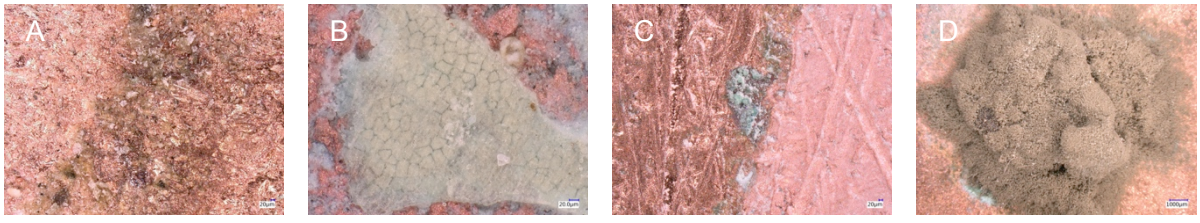

Figure 36: Used droppings (C4) – A) 1 day: Darker outer ring; B) 1 week: Crust formation; C) 2 weeks: Blue crystals forming around RH + SO_2 sample; D) 4 weeks: Mould growth on sample

Uric acid + potassium chloride (C5): After one day, the drop area was brown. Turquoise crust had formed around the drop area. A pink outer ring had also formed with a significant amount of discolouration. The turquoise crust had begun lifting after one week of exposure. A darker tarnish had formed surrounding the sample along with a darker outer ring with colours forming such as purple and blue. The RH + SO_2 sample was not as uniform in colour distribution as the RH sample, was more yellow and pink in its interior. After two weeks, the contaminant had begun to crack and more black deposits could be seen. The RH + SO_2 sample had more black spots than the RH sample. Red areas were interspersed throughout the samples.

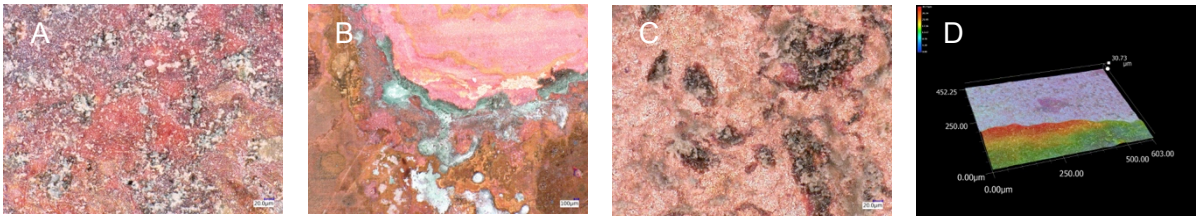

Figure 37: Uric acid + potassium chloride (C5) – A) 1 day: Discolouration; B) 1 week: Not uniform discolouration distribution in the RH + SO_2 sample; C) 2 weeks: Black corrosion areas; D) 4 weeks: Height map of the red layer on the RH + SO_2 sample

Uric acid + potassium sulphate (C6): After one day, the interior was more yellow with dark corrosion spots. The RH + SO_2 sample had a darker interior than the RH sample. It is evident that the uric acid + potassium chloride (C5) had influenced the results, as it had dripped into the uric acid + potassium sulphate (C6) and its remnants can be seen. This caused the interior to be pink for the RH sample and yellow for the RH + SO_2 sample. The two-week sample of the RH sample had a dark interior, whereas the uric acid + potassium chloride (C5) influenced the RH + SO_2 sample again with a pink interior. After four weeks, the RH sample had a dark interior and had red sections, also most likely affected by the uric acid + potassium chloride (C5). The RH + SO_2 sample had a yellow interior and was not influenced by any dripping from the uric acid + potassium chloride (C5).

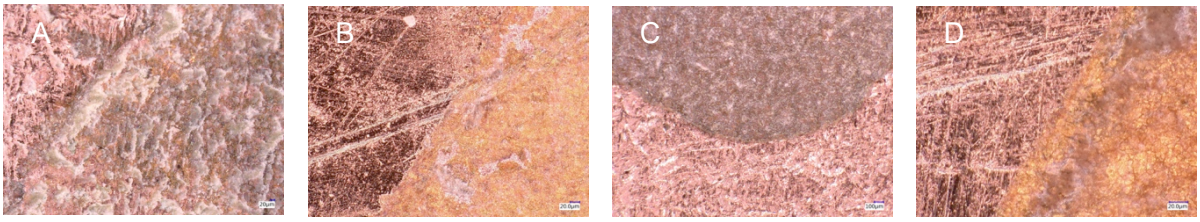

Figure 38: Uric acid + potassium sulphate (C6) – A) 1 day: Discolouration in RH sample; B) 1 week: Yellow interior of RH + SO_2 sample; C) 2 weeks: Dark interior of RH sample; D) Yellow interior of RH + SO_2 sample

Table 16: Visual transition of the roof under contamination. Sometimes a dark green/blue marker was utilized to mark out where the drop was

Contaminant	1 Day Exposure	1 Week Exposure	2 Weeks Exposure	4 Weeks Exposure
RH Exposure				
Uric Acid (C1)				
Uric acid + sodium nitrate (C2)				
Uric acid + potassium dihydrogen phosphate (C3)	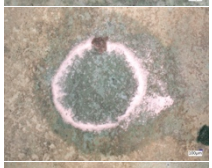		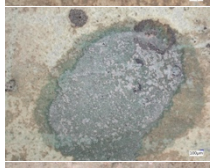	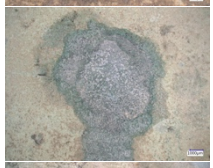
Used Droppings (C4)				
Uric acid and potassium chloride (C5)				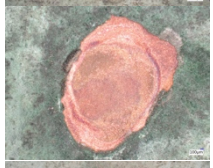
Uric acid and potassium sulphate (C6)		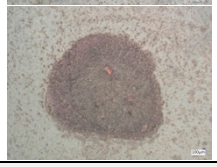		
RH + SO_2 Exposure				
Uric Acid (C1)				
Uric acid + sodium nitrate (C2)				
Uric acid + potassium dihydrogen phosphate (C3)	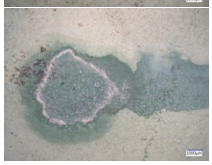	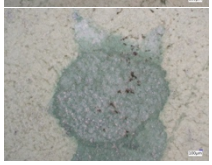		

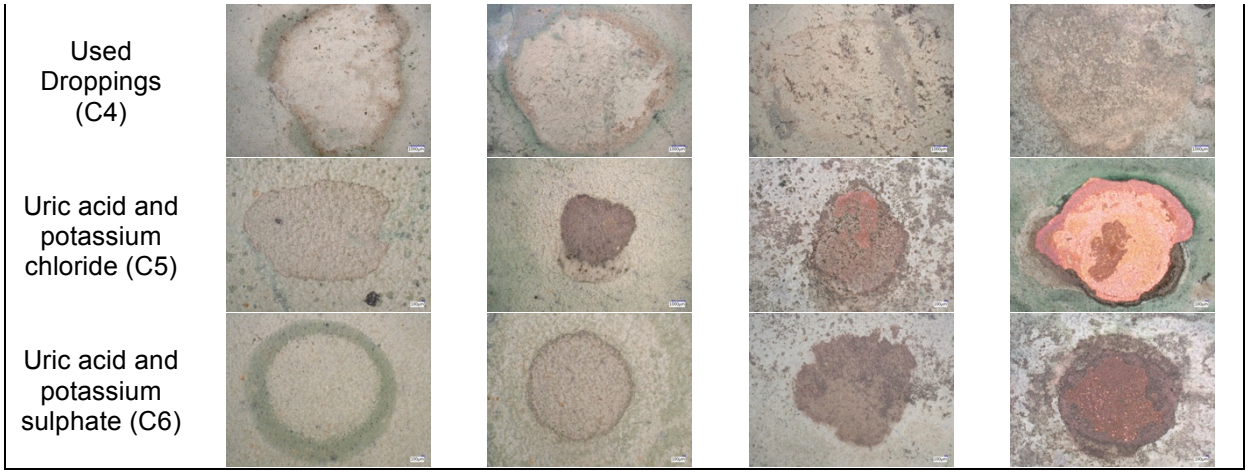

Uric Acid (C1): After one day of exposure, yellow crystals could be seen. There were less yellow crystals with the RH + SO_2 sample. Black corrosion spots were visible after one week. After two weeks, the sample showed surface erosion and red crystals could be seen in the RH + SO_2 sample. At the end of four weeks, the entire spot surface was darker, and green/brown fragments were evident on the salt sample. This could either be specks of the patina that had transferred to the salt, or it was the growth of mould.

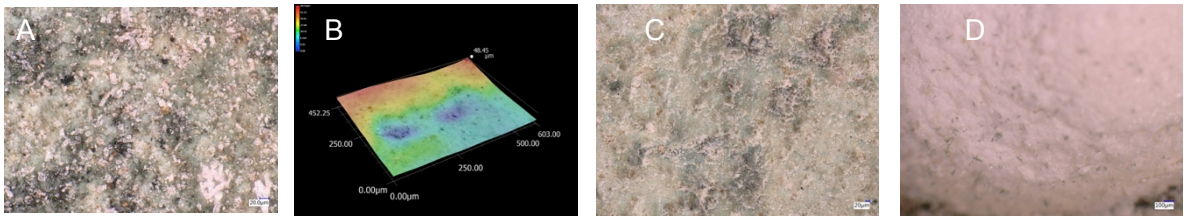

Figure 39: Uric Acid (C1) - A) 1 day: Yellow crystals visible; B) 1 week: Black corrosion pits; C) 2 weeks: Eroded surface; D) 4 weeks: Green/brown spots on the salt

Uric acid + sodium nitrate (C2): No surface change could be seen after one day. After one week, minimal change was visible. Dark corrosion spots and a red area were seen. Marks were visible on the salt after two weeks, and the surface was more eroded with red spots after four weeks.

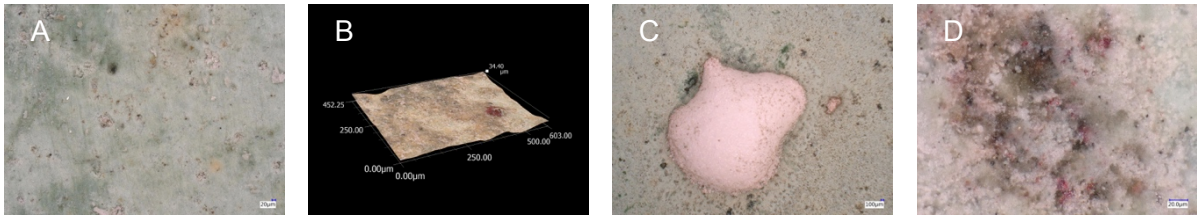

Figure 40: Uric acid + sodium nitrate (C2) – A) 1 day: No change; B) 1 week: Red area; C) 2 weeks: Spots visible on salt; D) 4 weeks – Eroded surface with red crystals.

Uric acid + potassium dihydrogen phosphate (C3): After one day, the surface was a darker blue/green colour. A red area was observed on the RH sample after one week. The darker blue/green colour continued to develop and more black corrosion spots were visible on the RH + SO_2 sample

after two weeks. At the end of four weeks, the spots were darker and different colours could be seen around the outer ring.

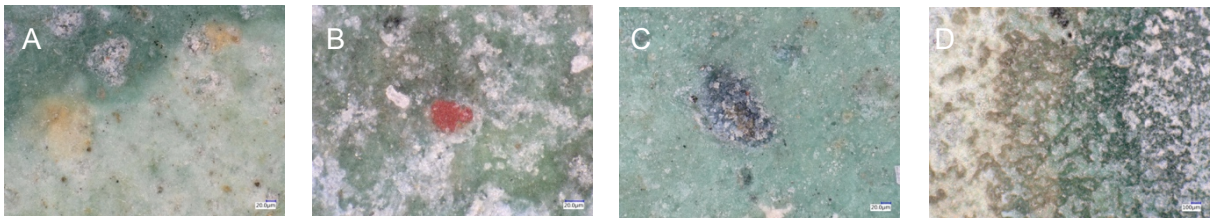

Figure 41: Uric acid + potassium dihydrogen phosphate (C3) – A) 1 day: Darker blue/green contaminant area colour; B) 1 week: Red crystal on the RH sample; C) 2 weeks: Corrosion spots on RH + SO_2 sample; D) 4 weeks: Different outer ring colours

Used droppings (C4): After one day, a slightly darker outer ring could be seen with some black corrosion spots. The RH + SO_2 sample was lighter inside and blue and yellow crystals were visible. Mould began growing on the contaminant after one week and a visible outer ring had formed. After two weeks, more mould had formed on the contaminant and the spot area was light brown for the RH Sample. The RH + SO_2 sample showed that the drop area was protected from the dripping uric acid + potassium dihydrogen phosphate (C3), as it was generally the same colour as the surrounding patina. At the end of four weeks, more mould had grown (more extensively than the copper sample). The RH + SO_2 sample showed red and turquoise crystals forming from the edge. These may have formed from the dripping of uric acid + potassium dihydrogen phosphate (C3).

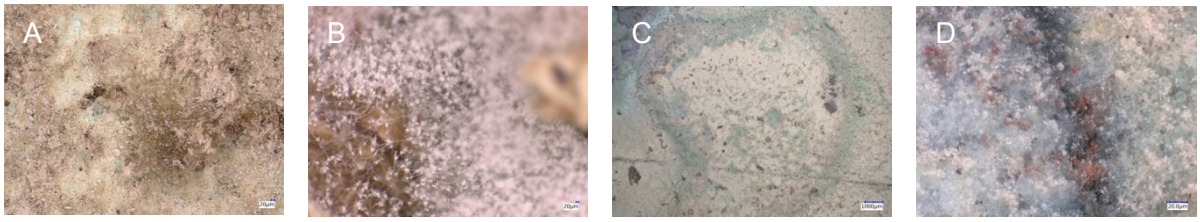

Figure 42: Used droppings (C4) – A) 1 day: Black corrosion spots visible; B) 1 week: Mould formation on the contaminant; C) 2 weeks: RH + SO_2 contaminant showing protection from the uric acid + potassium dihydrogen phosphate (C3) dripping; D) 4 weeks: Red crystals around dark outer ring

Uric acid + potassium chloride (C5): Little change was evident after one day of exposure, except that the spot was slightly darker. After one week, a darker outer ring had formed around the drop. The inside was slightly darker and the surface was more eroded in the RH sample. A small area of exposed copper became visible. The RH + SO_2 sample had some yellow crystals and dense salt areas had begun forming pits in the patina. More copper became exposed around the outer ring of the spot in the RH sample after two weeks. The RH + SO_2 sample began to show very small dispersed areas of exposed copper. After four weeks, the sample areas were totally exposed copper. The exposed copper itself looked similar to that of the copper samples described before.

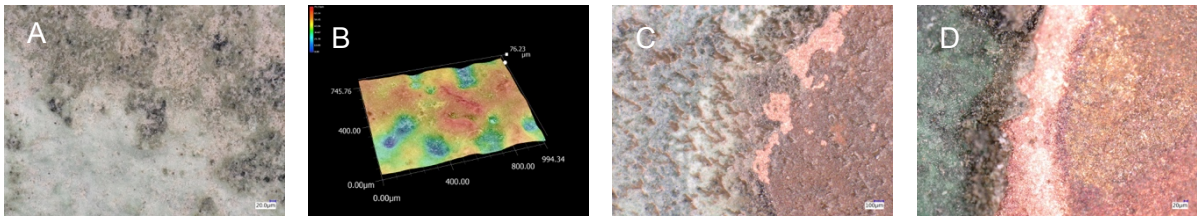

Figure 43: Uric acid + potassium chloride (C5) – A) 1 day: A slightly darker interior; B) 1 week: Salted areas causing pitting in RH + SO_2 sample; C) 2 weeks: Exposed copper around the outer ring in RH sample; D) 4 weeks: Exposed copper interior

Uric acid + potassium sulphate (C6): Little difference was seen after one day, except that there was a slightly darker outer ring caused by the moisture. After one week, the entire drop area was dark with some minor exposed copper in the RH sample. The RH + SO_2 sample was similar but less extensive. The exposed copper areas became more frequent after two weeks of exposure, but were not visible in the RH + SO_2 sample. After four weeks, the entire area of the RH sample was exposed copper with a dark outer ring. The RH + SO_2 sample began to show small areas of exposed copper with a dark interior.

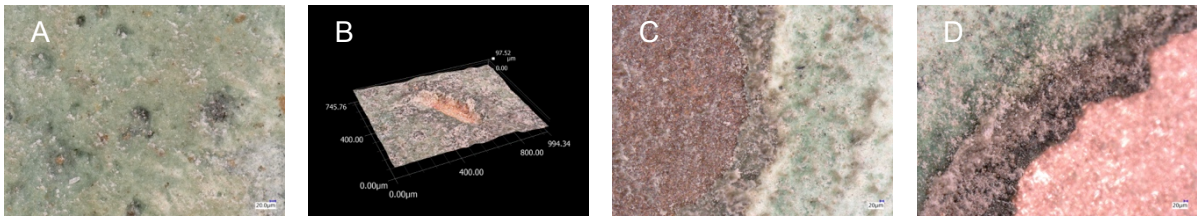

Figure 44: Uric acid + potassium sulphate (C6) – A) 1 day: Slightly darker outer ring; B) 1 week: Exposed copper in RH sample; C) 2 weeks: More frequent exposed copper areas in RH sample; D) 4 weeks: Exposed copper in RH sample

Table 17: Visual transition of the bronze under contamination

Contaminant	1 Day Exposure	1 Week Exposure	2 Weeks Exposure	4 Weeks Exposure
RH Exposure				
Uric Acid (C1)			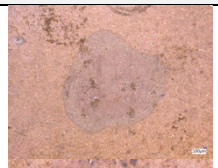	
Uric acid + sodium nitrate (C2)	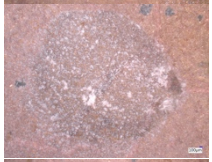	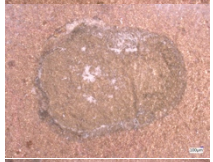	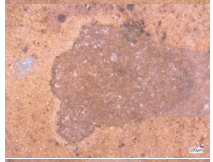	
Uric acid + potassium dihydrogen phosphate (C3)			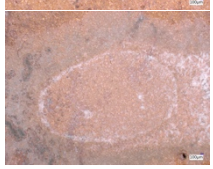	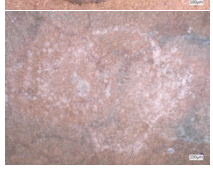

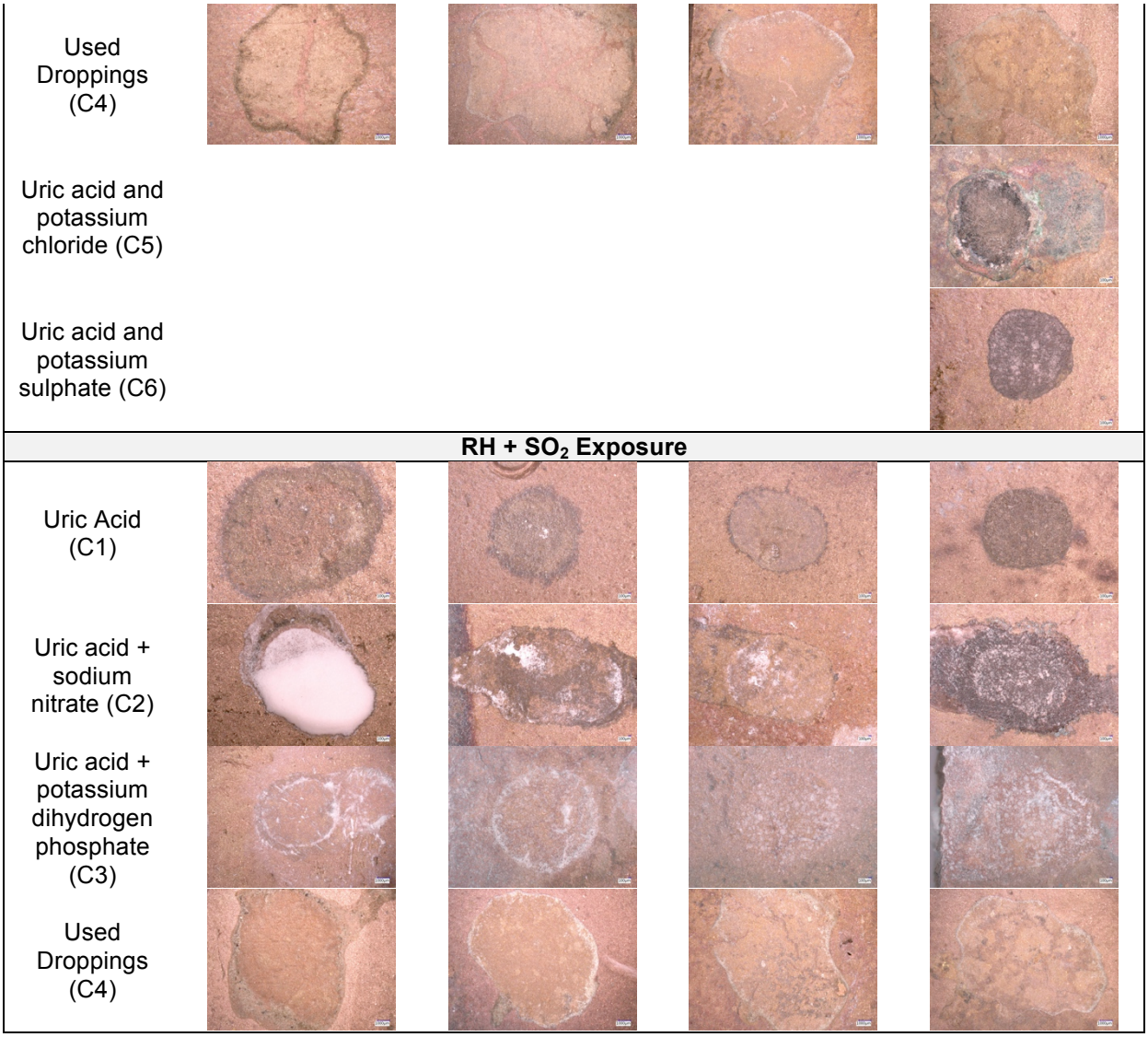

Uric Acid (C1): After one day of exposure, the bronze veins had darkened within the drop area and a dark outer ring had formed around the outside of the RH + SO_2 sample. A dark outer ring formed after one week of exposure for the RH sample, and pitting had occurred with the RH + SO_2 sample. After two weeks, red crystals could be seen with the RH sample. Lastly, after four weeks the entire drop area was dark.

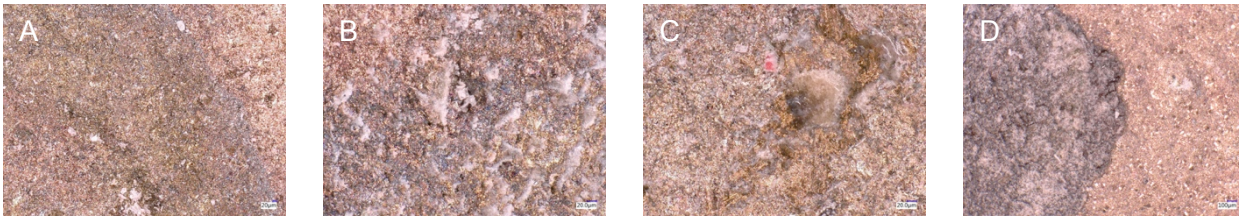

Figure 45: Uric Acid (C1) - A) 1 day: A dark outer ring forming; B) 1 week: Pitting and a pronounced outer ring; C) 2 weeks: Red crystal; D) 4 weeks: Entire spot area is dark

Uric acid + sodium nitrate (C2): After one day of exposure, the interior became darker and blue crystals could be seen in the RH sample. The RH + SO_2 sample showed a dark outer ring and slightly dark interior. The samples continued to darken for the next week. After two weeks, dark green crystal areas became visible. At the end of two weeks the samples showed dark green areas. After four weeks, yellow/green spots were seen on the salt and blue and purple crystals could be seen on the RH sample. The RH + SO_2 sample had a dark interior with blue-green crystals surrounding the exterior.

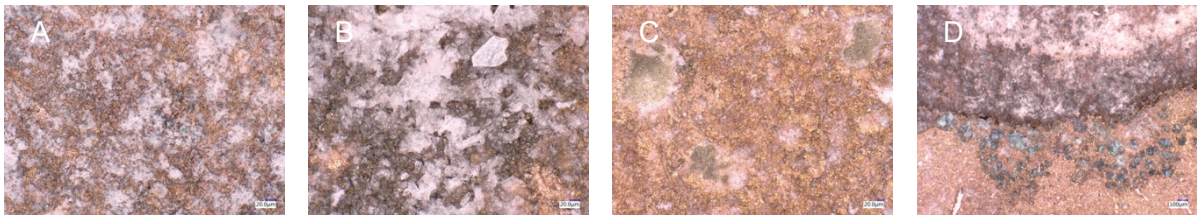

Figure 46: Uric acid + sodium nitrate (C2) – A) 1 day: Some blue crystals are seen on the RH sample; B) 1 week: The spot area is slightly darker; C) 2 weeks: Green areas; D) 4 weeks: Dark interior and surrounding turquoise crystals

Uric acid + potassium dihydrogen phosphate (C3): After one day, black corrosion spots could be seen. The RH + SO_2 samples showed yellow crystals. The black corrosion spots continued for another week. After two weeks, the interior was lighter than the exterior. At the end of four weeks, the sample area was darker and the turquoise crystals had increased. The RH + SO_2 sample also showed red crystals.

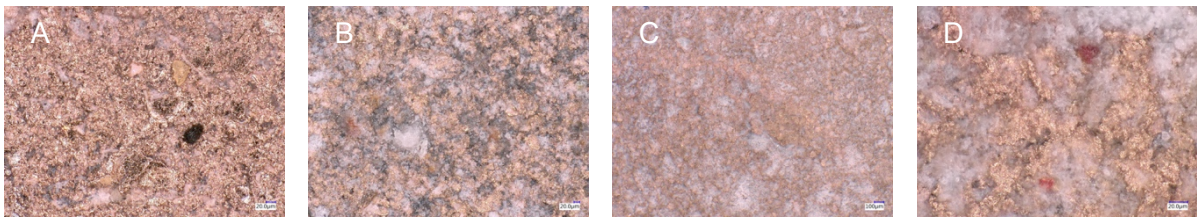

Figure 47: Uric acid + potassium dihydrogen phosphate (C3) – A) 1 day: Black corrosion spots are visible; B) 1 week: More dark corrosion spots; C) 2 weeks: The lighter interior; D) 4 weeks: Red crystals on RH + SO_2 sample

Used droppings (C4): After one day, a dark outer ring had formed and black corrosion spots were visible. The RH + SO_2 sample was darker and had yellow crystals. Mould had grown after one week and more black spots were visible. The RH + SO_2 sample was more yellow whereas the outside was pinker. Blue crystals could be seen. After two weeks, the samples were yellow on the interior and had more discoloured pink outside. At the end of four weeks, more mould had grown on the sample and yellow crystals could be seen. The interior was more yellow and had more black corrosion spots.

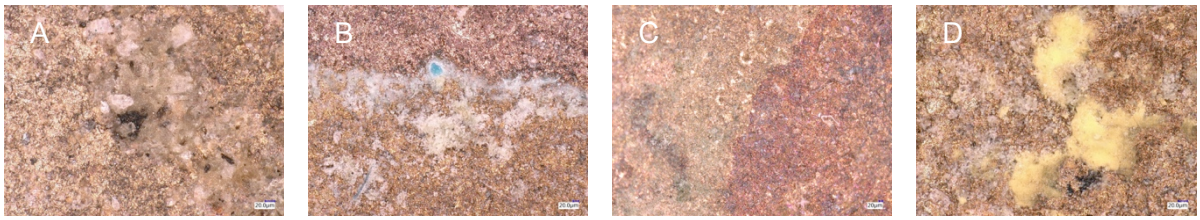

Figure 48: Used droppings (C4) – A) 1 day: Black corrosion spots; B) 1 week: Turquoise crystals on RH + SO_2 sample; C) 2 weeks: Yellow interior and pink exterior; D) 4 weeks: Yellow crystals on RH sample

Uric acid + potassium chloride (C5): There were no samples for the uric acid + potassium chloride (C5) for RH + SO_2, nor were there any samples removed for the first three weeks in the RH chamber. At the end of four weeks, the salt contaminant in the RH chamber was black and had turquoise crystals. The metal surface also had a black colour. Turquoise, red, yellow, and blue discolouration could be seen. The exterior ring was also blue, red, and yellow.

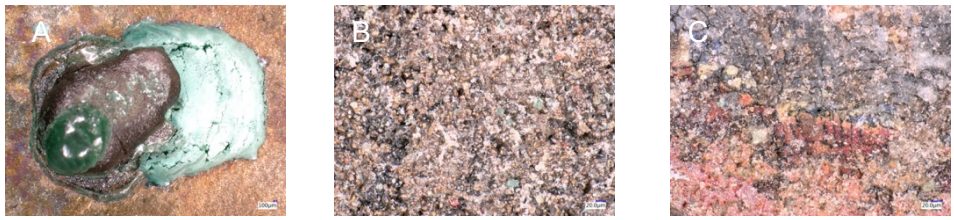

Figure 49: Uric acid + potassium chloride (C5) – A) 4 weeks: The black salt contaminant with turquoise crystals; B) 4 weeks: Dark interior with different colour crystals; C) 4 weeks: Various outer ring colours.

Uric acid + potassium sulphate (C6): There were no samples for the uric acid + potassium sulphate (C6) in RH + SO_2, nor were there any samples removed for the first three weeks in the RH chamber. At the end of four weeks, the interior of the sample was very dark.

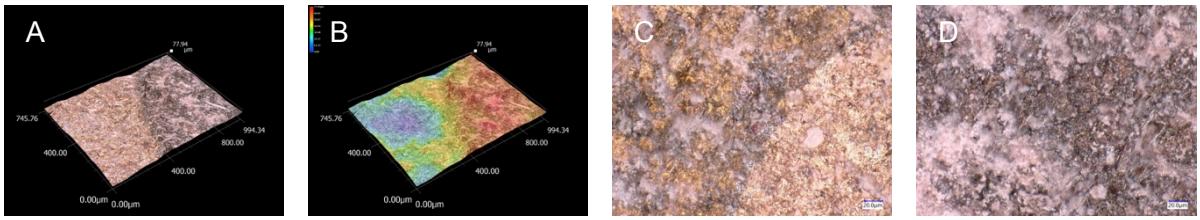

Figure 50: Uric acid + potassium sulphate (C6) – A and B) 4 weeks: The height differential between the dark interior and exterior; C) 4 weeks: Colour difference between the interior and exterior; D) 4 weeks: Interior

Many of the areas showed more corrosion happening around the outside ring of the drops. This is because those areas of the metal are more exposed to oxygen, thus increasing the rate of corrosion. In some cases, the drop acts as a protective agent towards corrosion as it is less exposed to the atmosphere. The blue crystals found were most likely copper (II) sulphate, whereas the more green crystals were most likely copper (II) hydroxide. Sulphur dioxide has a relatively high water

dissolution value, meaning that even low concentrations of sulphur dioxide can affect corrosion and the creation of the blue crystals. The turquoise crystals were probably a mixture of the two. The yellow crystals often found were most likely hydrated uric acid. The yellow crust found on the used droppings (C4) of the bronze sample was likely fluoride, as the used bird droppings contained a higher than usual amount of this element. The dark corrosion spots in the bronze were most likely the areas of zinc. The zinc is higher on the electrochemical series, causing corrosion to occur first in these concentrated areas instead of uniformly on the bronze surface.

Overall, the difference between the two testing environments (with and without SO_2) was quite minimal. It is recommended that future studies have a longer exposure time so that these differences can be noted. When comparing the presence of a patina versus exposed copper, it is believed that the patina acts as a protective agent. It was often difficult to visually see an impact on the surface material, and the salt contaminants were easier to brush off of the patina surface compared to the contaminants on the exposed copper and bronze.

4.2.2.2 Colourimetry

Though the microscope gave a good visual representation of the colour transitions during the experiment, colourimetry allowed quantification of colour changes. A fine brush removed the contaminants, and an ultrasonic bath was used to clean some samples. Care was taken as the ultrasonic bath began removing some of the patina. Therefore this cleaning method was stopped once this was discovered. The change in colour was analyzed for 1) the inside and outside of each contaminant area, 2) inside the contaminant area between 2-week and 4-week samples, and 3) outside the contaminant area between 2-week and 4-week samples. The comparisons also allow one to interpret the contribution of SO_2 gas. It is important to note that some of the sample may have still contained some of the salt contaminants, which would have affected the colour recorded.

When comparing the total colour change, there is no consistent pattern throughout all of the samples. The data shows that the fifth (uric acid and potassium chloride) and sixth contaminants (uric acid and potassium sulphate) tend to have the greatest change in colour. Contaminant four (bird droppings) has the least affect on colour change. In general, the colour change for RH exposure has similar values between the 2-week and 4-week samples as compared to the RH + SO_2 exposed samples. This means that the colour does not change as drastically between the two times for the RH exposed samples versus the RH + SO_2 exposed samples. In terms of colour change between the materials, on average copper has the highest colour change, followed by bronze and then the roof. Though these conclusions are made, they are based off of slight correlations between the data, meaning there are no strong trends.

The data was also broken into its components to make a better comparison. The lightness component (ΔL^*) of the data showed that most of the spots were darker than the surrounding areas. There is no major trend between the two-week and four-week components, as well as the RH and RH

+ SO_2 exposure. Uric acid + potassium sulphate (C6) for the four-week RH copper sample became the darkest and the uric acid + potassium dihydrogen phosphate (C3) from the two-week RH + SO_2 bronze sample became the lightest as compared to its surroundings.

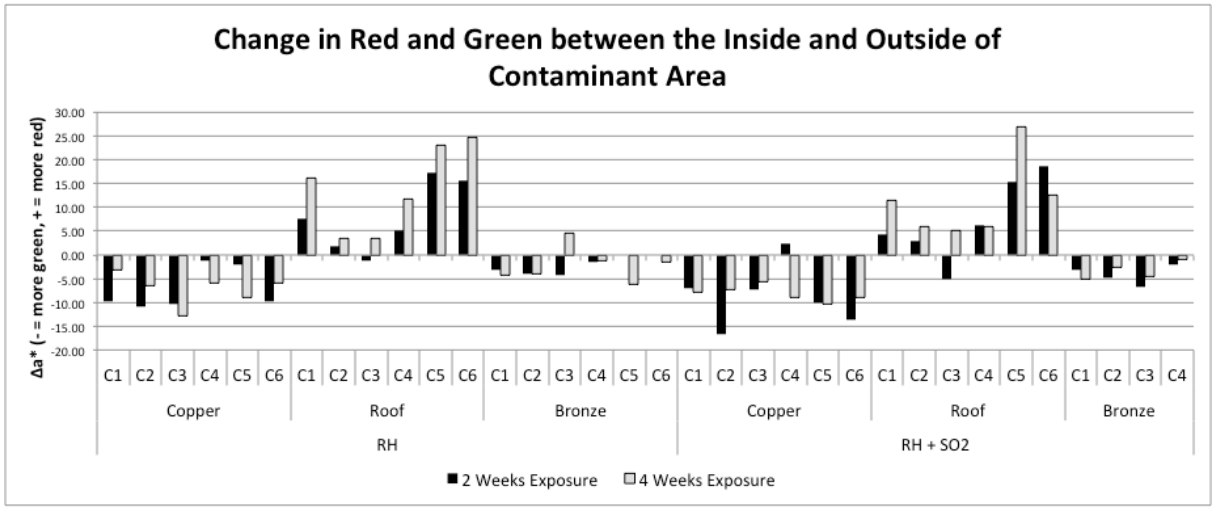

Figure 51: The difference in red and green between the inside and outside of drops

The change between red and green (Δa*) shows more visible correlations, as can be seen in Figure 51. The copper and bronze samples became a more green colour, whereas the roof in general became more red. It makes sense that uric acid + potassium chloride (C5) and contaminant 6 become more red with the roof sample as the copper became exposed. Also, the uric acid + potassium dihydrogen phosphate (C3) of the roof samples becomes more green with the RH sample, which can be correlated with the blue-green colour that is evident after exposure. Bronze has the least change in red/green between the three materials. There is no large difference between the RH and RH + SO_2 samples.

Lastly, the change between yellow and blue (Δb*) proves that most of the drop areas become blue compared to their surrounds rather than yellow. Uric acid + sodium nitrate (C2) from the two-week RH + SO_2 copper has the most blue colour change. Few samples, mostly after four-week exposure, become more yellow. There is no real correlation between RH and RH + SO_2 samples, as well as two-week versus four-week samples.

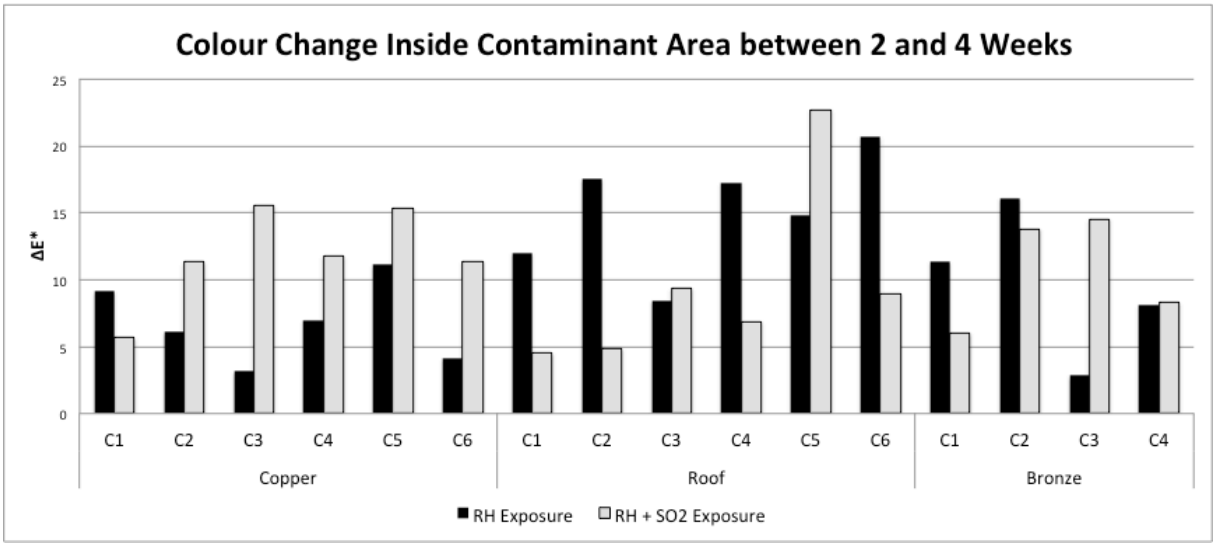

Figure 52: Total colour change inside the drop areas between two and four week samples

As with the previous data, there is no strong trend in the change of colour between the drop areas in a two-week timespan. With copper, it is evident that there is more of a change with RH + SO_2 exposure. In general, the RH exposed roof samples seem to have a greater change than that of the RH + SO_2 samples. The highest changes can be seen with the roof samples. This is especially visible since the patina was removed in some contaminants, leaving the bare copper exposed underneath. There are no major patterns that can be seen with bronze.

The lightness was compared between the drops. The changes were quite minimal are not consistent. Uric acid + potassium chloride (C5) from the RH + SO_2 copper sample became the most light, whereas the uric acid + sodium nitrate (C2) from the RH + SO_2 bronze sample became the darkest. There were very minimal changes and no pattern with the red/green component. Uric acid + sodium nitrate (C2) from the RH + SO_2 copper sample became the most green whereas the uric acid + potassium sulphate (C6) from the RH + SO_2 roof sample became the most green. There is no real correlation between RH and RH + SO_2 exposure, as well as between the different materials for the blue/yellow comparison. Uric acid + sodium nitrate (C2) from the RH roof sample became the most blue, whereas the uric acid + potassium chloride (C5) from the RH + SO_2 roof sample became the most yellow.

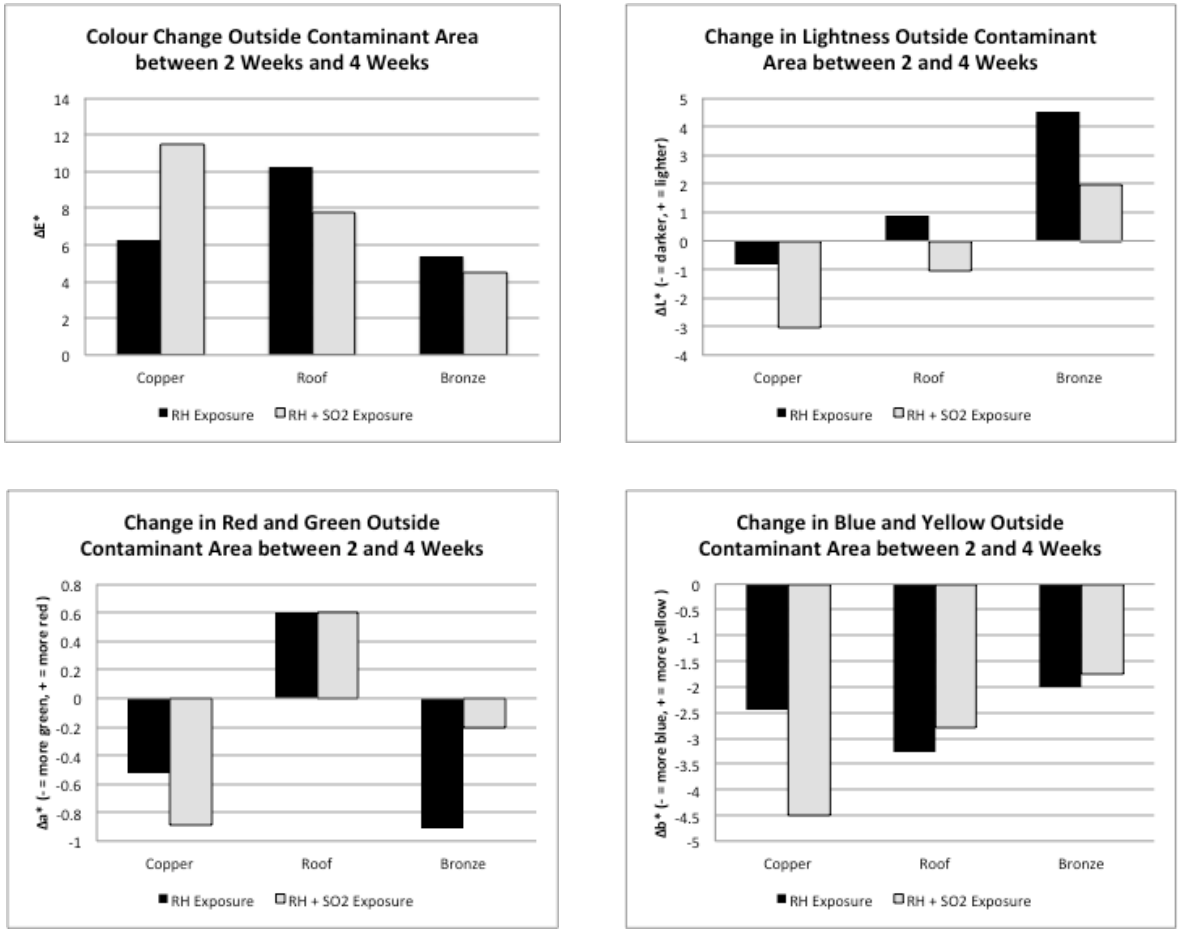

Figure 53: Clockwise from top left. The total colour change, the lightness change, the red/green change, and the blue/yellow change in the metals outside the drop areas between two and four weeks.

The colour change data of the metals was averaged and compared. Therefore, since these areas were not contaminated by any contaminants, they were only affected by humidity and/or SO_2. Again there is no significant pattern. In general, the colour decreases from copper, roof, and then bronze. The copper got darker whereas the bronze overall got lighter. The copper and bronze became more green and the roof became more red. Lastly, all of the metals became more blue and none became yellow. Colour change for the copper specimens was greater with the RH + SO_2 samples and the RH samples had a greater change for bronze. There is no consistent trend for the roof samples.

The colourimetry analysis allowed the numerical colour comparison analysis between the samples. Difficulties resulted from samples not being entirely uniform in colour and it is recommended for future experiments to ensure samples are entirely clean from any salts as they may affect the colours recorded. It is not recommended to perform colourimetry for the purposes conducted in this experiment, as there are too many variables that affect the reliability of the results. All other graphs can be seen in the Appendix.

4.2.2.3 SEM/EDS

All four-week samples were investigated using SEM/EDS. Due to technical difficulties with the equipment, EDS data could not be obtained for a few samples. Also, though the samples did not require a carbon or gold coating as they were already conductive, 'over-charging' often occurred, thus producing images with many white sections. This sometimes compromised the contrast in some images. Below are summary tables with images taken inside and outside of the drop areas at 5000x magnification.

Table 18: SEM images for the copper samples

Contaminant	RH Chamber		RH + SO_2 Chamber	
	Inside Drop	Outside Drop	Inside Drop	Outside Drop
Uric Acid (C1)	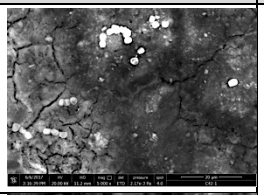	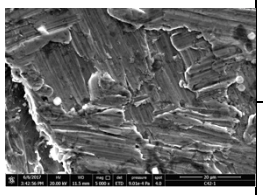	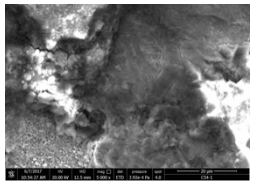	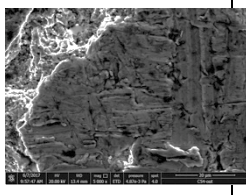
Uric acid + sodium nitrate (C2)	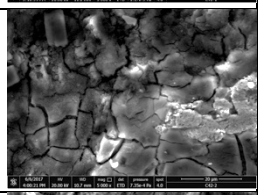		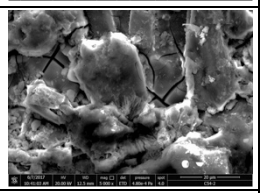	
Uric acid + potassium dihydrogen phosphate (C3)	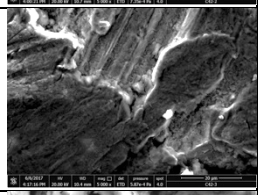		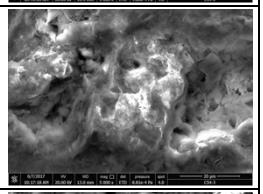	
Used Droppings (C4)	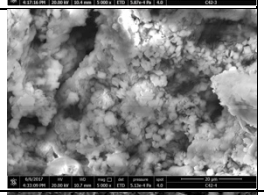		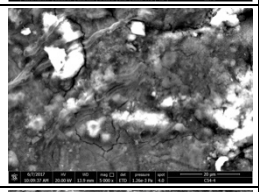	
Uric acid and potassium chloride (C5)	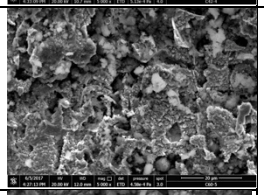	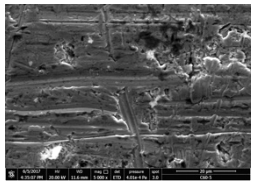	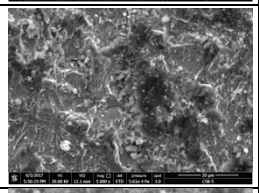	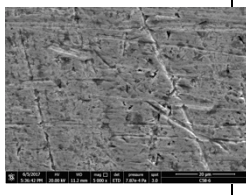
Uric acid and potassium sulphate (C6)	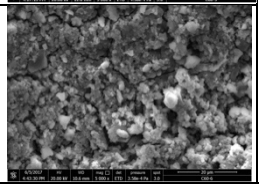		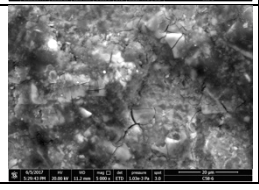	

The copper surface was generally smooth. Small-pitted areas as well as scratches could be seen. The copper surface outside the first four samples showed a more layered appearance. Perhaps

this area was in a location subject to some contamination, thus beginning the deterioration process. The EDS for these areas was similar and only showed evidence of copper being present. Figure 54 shows an example of this area.

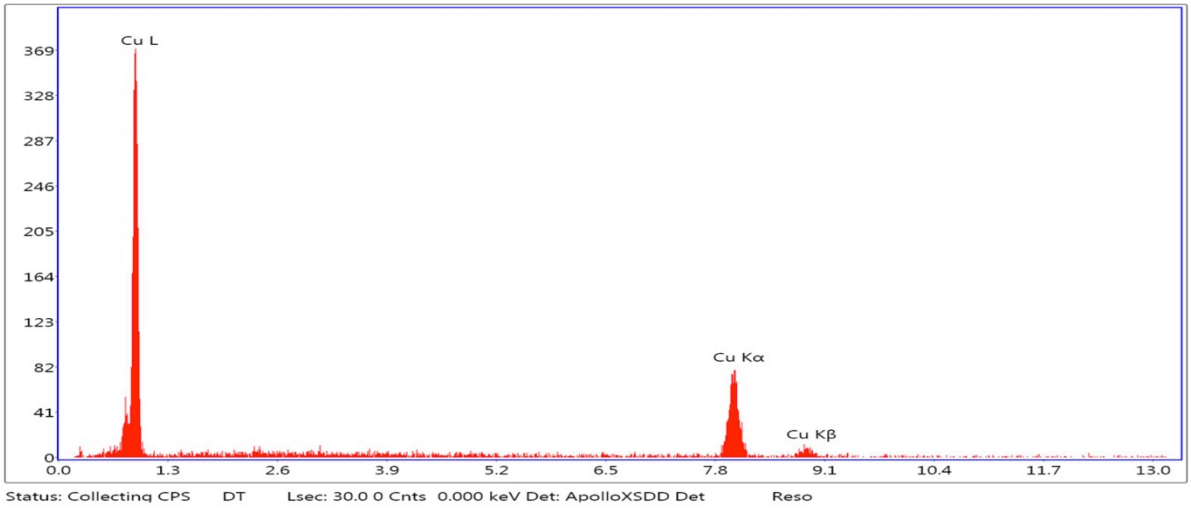

Figure 54: Copper – Outside: The copper sample EDS outside of the spot areas.

Uric Acid (C1): The surface of the drop area is more cracked than its exterior. Fragments of material and chains of white spheres are visible throughout. With EDS, it was determined that these were primarily carbon. It is believed that these are mould spores.

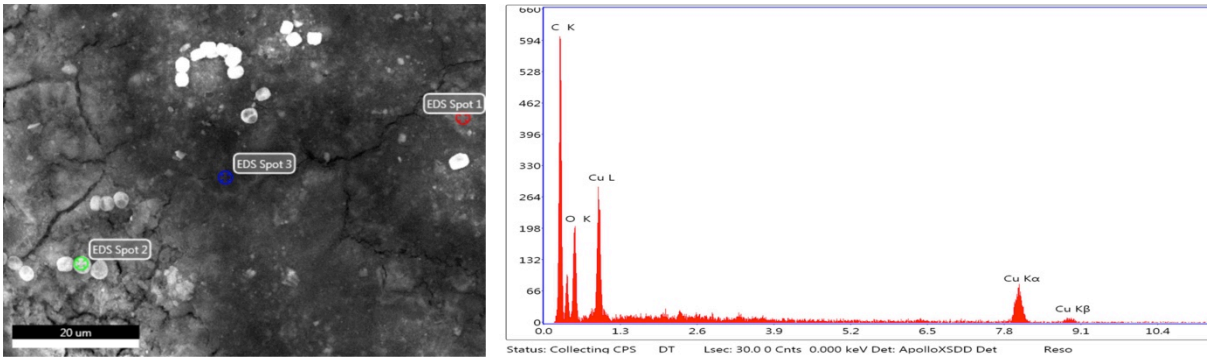

Figure 55: RH Copper – Uric Acid (C1): The EDS result of RH sample Spot 2 representing the sphere composition. Spots 1 and 3 were primarily Cu.

Similarly with the RH + SO_2 sample, mostly it was comprised of copper, except for the fragmented section that was primarily carbon. There is a potential that the sulphur that is seen could be the beginning of the formation of brochantite [$Cu_4(SO_4)(OH)_6$] or from the small amount in the atmosphere. The potassium could be fragments from the uric acid + potassium dihydrogen phosphate (C3). The nitrogen that is present is most likely from the uric acid itself [$C_5H_4N_4O_5$]. Chloride comprises dust particles in Prague due to winter de-icing processes. Since the samples were never stored in a vacuum and were transported between laboratories many times, these dust particles could have easily set on the samples.

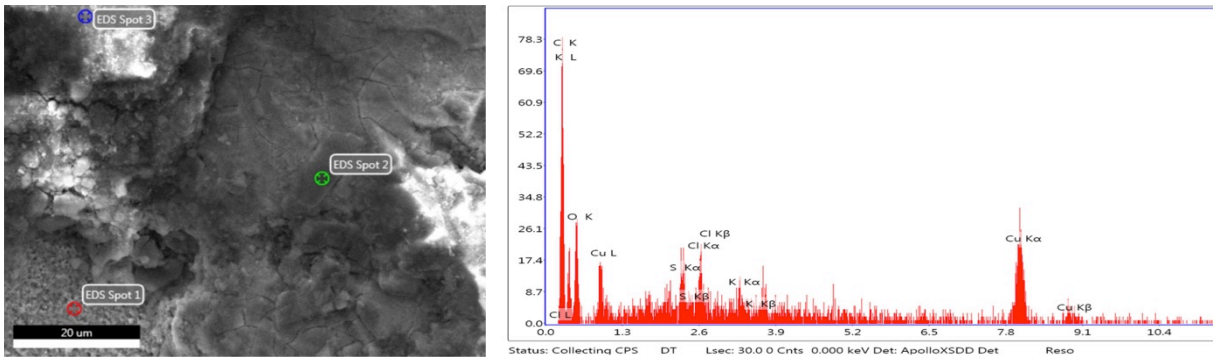

Figure 56: RH + SO_2 Copper – Uric Acid (C1): The EDS result of Spot 3. Spots 1 and 2 were primarily copper.

Uric acid + sodium nitrate (C2): The surface of this contaminant was again, rougher than that of the exterior. In the RH sample, the surface contained primarily oxygen and copper, followed by carbon, nitrogen, and sodium. This makes sense as this contaminant contains sodium nitrate [$NaNO_3$]. The iron found is most likely from dust particles. It makes sense that Spot 1 at the edge of the drop area has more of these components since it was more difficult to remove the surrounding area and more corrosion occurs in this zone than in the middle. The other spots are mainly copper.

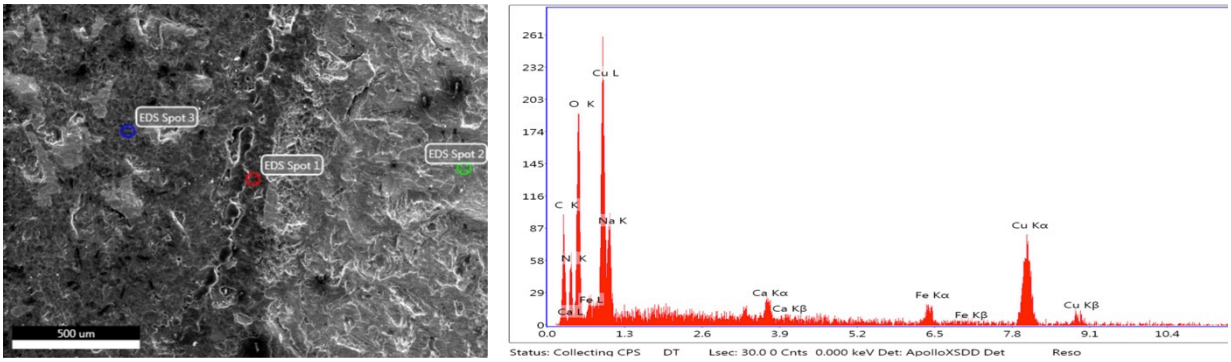

Figure 57: RH Copper – Uric acid + sodium nitrate (C2): The EDS result of Spot 1. Spots 2 and 3 were primarily copper.

The RH + SO_2 sample gave similar results, but had a couple different components. Spot 1, on the copper surface, contained primarily copper and nitrogen. Spots 2 and 3 mainly consisted of carbon, nitrogen, and oxygen. Lastly, spots 4 and 5 contained oxygen and carbon primarily. This coincides with the fragment data from the uric acid (C1).

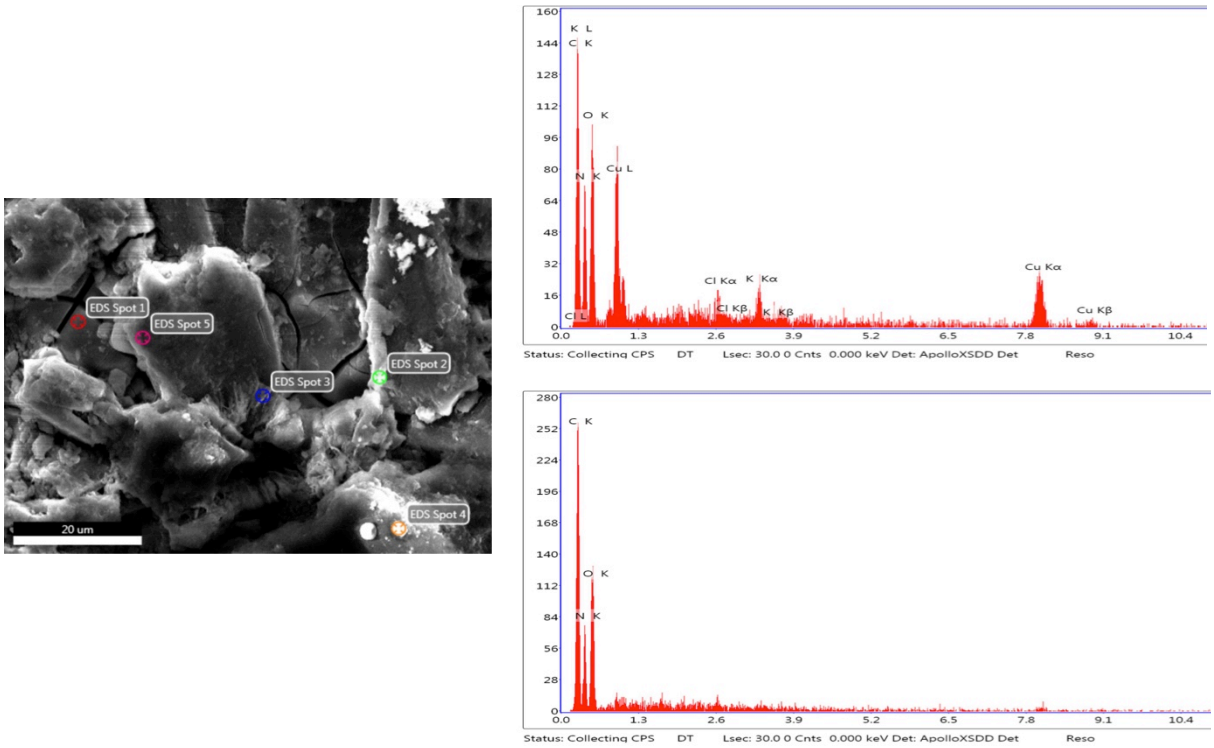

Figure 58: RH + SO_2 Copper – Uric acid + sodium nitrate (C2): The EDS results of Spot 2 (above) and Spot 4 (below)

Uric acid + potassium dihydrogen phosphate (C3): The RH sample primarily contained copper and oxygen. The points also contained traces of phosphorous, nitrogen, potassium, and calcium. The potassium, nitrogen, and phosphorous are reasonable products as they are present in the uric acid – potassium dihydrogen phosphate mixture. The calcium may be some stray particles from the used droppings (C4).

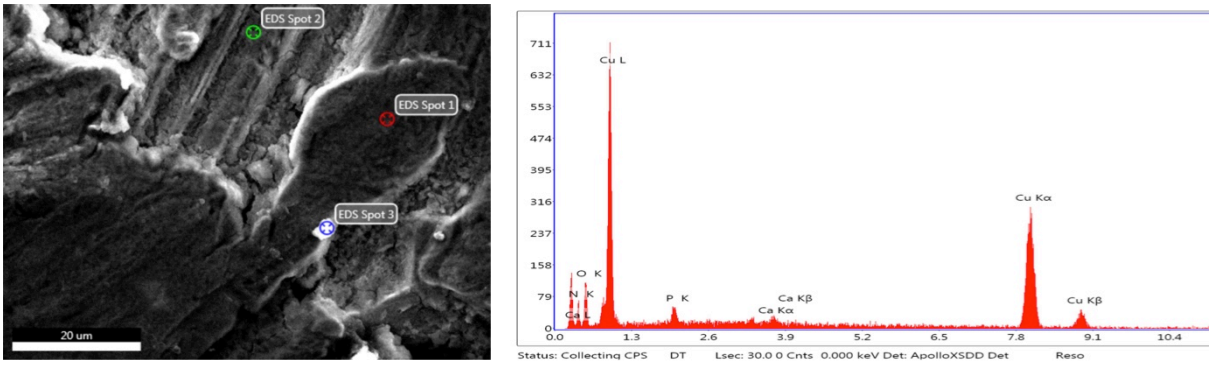

Figure 59: RH Copper – Uric acid + potassium dihydrogen phosphate (C3): The EDS results of RH Spot 2

The RH + SO_2 sample had very similar products, but had higher concentrations of phosphorous, sodium, and potassium. The sodium is most likely from uric acid + sodium nitrate (C2) particles.

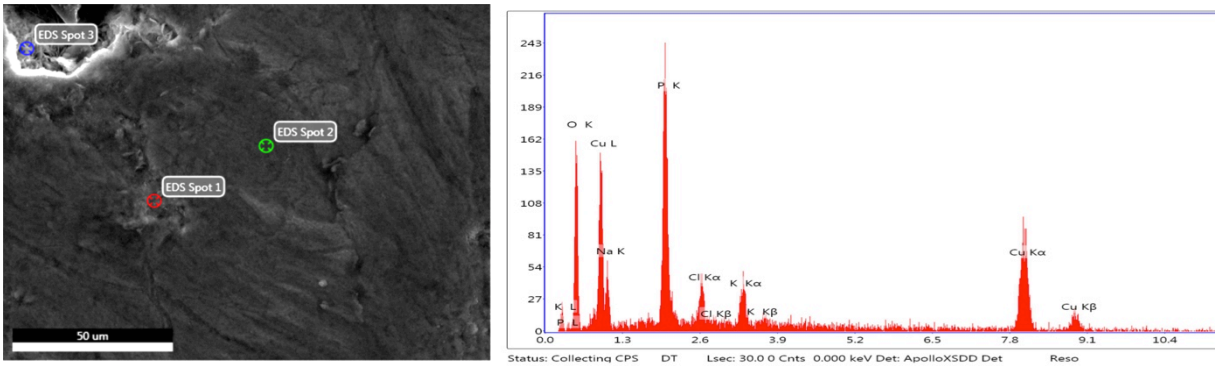

Figure 60: RH + SO_2 Copper – Uric acid + potassium dihydrogen phosphate (C3): The EDS results of Spot 1, showing higher concentrations of phosphorous and potassium.

Used droppings (C4): The surface of the RH used droppings (C4) was quite rough and full of fragments. The surface comprises primarily of copper and oxygen, though large amounts of calcium, phosphorous, and potassium are also visible. Traces of iron (dust) and magnesium (droppings) can also be seen.

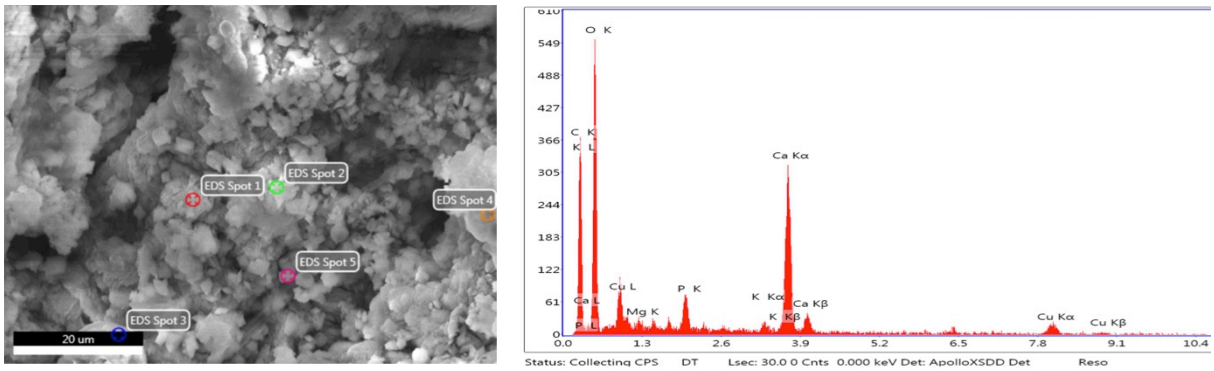

Figure 61: RH Copper – Used droppings (C4): The EDS results of Spot 4.

The RH + SO_2 surface was not as fragmented as the RH sample. Perhaps it was cleaned better before observation. The composition is similar to that of the RH sample, except no iron and magnesium is documented.

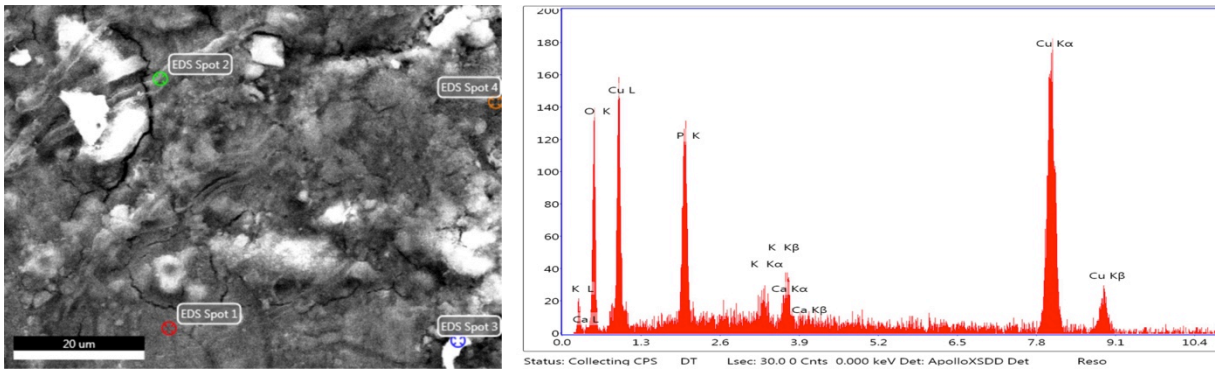

Figure 62: RH + SO_2 Copper – Used droppings (C4): The EDS results of Spot 2

Uric acid + potassium chloride (C5): The surface of the uric acid + potassium chloride (C5) is much more pitted and not uniform compared to that outside of the drop area. Again, the composition is primarily copper, carbon, and oxygen. Potassium and chlorine are also visible, thus coinciding with the salt contaminant uric acid – potassium chloride.

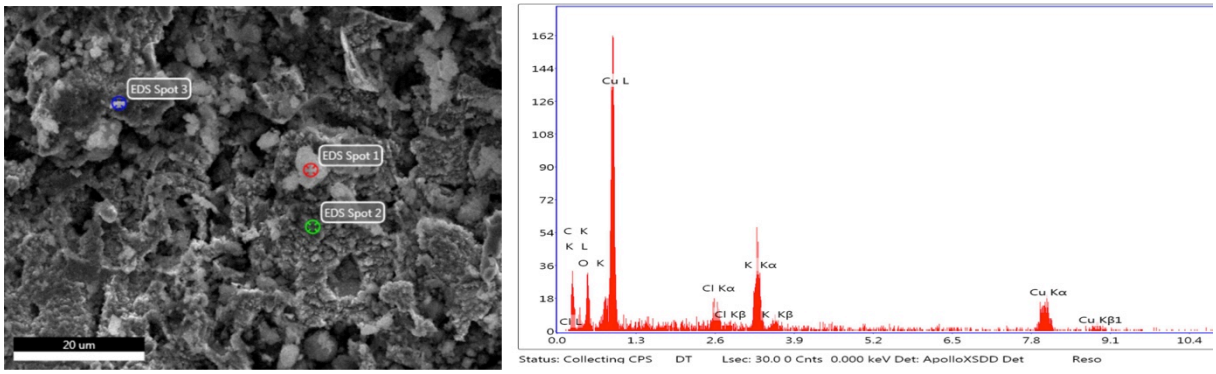

Figure 63: RH Copper – Uric acid + potassium chloride (C5): EDS results for Spot 1

The RH + SO_2 results were similar to that of the RH samples. The surface was not as pitted as the RH sample, but still showed that it had a much rougher surface than the surrounding copper.

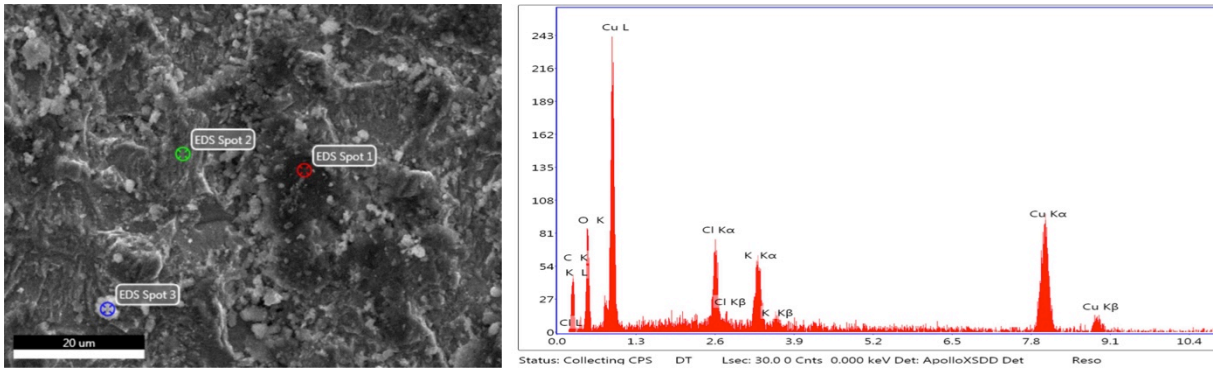

Figure 64: RH + SO_2 Copper – Uric acid + potassium chloride (C5): EDS results for Spot 1

Uric acid + potassium sulphate (C6): The interior of the drop is quite rough compared to that of the exterior. As with the other contaminants, the surface composition of the RH sample was composed primarily of oxygen, and copper. Large amounts of potassium, sulphur, and chlorine can also be seen. The chlorine is likely from the uric acid + potassium chloride (C5), which may have dripped into the uric acid + potassium sulphate (C6).

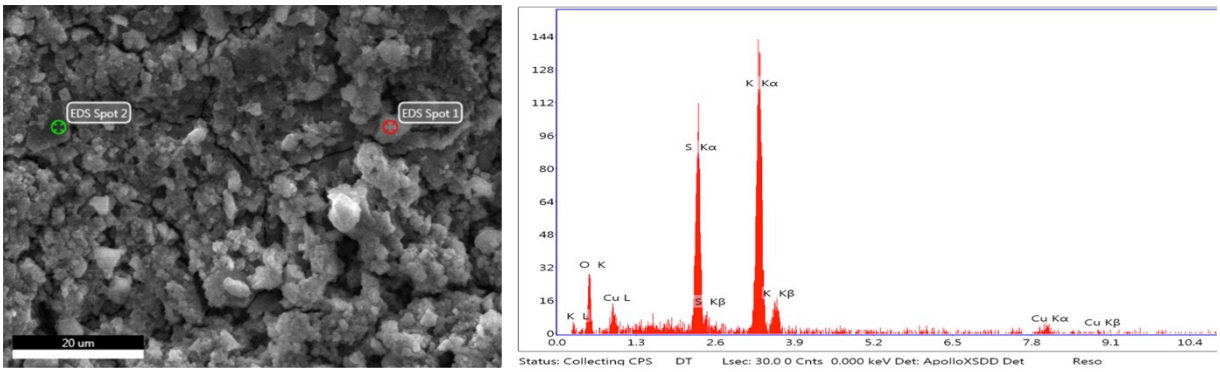

Figure 65: RH Copper – Uric acid + potassium sulphate (C6): EDS results for Spot 1, showing high concentrations of potassium and sulphur

The composition of the RH + SO_2 sample was similar, except that the main components consist of carbon, oxygen, copper, and nitrogen. Chlorine was not recorded; meaning that perhaps dripping from Contaminant 5 had not influenced this sample. The surface of the sample is still more rough than its exterior, but is not as dramatic as its RH counterpart.

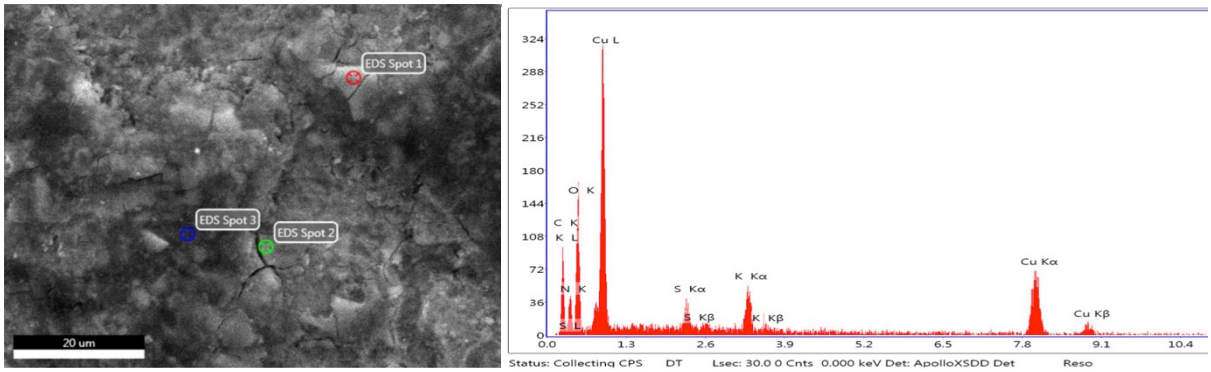

Figure 66: RH + SO_2 Copper – Uric acid + potassium sulphate (C6): EDS results for Spot 2

Table 19: SEM images for the roof samples

Contaminant	RH Chamber		RH + SO_2 Chamber	
	Inside Drop	Outside Drop	Inside Drop	Outside Drop
Uric Acid (C1)	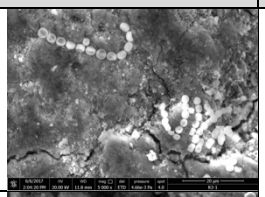		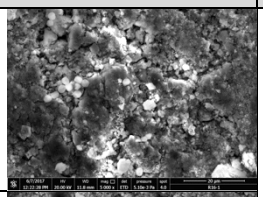	
Uric acid + sodium nitrate (C2)	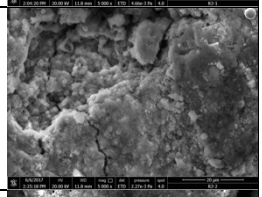	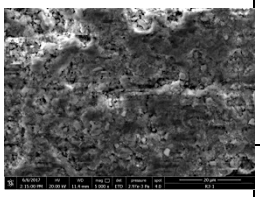	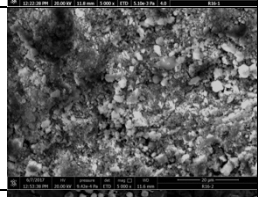	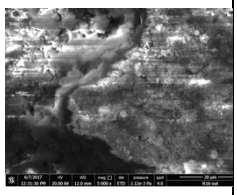
Uric acid + potassium dihydrogen phosphate (C3)	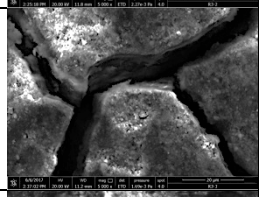		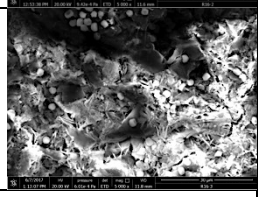	
Used Droppings (C4)	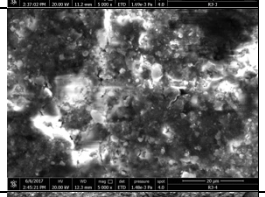			
Uric acid and potassium chloride (C5)	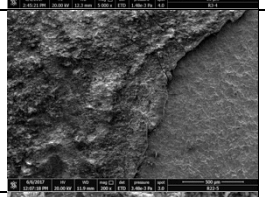	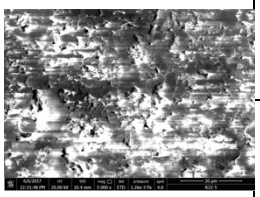	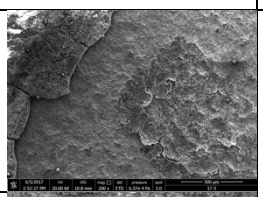	
Uric acid and potassium sulphate (C6)	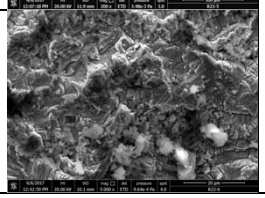		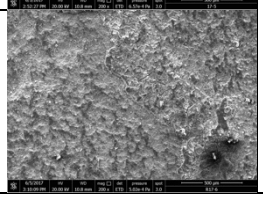	

The roof sample was the most difficult material to analyze as the patina affected the conductivity of the sample. The overcharged areas are mostly the white sections on the SEM images. In some cases, images of spot areas at a magnification of 5000x was not possible, as is seen with inside sample RH and RH + SO_2 Contaminant 5, and RH + SO_2 Contaminant 6. An exterior picture of the RH + SO_2 sample holding contaminants 5 and 6, as well as an interior image of the used droppings (C4) could not be obtained due to difficulties with the equipment. For the sake of the analysis, the exterior section is assumed to be very similar to that of the sample holding the first four contaminants.

The patina of the roof sample has a rough appearance as compared to the copper samples. It is comprised primarily of brochantite, which was known from previous studies and is evident with its

green appearance. Using EDS, similar results between the RH and RH + SO_2 chambers were determined. Its main elements include copper, oxygen, sulphur, and phosphorous.

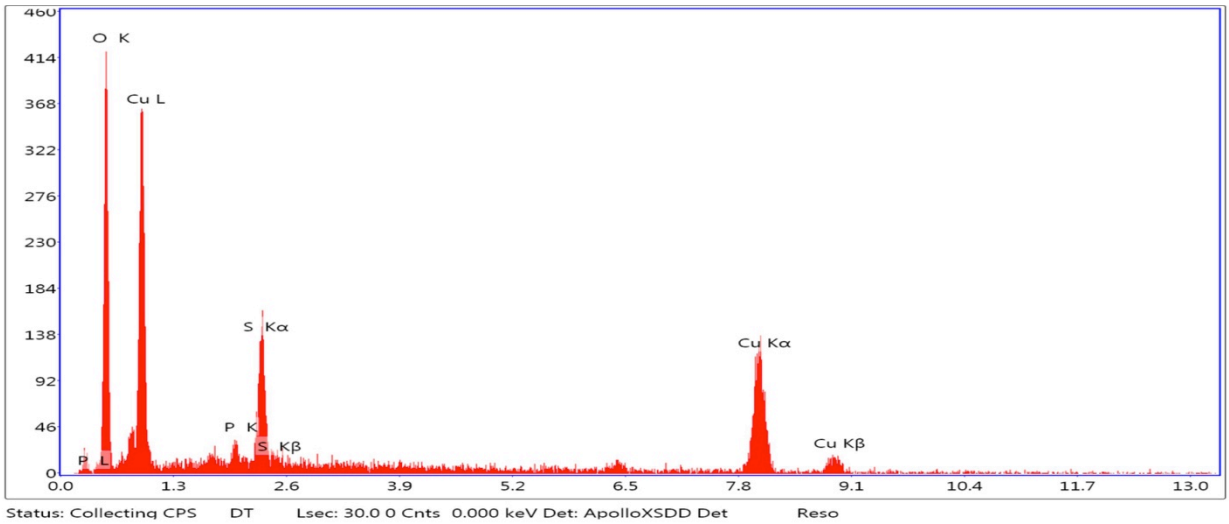

Figure 67: Roof – Outside: The typical diffractogram of the uncontaminated roof patina

Uric Acid (C1): The RH spot area has a very similar appearance to that of the exterior patina. Its composition has similar products to that of the exterior as well (copper, oxygen, and sulphur). Iron is also present in a small amount (Spot 3). This is most likely from dust particles that are impregnated within the patina itself. In Spot 4, nitrogen is also present, which is most likely from the uric acid (C1). The major difference between the interior and exterior is the presence of the circular chains that were also seen in the uric acid (C1) of the copper samples. It has a very similar composition as found before, containing carbon, oxygen, and copper. Again, it is estimated that it is the growth of mould spore from the uric acids.

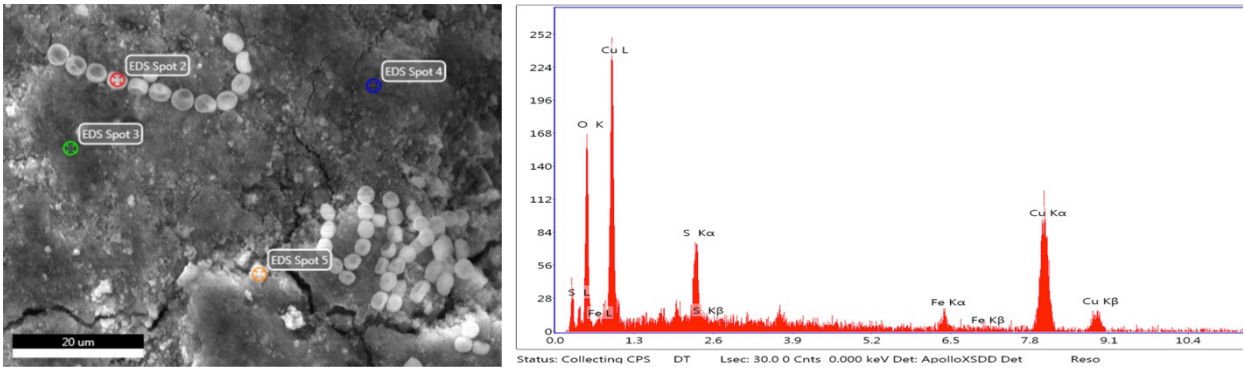

Figure 68: RH Roof – Uric Acid (C1): The EDS image of Spot 3, showing the presence of iron

The RH + SO_2 sample has a rougher surface but has the same composition. The main difference is a higher concentration of iron particles, again most likely from dust.

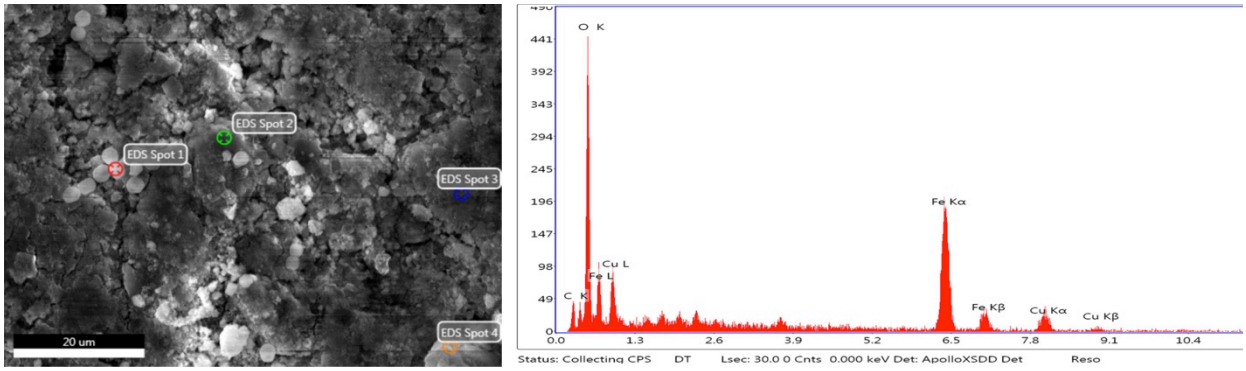

Figure 69: RH + SO_2 Roof – Uric Acid: EDS results of Spot 2 showing more iron particles.

Uric acid + sodium nitrate (C2): The surface of the drop area is quite similar to that of its exterior. Apart from the usual composition of copper, oxygen, and carbon, the surface also shows evidence of nitrogen, silicon, phosphorous, sulphur, and large iron particles. The nitrogen is most likely from the sodium nitrate contaminant or uric acid. The silicon is most likely from dust along with the iron. Phosphorous could either be from the uric acid + potassium dihydrogen phosphate (C3) or used droppings (C4) particles. Lastly, the sulphur is most likely from the patina material (brochantite or posnjakite). The EDS data could not be retrieved for the RH + SO_2 sample.

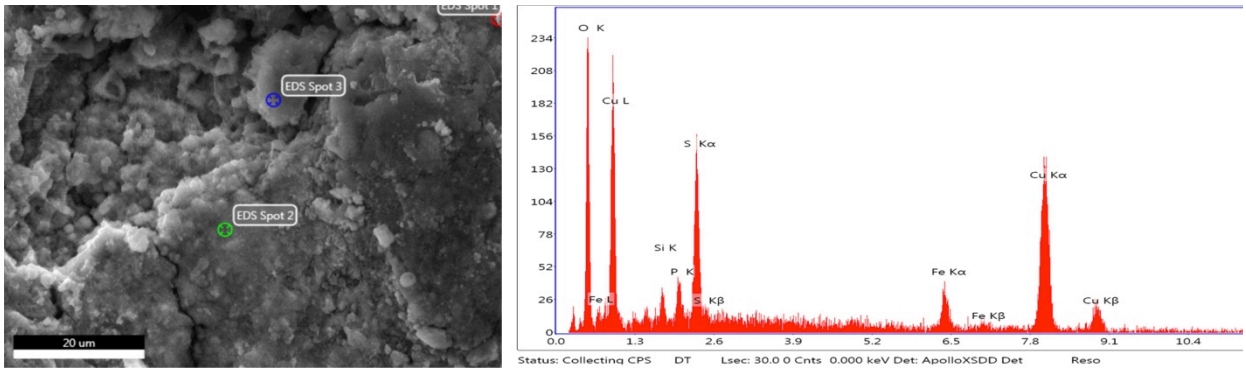

Figure 70: RH Roof – Uric acid + sodium nitrate (C2): The EDS results for Spot 2

Uric acid + potassium dihydrogen phosphate (C3): The surface of the RH sample was very cracked compared to the exterior surface. The composition of the surface is primarily oxygen and copper, followed by phosphorous, sulphur, and potassium. These elements match those in the uric acid + potassium dihydrogen phosphate (C3) and in the patina. In some areas, high amounts of oxygen and iron are also present. As before, no EDS data could be obtained for the RH + SO_2 sample. Its surface was not as cracked as the RH sample, but it has a rougher texture.

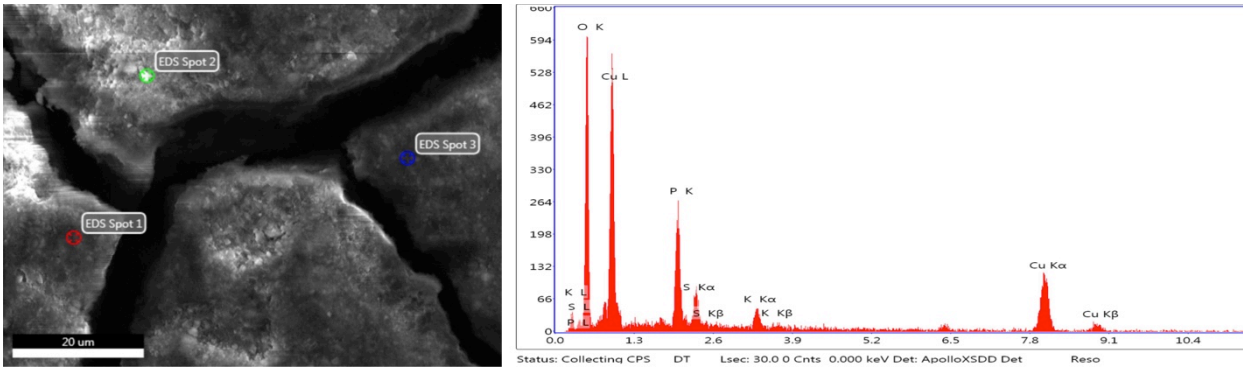

Figure 71: RH Roof – Uric acid + potassium dihydrogen phosphate (C3): The EDS results for Spot 2

Used droppings (C4): The surface of Contaminant 4 is rough in comparison to the uncontaminated area. The composition reflects that of the metal and contaminant materials. These include oxygen, copper, carbon, sulphur, iron (dust), phosphorous, potassium, magnesium, silicon (dust), and calcium. SEM and EDS analysis was not conducted for the RH + SO_2 Contaminant 4 due to technical difficulties.

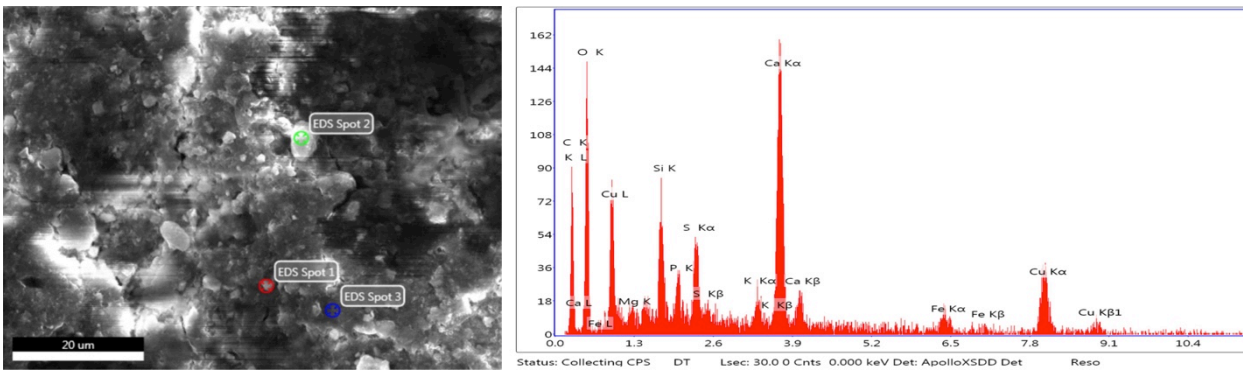

Figure 72: RH Roof – Used droppings (C4): The EDS results for Spot 2 showing the diverse composition

Uric acid + potassium chloride (C5): The surface of the RH spot area is very smooth compared to the patina surrounding the drop area, as it is pure copper. The patina surrounding the drop is also rougher than the general patina covering the metal. The spot area is 100% copper and the surrounding patina contains copper, oxygen, chlorine, potassium, and sulphur, which reflects the composition of the contaminant and patina.

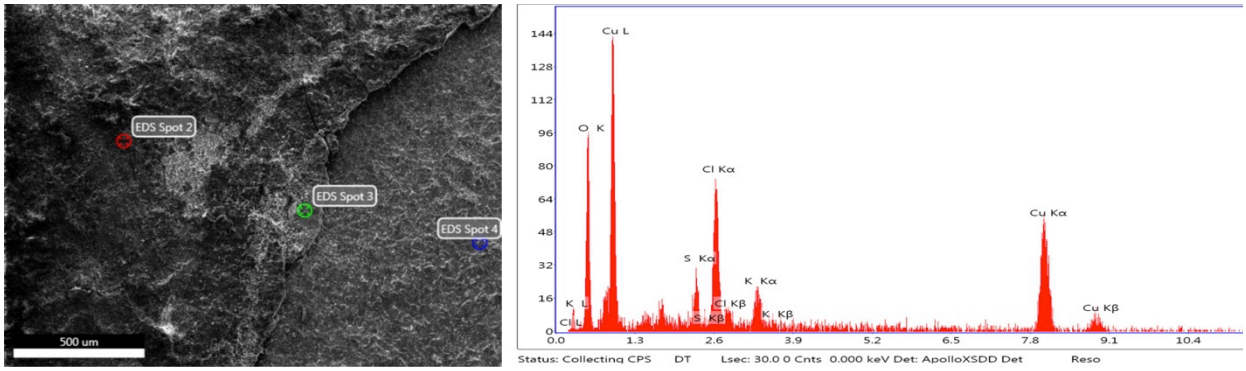

Figure 73: RH Roof – Uric acid + potassium chloride (C5): The EDS results for Spot 2.

The RH + SO_2 sample had very similar results, except that the interior of the drop was not fully exposed copper. All other components were the same as the RH sample, and the small crust remained on the surface was comprised of copper and potassium.

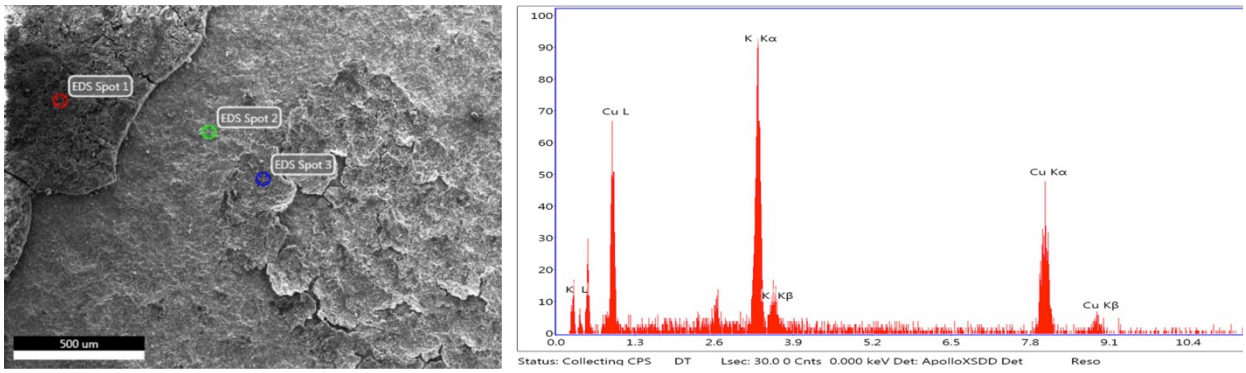

Figure 74: RH + SO_2 Roof – Uric acid + potassium chloride (C5): The EDS results for Spot 3, showing the composition of the remaining crust on the spot surface.

Uric acid + potassium sulphate (C6): The drop area of the RH sample was exposed copper. Traces of oxygen, potassium, sulphur, silicon (dust), and chlorine reflect minimal amounts of the contaminant left on the surface.

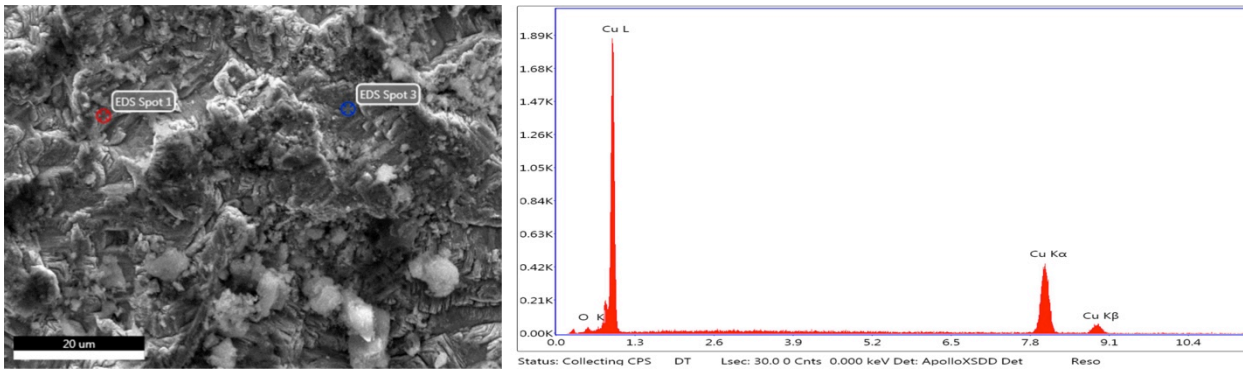

Figure 75: RH Roof – Uric acid + potassium sulphate (C6): The EDS results for Spot 1 on the exposed copper section.

The RH + SO_2 sample on the other hand had very minimal amounts of exposed copper. Its interior composition reflects that of the contaminant and patina surface (though there are minimal amounts left). These include copper, oxygen, sulphur, and potassium. Small amounts of chlorine can be seen in some cases, which is most likely from the uric acid + potassium chloride (C5) drippings.

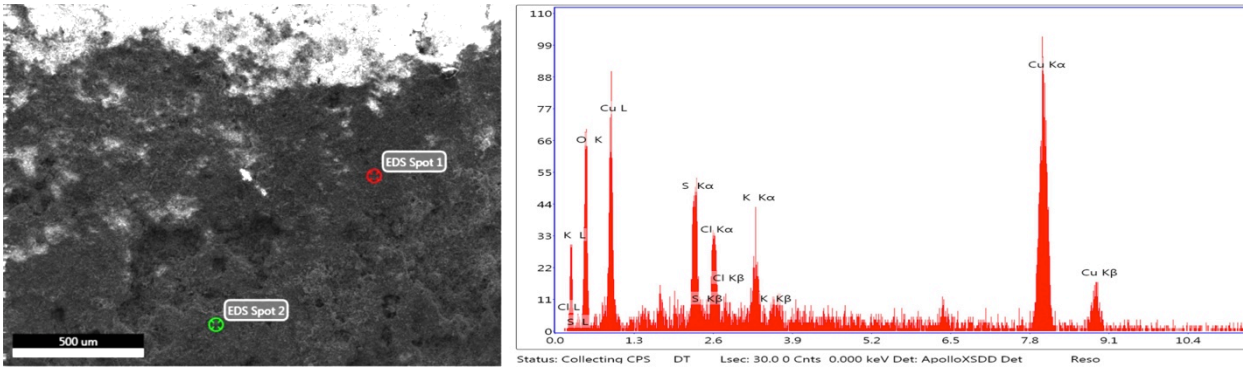

Figure 76: RH + SO_2 Roof – Uric acid + potassium sulphate (C6): The composition of Drop 1 on the RH + SO_2 sample, showing small amounts of chlorine most likely from the uric acid + potassium chloride (C5).

Table 20: SEM images of the bronze samples

Contaminant	RH Chamber		RH + SO_2 Chamber	
	Inside Drop	Outside Drop	Inside Drop	Outside Drop
Uric Acid (C1)	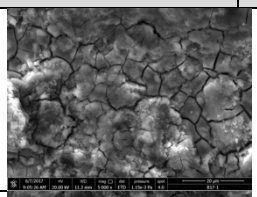		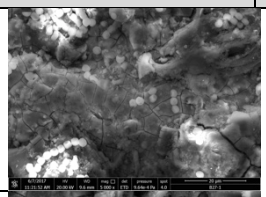	
Uric acid + sodium nitrate (C2)	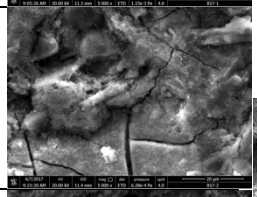	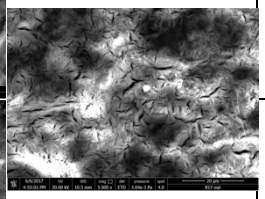	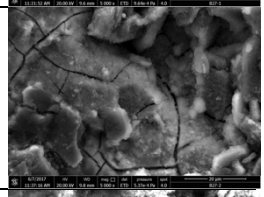	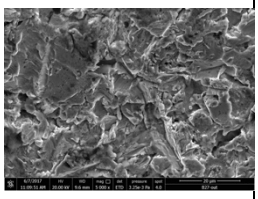
Uric acid + potassium dihydrogen phosphate (C3)	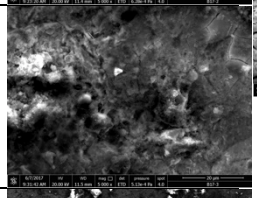		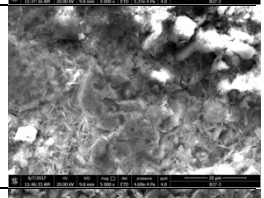	
Used Droppings (C4)	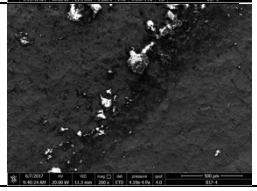		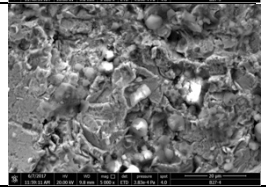	

Uric acid and potassium chloride (C5)	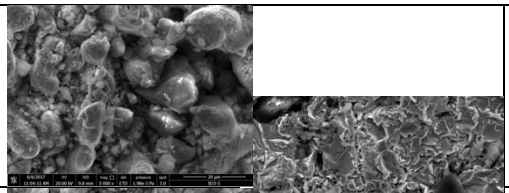		
Uric acid and potassium sulphate (C6)	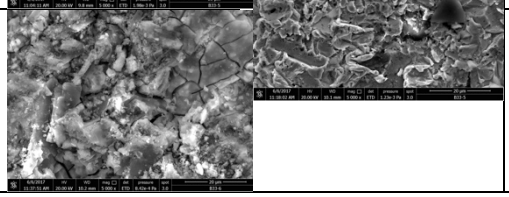		

The bronze sample surfaces were a lot less uniform, consisting of small fragmented layers. A 5000x-magnified photo of RH Contaminant 4 was unable to be conducted; therefore a 200x-magnified photo is shown. As previously stated, due to limited materials, there were no four-week bronze samples with RH + SO_2 exposure. The exterior bronze surfaces primarily consist of copper. In some cases its other components such as tin, lead, zinc, silicon, nickel, and iron are present. Other elements were detected and were must likely from dust or the salt powders blown across the surface.

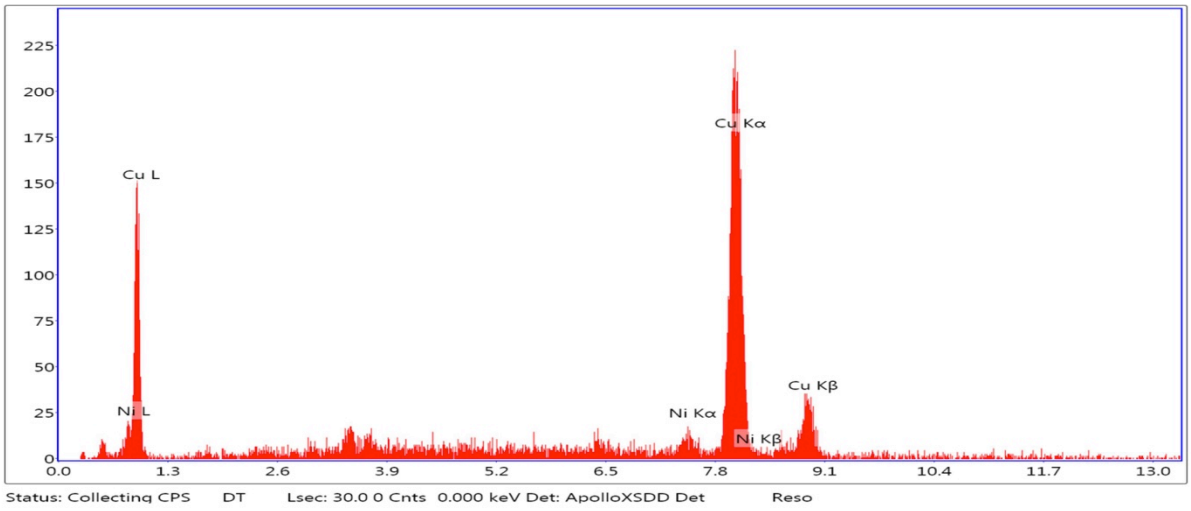

Figure 77: Bronze – Outside: EDS image of the uncontaminated bronze surface

Uric Acid (C1): The RH surface has a cracked texture and is comprised of elements that reflect either the bronze composition or contaminant composition. This includes primarily copper, followed by oxygen, nitrogen, and carbon. Some samples also contain silicon, chlorine, and tin. The chlorine is most likely from the used droppings (C4).

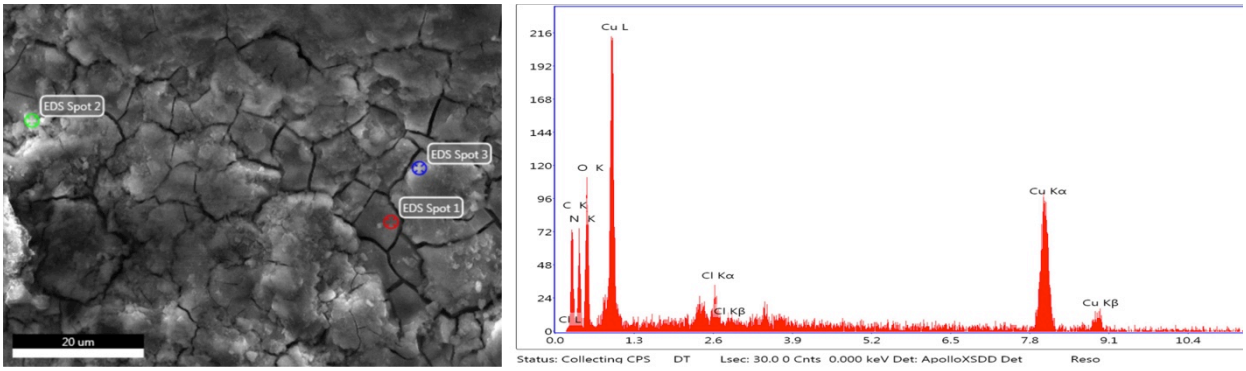

Figure 78: RH Bronze – Uric Acid: EDS image of Spot 2

The RH + SO_2 sample had a very similar composition. The main difference was that it contained the same circular chains that were seen in previous Uric Acid compositions on the copper and roof. Copper, oxygen, nitrogen, silicon, and chlorine are detected from this chain. When comparing to the previous chains, the nitrogen, silicon, and chlorine could be from backscattering of the bronze surface.

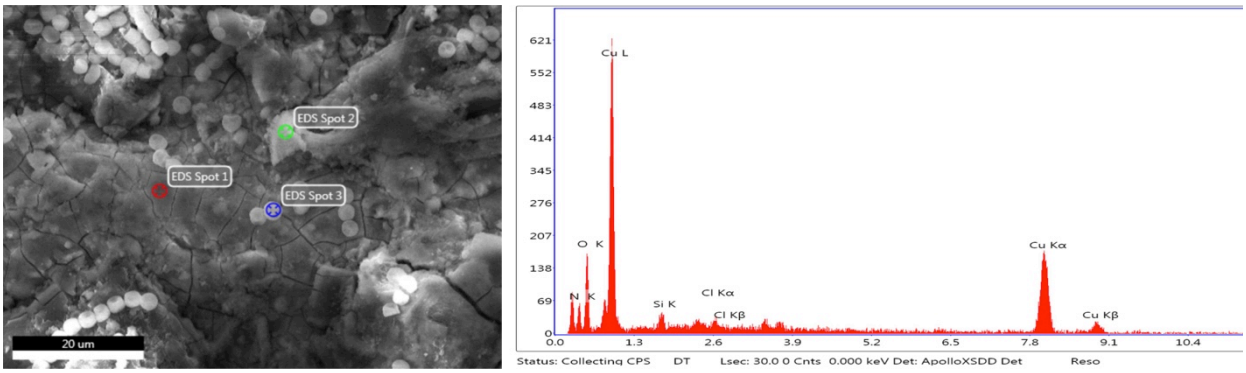

Figure 79: RH + SO_2 Bronze – Uric Acid: EDS image of the circular chain element (Spot 3)

Uric acid + sodium nitrate (C2): The RH surface of the drop area was cracked with large uneven surfaces. All of the elements present were expected to be found as they were from either the contaminant or the metal surface. These include, in order from greatest concentration to least, copper, oxygen, nitrogen, carbon, sodium, lead, chlorine, and calcium. It is predicted that the calcium is from the used droppings (C4).

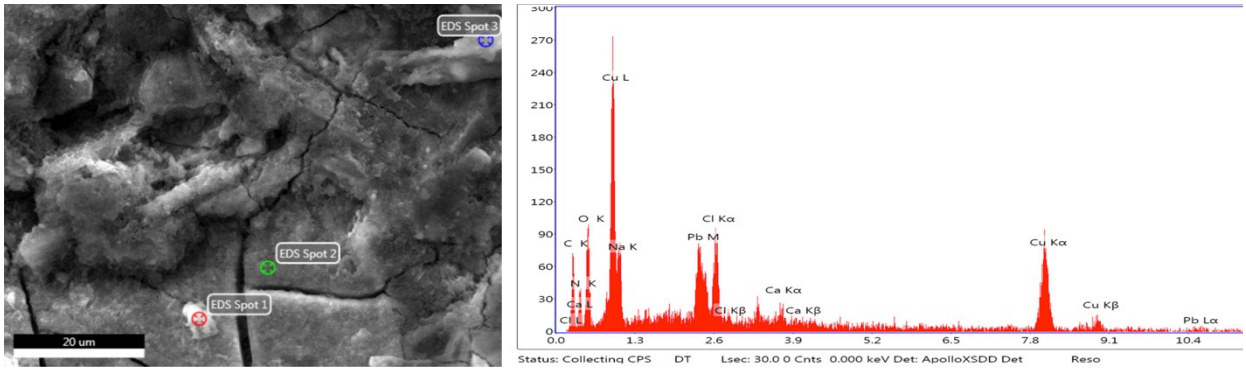

Figure 80: RH Bronze – Uric acid + sodium nitrate (C2): The EDS image of Spot 2.

The RH + SO_2 sample had a very similar composition. In some areas there was a very high concentration of lead. This is possible because the process of producing alloys is a particular process. The elements that have a higher melting point are melted first, followed by the other elements. In the case of bronze, copper has a higher melting point, followed by lead ("To Make Brass and Alloys," n.d.). Therefore, the lead may not have fully mixed with the copper upon its addition to the copper, creating concentrated areas.

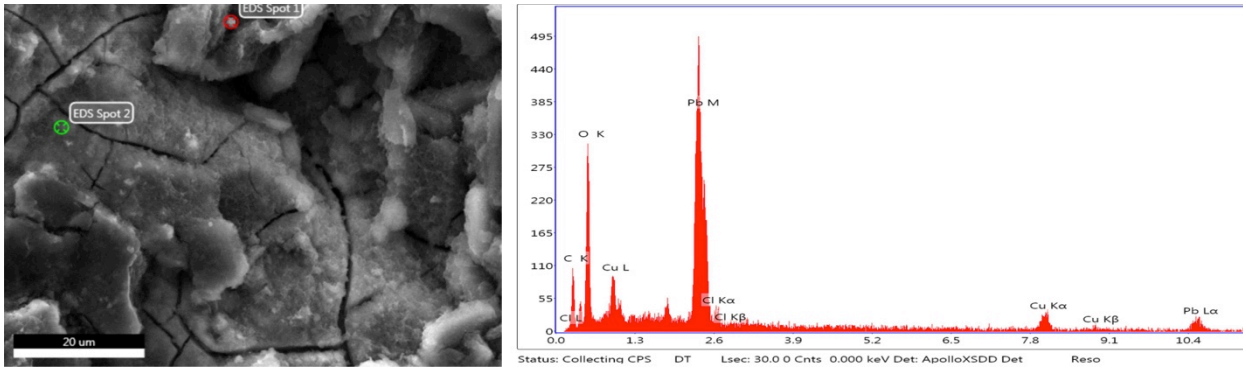

Figure 81: RH + SO_2 Bronze – Uric acid + sodium nitrate (C2): EDS image of Spot 1 showing the high concentration of lead

Uric acid + potassium dihydrogen phosphate (C3): The surface of the RH sample was cracked and pitted. Its composition is reflective of the components involved in the contaminant and bronze. The surface varies greatly on the ratio of these elements due to the fragmented pieces and somewhat inhomogeneous bronze material. Some areas show a very high copper concentration whereas the fragmented sections show more carbon, oxygen, and nitrogen.

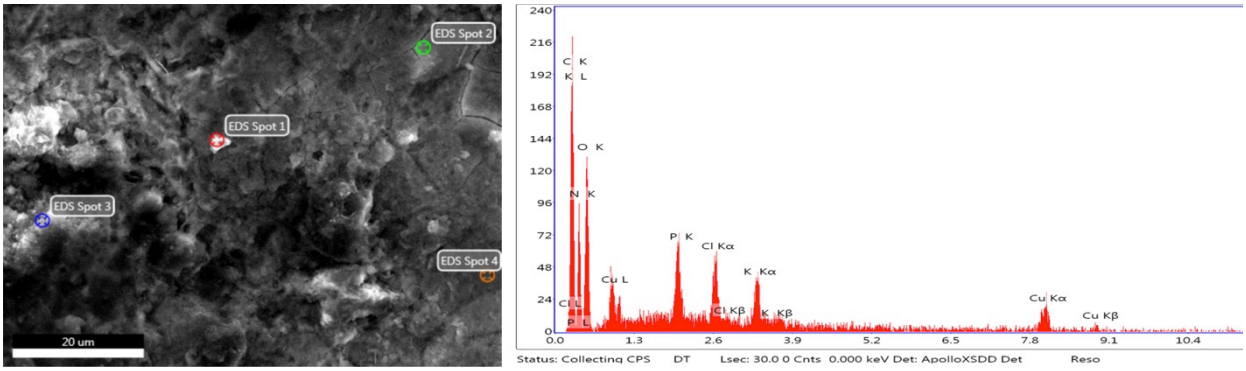

Figure 82: RH Bronze – Uric acid + potassium dihydrogen phosphate (C3): EDS image of Spot 3 showing a high concentration of carbon, nitrogen, and oxygen

As with the RH sample, the composition of the spot area for the RH + SO_2 sample is reflective of the components involved. Again, the more fragmented areas contain primarily carbon, oxygen, and nitrogen. In the data points taken, there is more phosphorous and potassium.

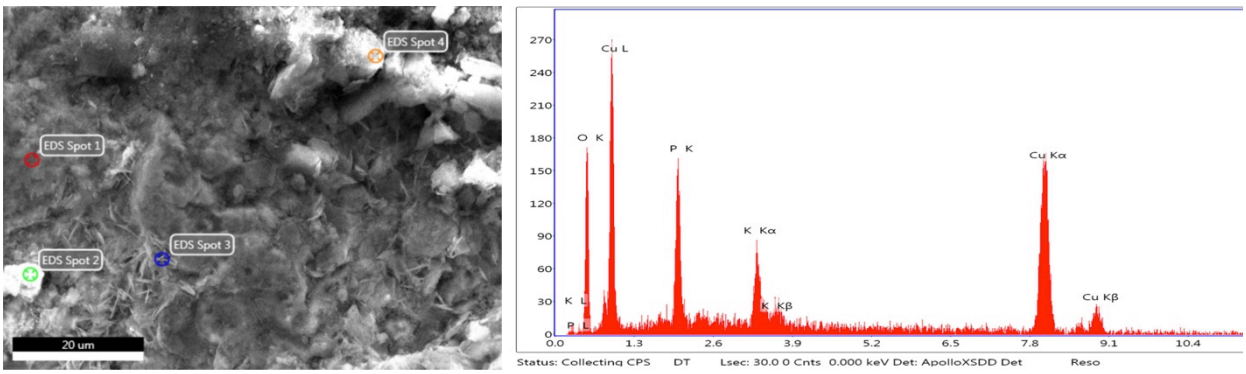

Figure 83: RH + SO_2 Bronze – Uric acid + potassium dihydrogen phosphate (C3): EDS image of Spot 1

Used droppings (C4): The surface of the RH drop is slightly rougher than that of the exterior. As with the other contaminants, there are no rogue elements that was not involved in the contaminant or material itself. As opposed to previous contaminants, there are higher concentrations of calcium (from the bird droppings), zinc, and tin.

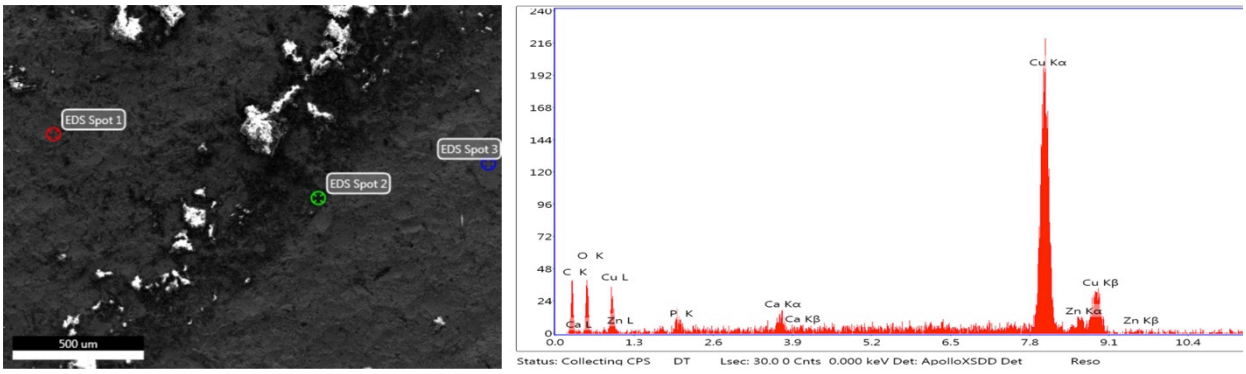

Figure 84: RH Bronze – Used droppings (C4): The EDS image of Spot 2, showing the presence of zinc.

The RH + SO_2 sample is less varied in its composition and shows a rougher surface. It consists primarily of copper, but also shows carbon, oxygen, calcium, silicon, lead, and tin.

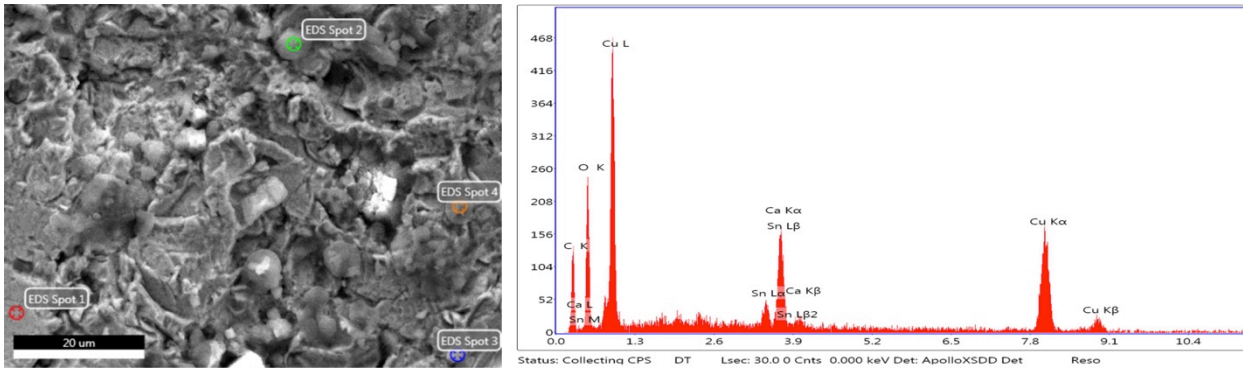

Figure 85: RH + SO_2 Bronze – Used droppings (C4): EDS image of Spot 3.

Uric acid + potassium chloride (C5): The surface of the RH drop area is very uneven and pitted. As with other samples, there are few elements that do not belong either to the bronze or contaminant. Though the ratio of these elements changes as one chooses different points, they are generally as follows: copper, oxygen, zinc, tin, nickel, silicon chlorine, nitrogen, sulphur, lead, potassium, and iron. The sulphur may be from the beginning formation of a patina. The iron may be from dust particles.

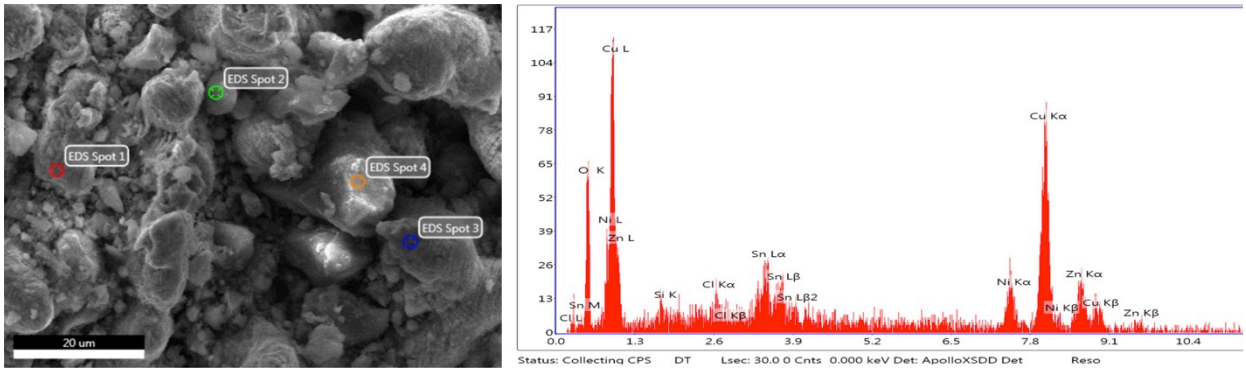

Figure 86: RH Bronze – Uric acid + potassium chloride (C5): EDS image of Spot 3

Uric acid + potassium sulphate (C6): The surface of the drop was not as varied as the uric acid + potassium chloride (C5), as there were more uniformed cracked regions. As with previous samples, the fragmented regions were comprised primarily of copper, oxygen, and carbon. Other major elements found on the surface include nitrogen, sulphur, and potassium. These are all found in the contaminant and/or metal.

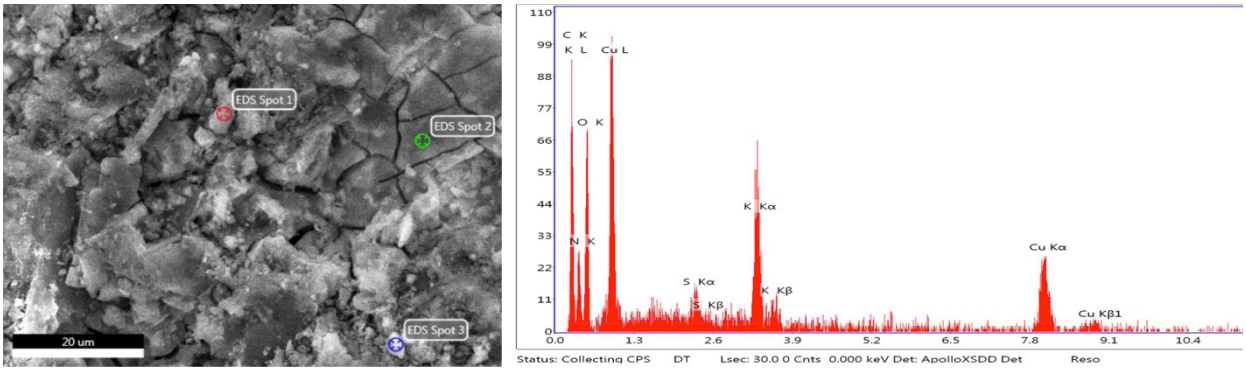

Figure 87: RH Bronze – Uric acid + potassium sulphate (C6): EDS image of Spot 3.

The surfaces in all of the samples changed dependent on the contaminant added. Some became cracked, whereas others became more fragmented and pitted than their surroundings. The surface roughness may affect the rate of corrosion, as water may be more likely to settle in a rough area versus a smooth flat surface. Most samples have uneven surfaces with an abundance of carbon, oxygen, and copper. The Contaminant 1 often has chains of spheres that are primarily carbon and oxygen. These are most likely mould spores growing from the uric acid. Separate spheres – or spores - can sometimes be seen in other samples, but the combination of other salt contaminants most likely does not make the ideal growth environment for the spores. After research into the different bacterial and fungal species found on bird droppings from previous studies, it is estimated that these are the spores from either penicillium cyclopium or penicillium expansum.

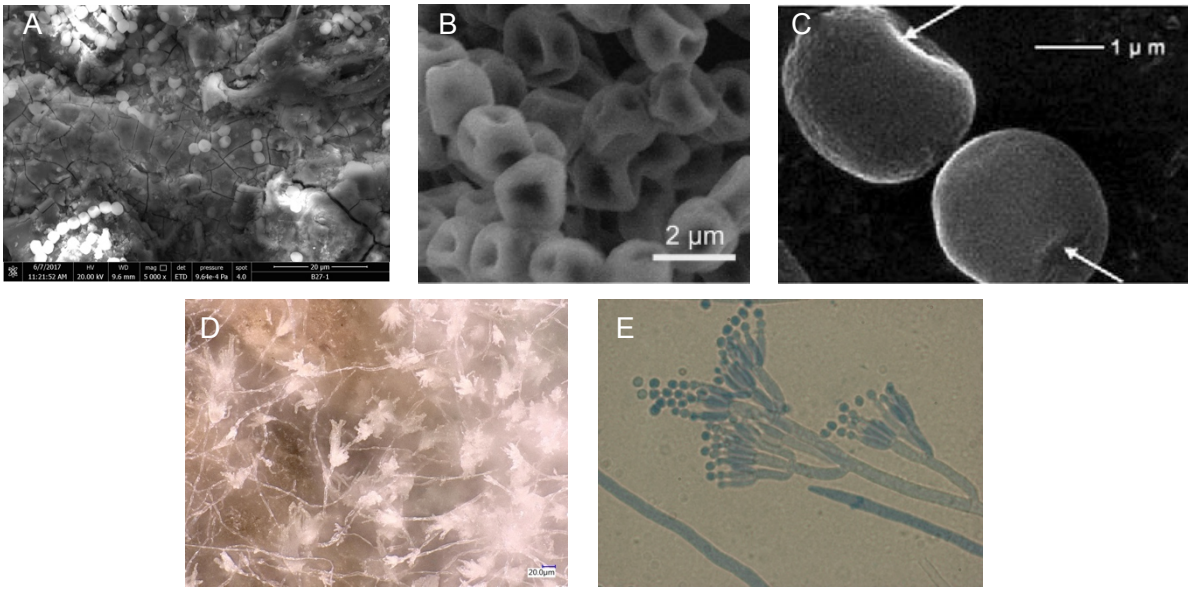

Figure 88: A) SEM image of the spores found on the bronze sample; B) Research SEM image of penicillium expansum (He, Liu, Mustapha, & Lin, 2011); C) Research SEM image of penicillium cyclopium (Zhang, Sun, Chen, Zeng, & Wang, 2017); D) Microscope image of the mould spores found on the used droppings (C4); D) Research microscope image of penicillium (Conidia, n.d.)

A study of the required pH states that penicillium expansum grows under a pH of 4 or 7, meaning that it is a resilient fungi that can grown in very acidic conditions (Barad et al., 2016). Another study determined that uric acid can aid in the growth of penicillium cyclopium (Helbig, Steighardt, & Roos, 2002). Unfortunately, the only way to really distinguish fungal species is by sequencing. Future studies may want to investigate this topic to determine the fungal growth's impact on the corrosion products.

Most elements located were either from the contaminant added or the metal itself. Elements such as iron and chlorine in some cases were attributed to dust particles.

4.2.2.4 ICP-OES

Due to complications with equipment and the high temperatures outside, this test was not conducted. It is recommended that future studies perform this test to aid in determining the rate of corrosion.

5. CONCLUSION

The composition of bird droppings was determined using ion exchange chromatography (IEC) and X-ray diffraction (XRD). The anions found in the used bird droppings from greatest concentration to least were: sulphate, chloride, phosphate, fluoride, bromide, and nitrate. The cations included potassium, calcium, sodium, magnesium, and ammonium. This composition was slightly different than that of real bird droppings. The anions included phosphate, chloride, and sulphate. The cations included ammonium, potassium, sodium, magnesium, and calcium. It is believed that the manufactured (used) droppings contained filler material. The XRD indicated that the used bird droppings contained calcite, quartz, weddellite, and magnesium hydrogen phosphate hydrate. The real bird droppings contained magnesium ammonium phosphate hydrate, quartz, weddellite, and aphthitalite. The used bird droppings were more acidic than the real bird droppings. Should this composition had been known before the experiment began, the following contaminants would have been recommended to test: 1) uric acid; 2) uric acid and ammonium chloride; 3) uric acid and sodium sulphate 4) uric acid and monomagnesium phosphate; 5) uric acid and potassium chloride; 6) Uric acid and ammonium sulphate; 7) potassium sulphate; and 8) real bird droppings.

The microscopy and colourimetry provided a good analysis of the visual impact of the contaminants. Sometimes the contaminant acted as a protective agent and the surrounding metal tarnished. In most cases, the copper and bronze became a darker brown colour, most likely indicating the initial formation of posnjakite or cuprite. The turquoise colour from some of the contaminants was most likely copper (II) hydroxide. Contaminants 5 and 6 removed the patina on the roof sample, but overall the patina acted as a protective agent against the contaminants. The colourimetry gave numerical values for these colour changes between the inside, outside, two-week, and four-week samples.

The scanning electron microscope (SEM) and energy dispersive spectroscopy (EDS) allowed for the analysis of structure and composition of the metal surfaces. In most cases, the elements present reflected those of the applied contaminant or the metal. Evidence of fungi and dust was present in some samples and the surface texture often became rougher. The inductively coupled plasma optical emission spectrometry (ICP-OES) testing did not occur due to equipment issues.

Overall it is evident that bird droppings do have a chemical effect on metals. It is recommended that further research occur that better imitates the real bird droppings. Obtaining droppings should be conducted first, followed by XRD and IEC to determine its contents. Following this, choosing the appropriate salt contaminants with the results of the XRD and IEC should be done. It is recommended that the testing process last longer than four weeks. Though the conditions do accelerate the corrosion process, it is not long enough to see any extreme changes. Perhaps testing sheltered and unsheltered metals could provide more information about environmental effects. The orientation of the metal samples should be considered to ensure no dripping occurs on other contaminants. Also, though best efforts were made to not contaminate the metal surfaces with

fingerprints and other elements, storage of the elements within (and limited removal from) a near-vacuum-sealed chamber is recommended. Due to the time constraint of the analyses, performing the tests on all removed specimens to evaluate the effect of duration did not occur and is therefore recommended for future testing programs.

Cleaning to remove stagnant water on metal surfaces is an easy way to decrease the rate of corrosion. Current successful bird deterrent methods often require mechanical or chemical fastening. Research into the effects of the adhesives (glue) or bird gel on metals is a recommended topic. In the end, the best way to protect metals from bird droppings is to prevent birds from perching on them in the first place.

REFERENCES

Abrahams, M. (2012, February 6). Pigeon deterrents: a question of chemistry. *The Guardian*. Retrieved from https://www.theguardian.com/education/2012/feb/06/research-pigeon-behaviour-clean-statues

Absolute Pest Control Ltd. (n.d.). Bird Control. Retrieved May 28, 2017, from http://www.absolutepestcontrol.biz/bird-control

Barad, S., Sela, N., Kumar, D., Kumar-Dubey, A., Glam-Matana, N., Sherman, A., & Prusky, D. (2016). Fungal and host transcriptome analysis of pH-regulated genes during colonization of apple fruits by Penicillium expansum. *BMC Genomics*, *17*(330), 1–27. Retrieved from https://bmcgenomics.biomedcentral.com/articles/10.1186/s12864-016-2665-7

Bassi, M., & Chiatante, D. (1976). The Role of Pigeon Excrement in Stone Biodeterioration. *International Biodeterioration & Biodegredation*, *12*(3), 73–79.

BBC News. (1999, January 19). UK Pigeons: Not a problem to poo-poo. *BBC News Online Network*. London. Retrieved from http://news.bbc.co.uk/2/hi/uk_news/257284.stm

BBC News. (2003, November 17). Feeding Trafalgar's pigeons illegal. *BBC News Online Network*. London. Retrieved from http://news.bbc.co.uk/2/hi/uk_news/england/london/3275233.stm

Bernardi, E., Bowden, D. J., Brimblecombe, P., Kenneally, H., & Morselli, L. (2009). The effect of uric acid on outdoor copper and bronze. *Science of the Total Environment*, *407*(7), 2383–2389. https://doi.org/10.1016/j.scitotenv.2008.12.014

Blum, P. (1997). Reflectance Spectrophotometry and Colorimetry. In *Physical Properties Handbook: A guide to the shipboard measurement of physical properties of deep-sea cores* (pp. 1–11). ODP Tech Note. Retrieved from http://www-odp.tamu.edu/publications/tnotes/tn26/CHAP7.PDF

Chemical Book. (n.d.). Chemical Properties. Retrieved June 4, 2017, from http://www.chemicalbook.com/

Clarelli, F., De Filippo, B., & Natalini, R. (2014). Mathematical model of copper corrosion. *Applied Mathematical Modelling*, *38*(19–20), 4804–4816. https://doi.org/10.1016/j.apm.2014.03.040

Conidia. (n.d.). Molds. Retrieved June 24, 2017, from http://conidia.fr/en/molds/

Drdácký, M., & Slížková, Z. (2005). *Posouzení stavu budovy Národního muzea v Praze, Zpráva k hospodářské smlouvě s NM v Praze*. Prague.

Dutrow, B., & Clark, C. (2017). X-ray Powder Diffraction (XRD). Retrieved June 4, 2017, from http://serc.carleton.edu/research_education/geochemsheets/techniques/XRD.html

Fabjan, E. Š., Kosec, T., Kuhar, V., & Legat, A. (2011). Corrosion stability of different bronzes in

simulated Urban rain. *Materiali in Tehnologije*, *45*(6), 585–591.

Finamore, E. (2016). Where Did Trafalgar Square's Pigeons Come From? Retrieved April 18, 2017, from http://londonist.com/2016/07/where-did-trafalgar-square-s-pigeons-come-from

FitzGerald, K. P., Nairn, J., Skennerton, G., & Atrens, A. (2006). Atmospheric corrosion of copper and the colour, structure and composition of natural patinas on copper. *Corrosion Science*, *48*(9), 2480–2509. https://doi.org/10.1016/j.corsci.2005.09.011

Fretwell, S. D., & Lucas, H. L. (1968). *On Territorial Behaviour and Other Factors Influencing Habitat Distribution in Birds*. Raleigh. Retrieved from http://izt.ciens.ucv.ve/ecologia/Archivos/Tomas_references-II/articles/def/fretwell_lucas-actabiot69.pdf

Gómez-Heras, M., Benavente, D., Álvarez De Buergo, M., & Fort, R. (2004). Soluble salt minerals from pigeon droppings as potential contributors to the decay of stone based Cultural Heritage. *European Journal of Mineralogy*, *16*(3), 505–509. https://doi.org/10.1127/0935-1221/2004/0016-0505

Gra Research - Center for Public Buildings. (2016). Methods of Bird Control: Advantages and Disadvantages. Retrieved May 28, 2017, from https://www.gsa.gov/portal/content/113310

Hafner, B. (n.d.). Energy Dispersive Spectroscopy on the SEM: A Primer. Retrieved June 4, 2017, from http://www.charfac.umn.edu/instruments/eds_on_sem_primer.pdf

He, L., Liu, Y., Mustapha, A., & Lin, M. (2011). Antifungal activity of zinc oxide nanoparticles against Botrytis cinerea and Penicillium expansum. *Microbiological Research*, *166*, 207–215. Retrieved from https://www.researchgate.net/publication/45187960_Antifungal_activity_of_zinc_oxide_nanoparticles_against_Botrytis_cinerea_and_Penicillium_expansum

Helbig, F., Steighardt, J., & Roos, W. (2002). Uric acid is a genuine metabolite of Penicillium cyclopium and stimulates the expression of alkaloid biosynthesis in this fungus. *Applied and Environmental Microbiology*, *68*(4), 1524–1533. Retrieved from https://www.ncbi.nlm.nih.gov/pubmed/11916664

Jacob, J. (2015). Avian Digestive System. Retrieved June 27, 2017, from http://articles.extension.org/pages/65376/avian-digestive-system

Knotkova, D., & Kreislová, K. (2007). Atmospheric corrosion and conservation of copper and bronze. In A. Moncmanova (Ed.), *Environmental Deterioration of Materials* (pp. 107–142). Southampton: WIT Press.

Kreislova, K., & Geiplova, H. (2016). Prediction of the long-term corrosion rate of copper alloy objects. *Materials and Corrosion*, *67*(2), 152–159. https://doi.org/10.1002/maco.201408112

Kreislová, K., Knotková, D., & Koukalová, A. (2010). *Posouzení korozního stavu plastik*. Prague.

Kreislová, K., & Koukalová, A. (2012). *Hodnocení stavu měděné krytiny letohrádku Belvedér*. Prague.

Lavenburg, G., Hall, D., Lewis, J., Wolfe, S., & Strange, M. (2011). Impacts of Bird Droppings and Deicing Salts on Highway Structures : Monitoring , Diagnosis , Prevention, *19716*(December), 1–22.

RS Innovative Solutions. (n.d.). Bird Control Solutions. Retrieved May 28, 2017, from http://www.reachnettings.com/Products/bird-control-solution/bird-gel/

Science Lab. (n.d.). MSDS. Retrieved June 4, 2017, from http://www.sciencelab.com/

Stuart, B. (2007). *Analytical Techniques in Materials Conservation*. West Sussex: John Wiley & Sons Ltd.

Swapp, S. (n.d.). What is Scanning Electron Microscopy (SEM). Retrieved June 4, 2017, from https://serc.carleton.edu/research_education/geochemsheets/techniques/SEM.html

Tidblad, J., Kucera, V., & Sherwood, S. (2009). Corrosion. In J. Watt, V. Kucera, J. Tidblad, & R. Hamilton (Eds.), *The Effects of Air Pollution on Cultural Heritage* (pp. 53–103). New York: Springer Science + Business Media. https://doi.org/10.1007/978-0-387-84893-8

To Make Brass and Alloys. (n.d.). Retrieved June 23, 2017, from https://www.scientificamerican.com/article/to-make-brass-and-alloys/

Vasiliu, A., & Buruiana, D. (2010). Are birds a menace to outdoor monuments? *International Journal of Conservation Science*, *1*(2), 75–82.

Viani, A. (2017). *XRD Analysis Report*. Telč.

Zhang, J., Sun, H., Chen, S., Zeng, L., & Wang, T. (2017). Anti-fungal activity, mechanism studies on α-Phellandrene and Nonanal against Penicillium cyclopium. *Botanical Studies*, *58*(13). Retrieved from https://as-botanicalstudies.springeropen.com/articles/10.1186/s40529-017-0168-8

APPENDIX A – COLOURIMETRY GRAPHS

Change between inside and outside of contaminated areas

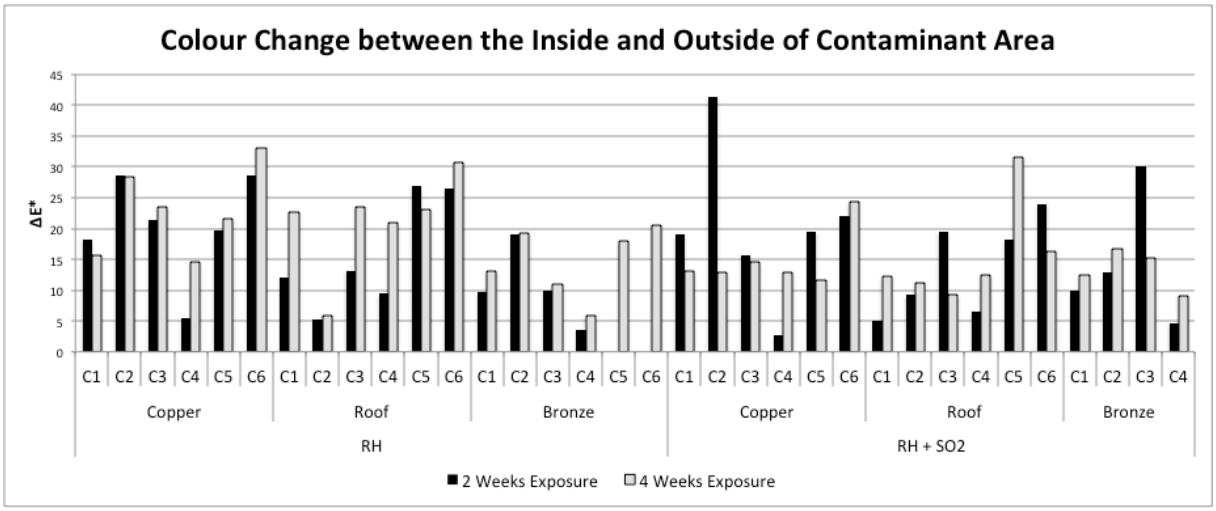

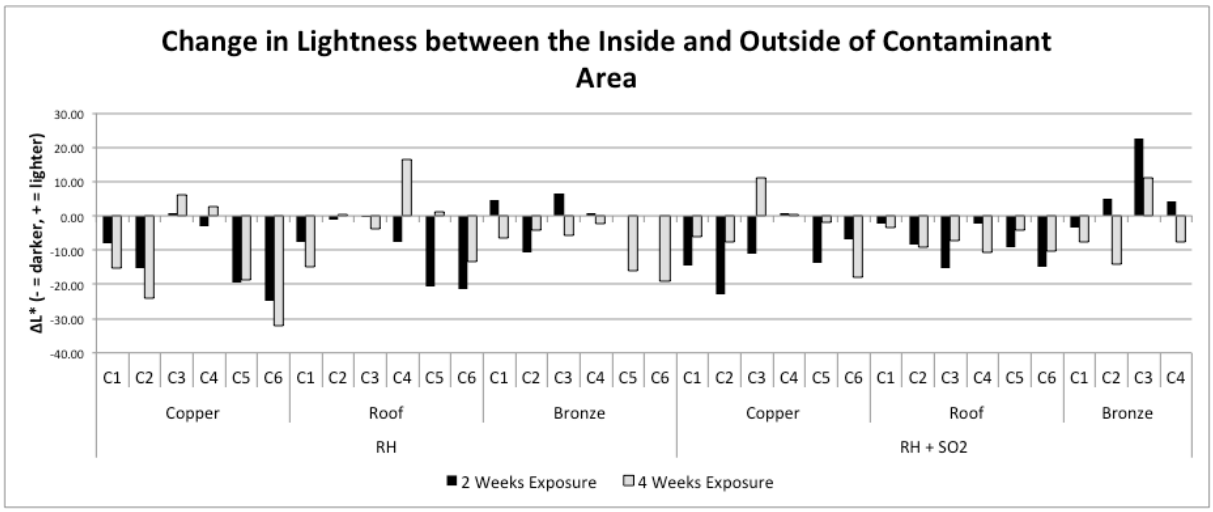

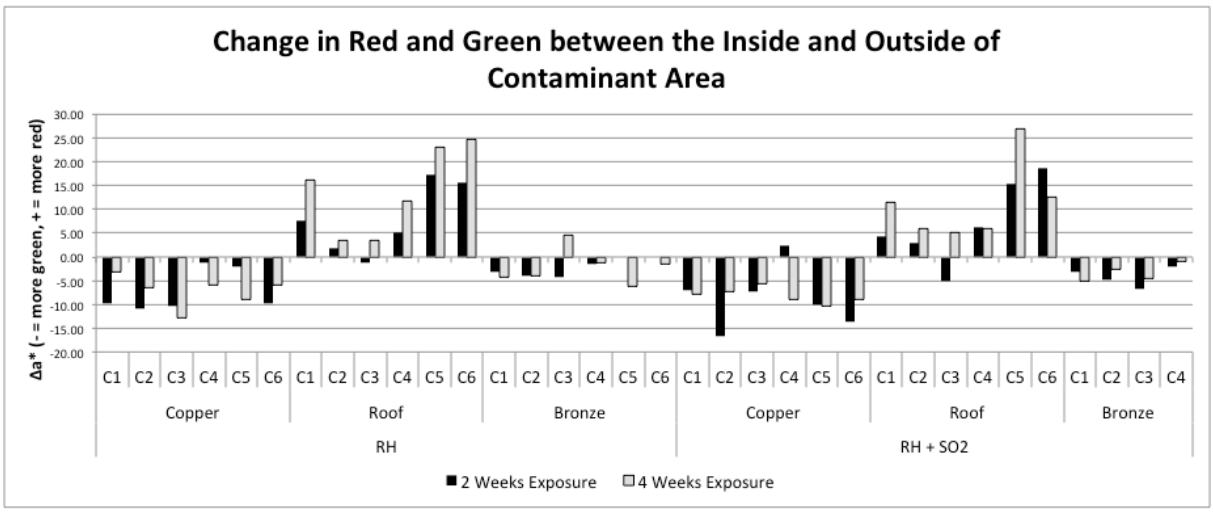

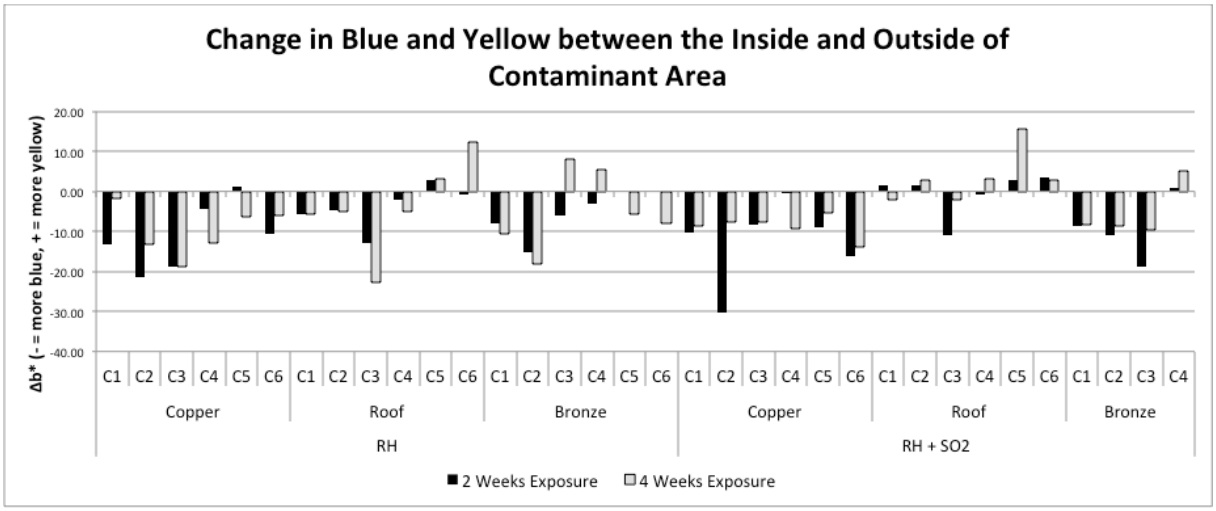

Change inside contaminated areas between two and four weeks

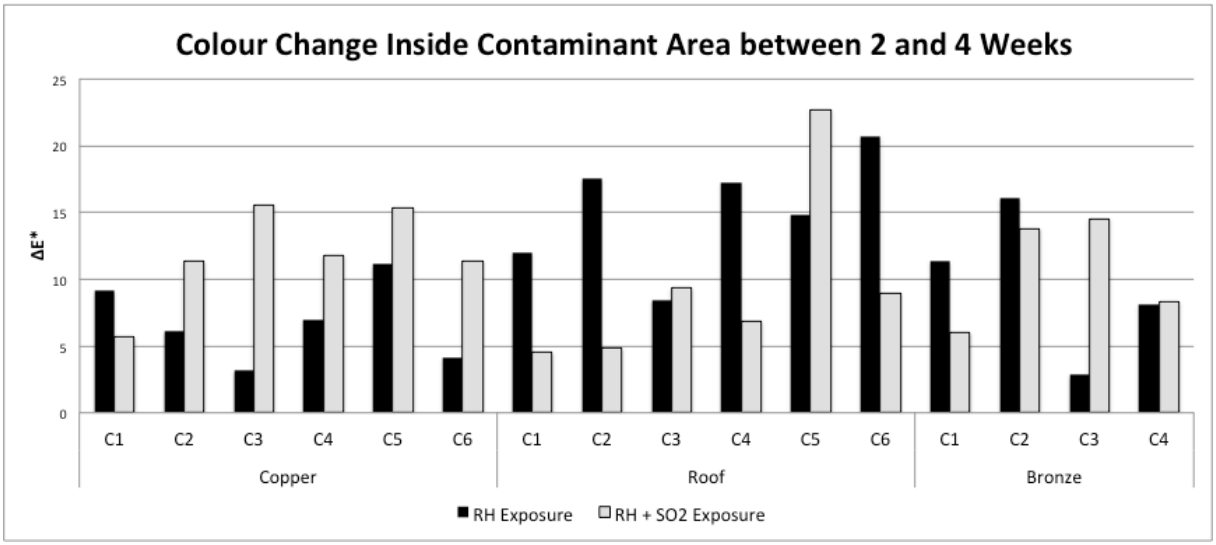

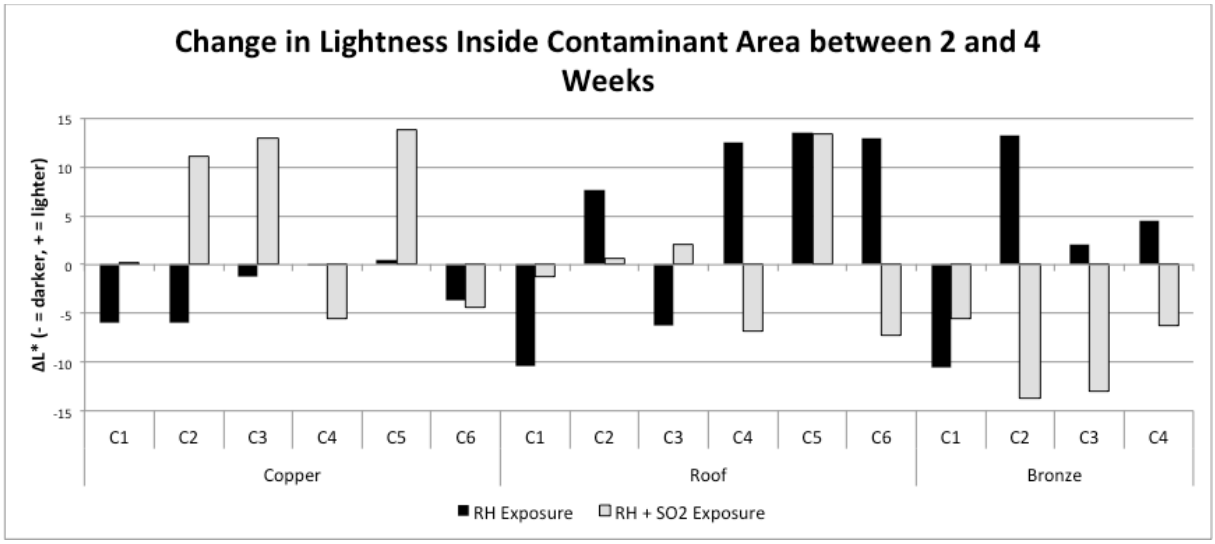

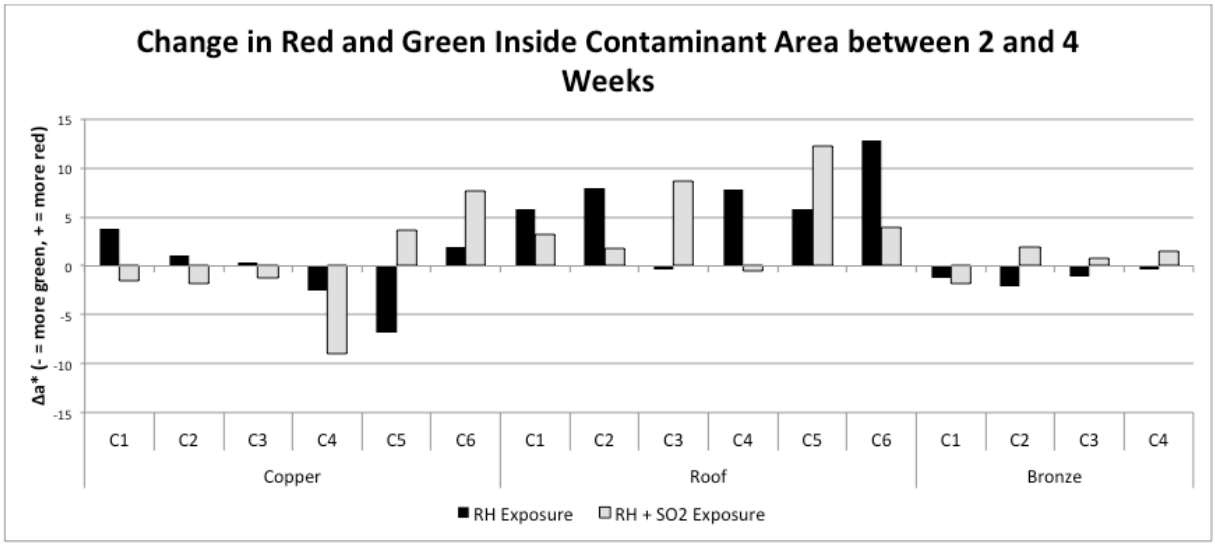
Change in Red and Green Inside Contaminant Area between 2 and 4 Weeks
Δa* (- = more green, + = more red)
15
10
5
0
-5
-10
-15
C1 C2 C3 C4 C5 C6 C1 C2 C3 C4 C5 C6 C1 C2 C3 C4
Copper
Roof
Bronze
RH Exposure
RH + SO2 Exposure

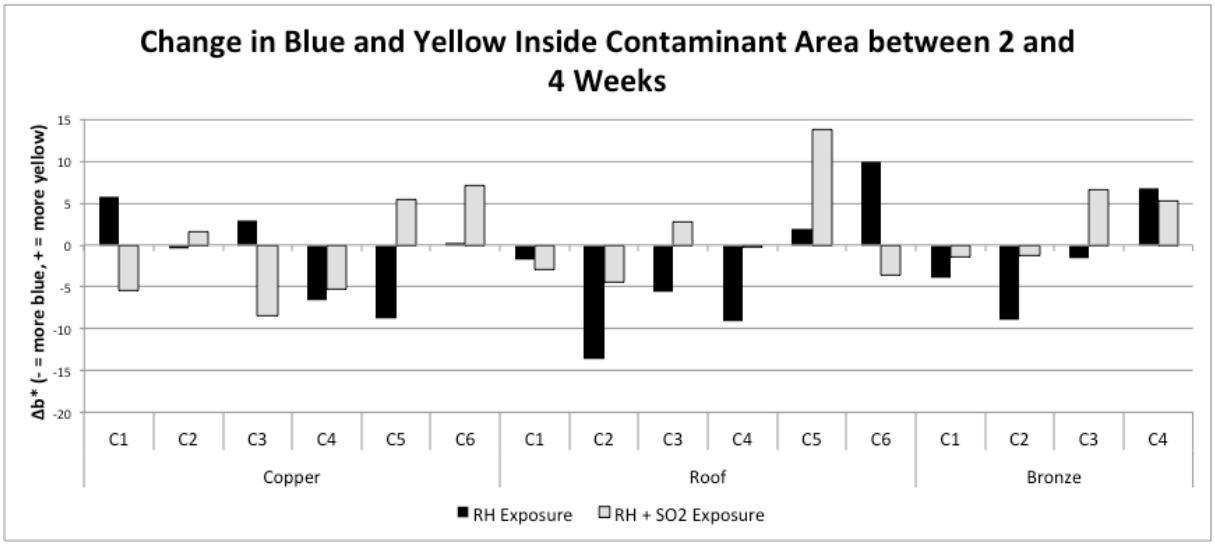
Change in Blue and Yellow Inside Contaminant Area between 2 and 4 Weeks
Δb* (- = more blue, + = more yellow)
15
10
5
0
-5
-10
-15
-20
C1 C2 C3 C4 C5 C6 C1 C2 C3 C4 C5 C6 C1 C2 C3 C4
Copper
Roof
Bronze
RH Exposure
RH + SO2 Exposure

Change outside contaminated areas between two and four weeks (not averaged)

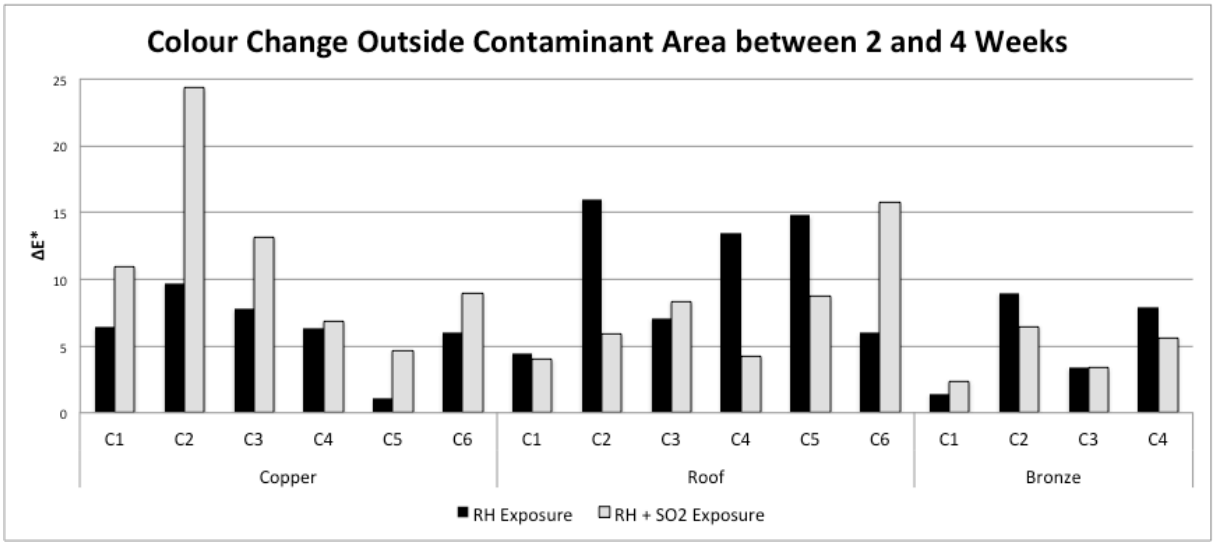

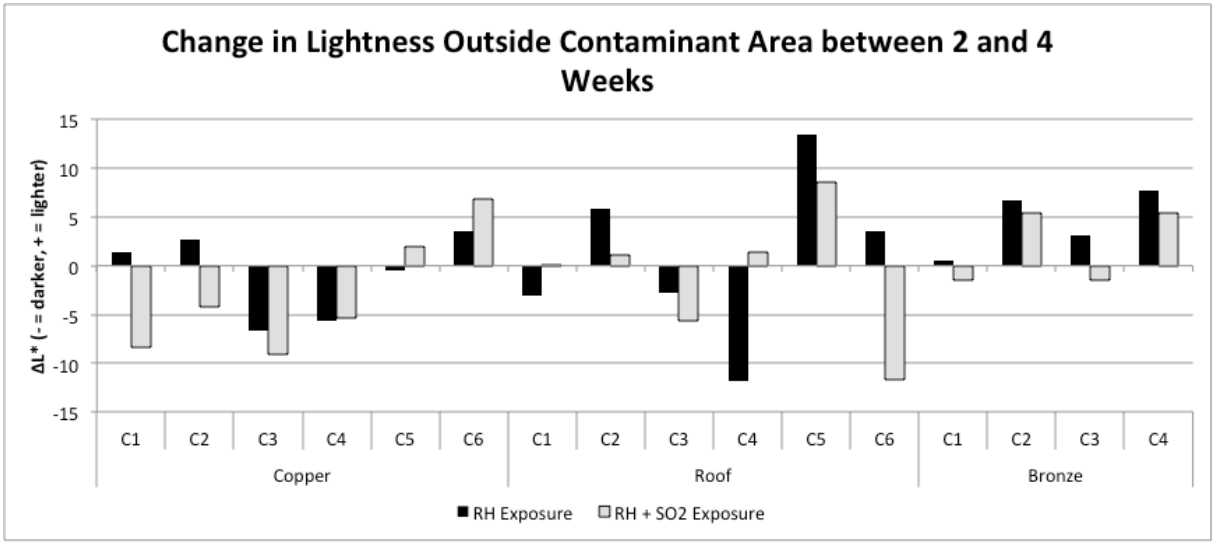

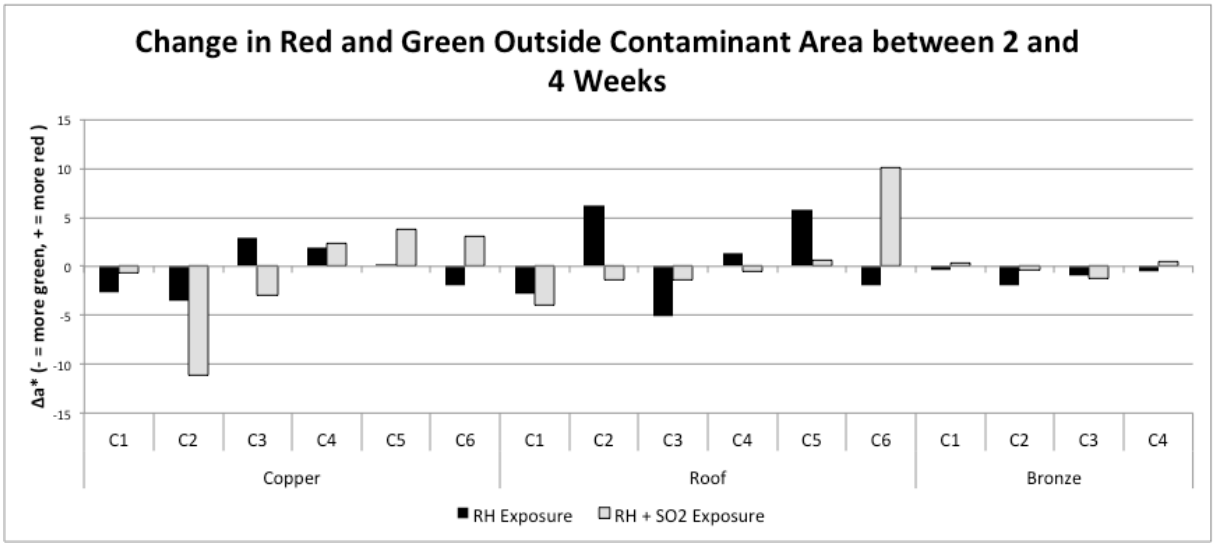

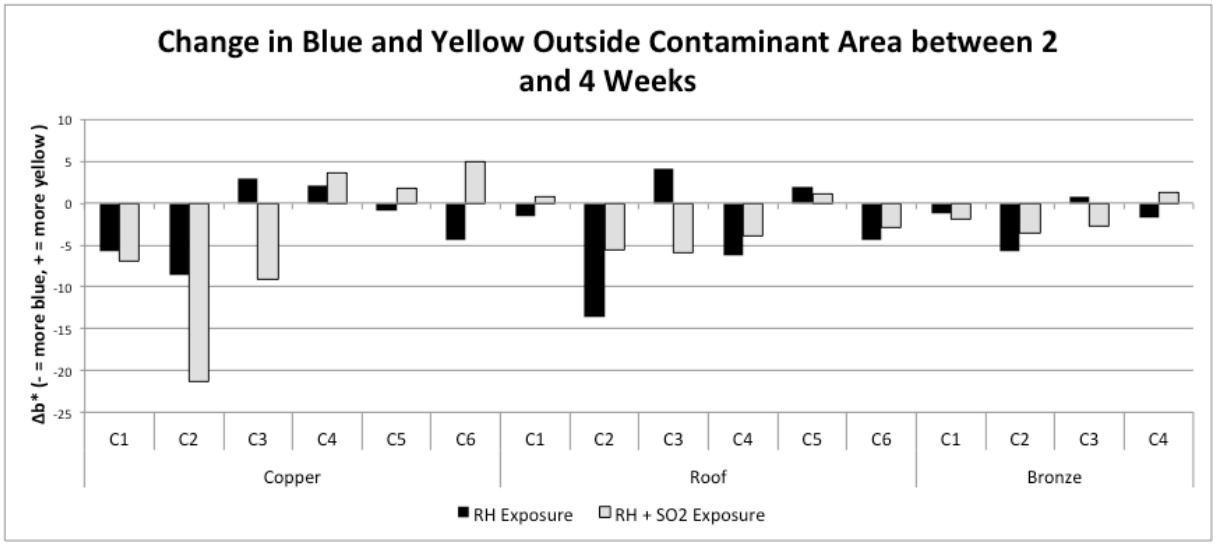
Change in Blue and Yellow Outside Contaminant Area between 2 and 4 Weeks
Δb* (- = more blue, + = more yellow)
10
5
0
-5
-10
-15
-20
-25
C1
C2
C3
C4
C5
C6
Copper
Roof
Bronze
RH Exposure
RH + SO2 Exposure